

**PHASE CHANGE MATERIALS BASED ON POLYETHYLENE,
PARAFFIN WAX AND WOOD FLOUR**

by

MFISO EMMANUEL MNGOMEZULU (B.Sc. Hons.)

2002121057

Submitted in accordance with the requirements for the degree

MASTER OF SCIENCE (M.Sc.)

Department of Chemistry

Faculty of Natural and Agricultural Sciences

at the

UNIVERSITY OF THE FREE STATE (QWAQWA CAMPUS)

SUPERVISOR: PROF A.S. LUYT

CO-SUPERVISOR: DR I. KRUPA

November 2009

DECLARATION

I declare that the dissertation hereby submitted by me for the Masters of Science degree at the University of the Free State is my own independent work and has not previously been submitted by me at another university/faculty. I furthermore, cede copyright of the dissertation in favour of the University of the Free State.

Mngomezulu M.E. (Mr)

Luyt A.S. (Prof)

DEDICATIONS

Kubazali bami abathandekayo: UBaba Vusimuzi Josiah Mngomezulu noMama Mafahatsi Jerminah Mngomezulu. Ngiswele imilomo eyizinkulungwane ngothando nemfundiso yenu kimi kusukela ngizalwa kuzekube kusekugcineni. Ngibonga abazali benu (Ogogo nomkhulu bami-Umkhulu Christmas Meshaek Mbuti Mngomezulu (odukile) nogogo Teboho Linah Mngomezulu, kanye nomkhulu Lehlohonolo Petrus Monareng (osekwelamathongo) nogogo Kukkie Violet Monareng). Anginalo iGolide neSiliva ukunibonga ngoba ningenze umuntu ebantwini. Ngakho ngiyakunibonga ngokuphila impilo ehlanzekile phambi kukaMvelinqangi naphambi kwenu. Thokozani niphile boMfiso nani boSebei abahle!!!

ABSTRACT

Phase change material (PCM) composites based on high-density polyethylene (HDPE) with soft (M3) and hard (H1) Fischer-Tropsch paraffin waxes and alkali-treated wood flour (WF) were investigated in this study. Both the blends and composites were prepared using a melt-mixing method with a Brabender-Plastograph. SEM, DSC, TGA, DMA, tensile testing and water absorption were used to characterize the structure and properties of the blends and composites. The HDPE as the supporting matrix kept the molten waxes in compact shape during its phase transition from solid to liquid. Immiscibility of the PCMs (waxes) and the supporting matrix (HDPE) is a necessary property for effective energy storage. M3 wax blends were immiscible, whereas H1 wax blends seemed to be partially miscible and co-crystallized with the polymer matrix. In the presence of WF, the wax seems to crystallize around and in the pores of the WF particles, thus reducing co-crystallization with the HDPE and improving the energy storage capacity. TGA results showed a reduction in the thermal stabilities of the blends and composites in the presence of both WF and waxes. The storage modulus was reduced in the presence of wax, but improved when both WF and wax are present, although the improvement was less significant in the case of the M3 wax. Depending on the type of wax, the γ - and α -transitions were influenced differently, and there was an emergence of a β -relaxation in the case of the M3 wax blends. Both waxes had different influences on the tensile modulus and strength of the blends, with H1 increasing and M3 decreasing these properties. The PCM composites, on the other hand, had high moduli. High content of WF in the composites showed high water absorption. However, in the wax containing composites, there was a general decrease in water uptake.

LIST OF ABBREVIATIONS

ASTM	American Society for Testing and Materials
BPE	Branched polyethylene
DMA/DMTA	Dynamic mechanical analysis/thermal analysis
DSC	Differential scanning calorimetry
CP	Chemically pure
EG	Expanded graphite
EVA	Ethylene-co-vinyl acetate
EVAl	Ethylene-vinyl alcohol copolymer
HDPE	High density polyethylene
LDPE	Low-density polyethylene
LHS	Latent heat storage
LLDPE	Linear low-density polyethylene
LPE	Linear polyethylene
MFI	Melt flow index
OMT	Organophilic montmorillonite
PCM	Phase change material
PE	Polyethylene
PEG	Polyethylene glycol
PP	Polypropylene
PPC	Polyethylene-paraffin compound
PPS	Poly(phenylene sulphide)
PS	Polystyrene
PU	Polyurethane
PVA/SBN	Polyvinyl alcohol/soybean nano-fibre
SBS	Styrene-butadiene-styrene
SEBS	Styrene-ethylene-butylene-styrene
SEM	Scanning electron microscopy
TES	Thermal energy storage
TGA	Thermogravimetric analysis
UHMW-PE	Ultra high molecular weight polyethylene
UV	Ultraviolet
Wax FT	Fischer-Tropsch paraffin wax

Wax S	Soft paraffin wax
WA	Water absorption
WF	Wood flour
WPE	Recycled polyethylene waste

TABLE OF CONTENTS

Contents	Page Number
DECLARATION	i
DEDICATIONS	ii
ABSTRACT	iii
LIST OF ABBREVIATIONS	iv
TABLE OF CONTENTS	vi
LIST OF TABLES	ix
LIST OF FIGURES	x
CHAPTER 1: General Introduction	1
1.1 Background	1
1.2 Aims and objective of the study	8
1.3 Thesis outline	8
1.4 References	9
CHAPTER 2: Literature review	13
2.1 Introduction	13
2.2 Preparation and morphology	13
2.2.1 Phase change materials (PCMs)	13
2.2.2 Polyolefin/paraffin wax blends	16
2.2.3 Polyolefin/natural fibre composites	17
2.3 Thermal properties	20
2.3.1 Melting and crystallization	20
2.3.1.1 Phase change materials (PCMs)	20
2.3.1.2 Polyolefin/wax blends	22
2.3.1.3 Polyolefin/natural fibre composites	23
2.3.2 Thermal stability	24
2.3.2.1 Phase change materials (PCMs)	24
2.3.2.2 Polyolefin/wax blends	25
2.3.2.3 Polyolefin/natural fibre composites	26

2.4	Thermo-mechanical and mechanical properties	26
2.4.1	Thermo-mechanical properties	26
2.4.1.1	Phase change materials (PCMs)	26
2.4.1.2	Polyolefin/natural fibre composites	28
2.4.2	Mechanical properties	28
2.4.2.1	Phase change materials (PCMs)	28
2.4.2.2	Polyolefin/wax blends	29
2.4.2.3	Polyolefin/natural fibre composites	30
2.5	Water absorption	31
2.5.1	Polyolefin/natural fibre composites	31
2.6	References	32
CHAPTER 3: Experimental		39
3.1	Materials	39
3.1.1	High density polyethylene	39
3.1.2	Waxes	39
3.1.3	Wood flour	39
3.1.4	Other chemicals	40
3.2	Methods	40
3.2.1	Wood four treatment	40
3.2.2	Blends and composites preparation	40
3.3	Analysis techniques	41
3.3.1	Scanning electron microscopy (SEM)	41
3.3.2	Differential scanning calorimetry (DSC)	42
3.3.3	Thermogravimetric analysis (TGA)	43
3.3.4	Dynamic mechanical analysis (DMA)	44
3.3.5	Tensile testing (TT)	45
3.3.6	Water absorption (WA)	45
3.4	References	46
CHAPTER 4: Results and discussion		48
4.1	Scanning electron microscopy (SEM)	48

4.2	Differential scanning calorimetry (DSC)	52
4.2.1	HDPE/M3 wax blends and HDPE/WF/M3 wax composites	52
4.2.2	HDPE/H1 wax blends and HDPE/WF/H1 wax composites	62
4.3	Thermogravimetric analysis (TGA)	68
4.3.1	HDPE/M3 wax blends and HDPE/WF/M3 wax composites	69
4.3.2	HDPE/H1 wax blends and HDPE/WF/H1 wax composites	73
4.4	Dynamic mechanical analysis (DMA)	75
4.4.1	HDPE/M3 wax blends and HDPE/WF/M3 wax composites	76
4.4.2	HDPE/H1 wax blends and HDPE/WF/H1 wax composites	79
4.5	Tensile testing	82
4.5.1	HDPE/M3 wax blends and HDPE/WF/M3 wax composites	82
4.5.2	HDPE/H1 wax blends and HDPE/WF/H1 wax composites	88
4.6	Water absorption (WA)	92
4.7	References	97
CHAPTER 5: Conclusions		100
5.1	HDPE/WF composites	100
5.2	HDPE/M3 wax blends and HDPE/WF/M3 wax composites	101
5.3	HDPE/H1 wax blends and HDPE/WF/H1 wax composites	104
ACKNOWLEDGEMENTS		108
APPENDICES		109

LIST OF TABLES

	Page
Table 3.1 Sample ratios used for the preparation of the different blends and composites	41
Table 4.1 Summary of DSC results for HDPE/M3 wax blends and HDPE/WF/M3 wax composites	54
Table 4.2 Summary of DSC results for HDPE/H1 wax blends and HDPE/WF/H1 wax composites	64
Table 4.3 Summary of TGA results of HDPE/M3 wax blends and HDPE/WF/M3 wax composites samples	70
Table 4.4 Summary of TGA results of HDPE/H1 wax blends and HDPE/WF/H1 wax composites samples	75
Table 4.5 Summary of tensile results for HDPE/M3 wax blends and HDPE/WF/M3 wax composites	84
Table 4.6 Summary of tensile results for HDPE/H1 wax blends and HDPE/WF/H1 wax composites	89
Table 4.7 Summary of results for water absorption of HDPE/WF/M3 wax and HDPE/WF/H1 wax composites	94

LIST OF FIGURES

	Page	
Figure 1.1	Classification of phase change materials (PCMs)	2
Figure 1.2	Schematic representation of a temperature-time graph	4
Figure 3.1	Dumb-bell shaped tensile testing sample	45
Figure 4.1	SEM micrographs of 80/20 w/w HDPE/WF (alkaline treated) Composite	48
Figure 4.2	SEM micrographs of 70/20/10 w/w HDPE/WF/M3 wax (a & b), 50/20/30 w/w HDPE/WF/M3 wax (c & d), and 30/20/50 w/w HDPE/WF/M3 wax (e & f) composites	49
Figure 4.3	SEM micrographs of 70/20/10 w/w HDPE/WF/H1 wax (a & b), 50/20/30 w/w HDPE/WF/H1 wax (c & d), and 30/20/50 w/w HDPE/WF/H1 wax (e & f) composites	51
Figure 4.4	DSC heating curves of HDPE, M3 wax and the HDPE/M3 wax blends	53
Figure 4.5	Comparison of experimental and calculated melting enthalpies of the M3 wax melting as a function of wax content in HDPE/M3 wax blends	85
Figure 4.6	Comparison of experimental and calculated melting enthalpies of the HDPE melting as a function of wax content in HDPE/M3 wax blends	55
Figure 4.7	DSC heating curves of HDPE and the HDPE/WF composites	56
Figure 4.8	Comparison of experimental and calculated melting enthalpies of the HDPE melting as a function of WF content in HDPE/WF composites	56
Figure 4.9	DSC heating curves of HDPE/WF/M3 wax PCM composites at 10% WF content	59
Figure 4.10	DSC heating curves of HDPE/WF/M3 wax PCM composites at 20% WF content	59
Figure 4.11	Comparison of experimental and calculated melting enthalpies	60

	of the M3 wax melting as a function of wax content in HDPE/10% WF/M3 wax composites	
Figure 4.12	Comparison of experimental and calculated melting enthalpies of the M3 wax melting as a function of wax content in HDPE/20% WF/M3 wax composites	60
Figure 4.13	Comparison of experimental and calculated melting enthalpies of the HDPE melting as a function of wax content in HDPE/10% WF/M3 wax composites	61
Figure 4.14	Comparison of experimental and calculated melting enthalpies of the HDPE melting as a function of wax content in HDPE/20% WF/M3 wax composites	62
Figure 4.15	DSC heating curves of HDPE, H1 wax and the HDPE/H1 wax blends	63
Figure 4.16	Comparison of experimental and calculated melting enthalpies as a function of wax content in HDPE/H1 wax blends	65
Figure 4.17	DSC heating curves of HDPE, the HDPE/WF composite and the HDPE/WF/H1 wax composites at 10% WF content	66
Figure 4.18	DSC heating curves of HDPE, the HDPE/WF composite and the HDPE/WF/H1 wax composites at 20% WF content	66
Figure 4.19	Comparison of experimental and calculated melting enthalpies as a function of wax content in HDPE/10% WF/H1 wax composites	67
Figure 4.20	Comparison of experimental and calculated melting enthalpies as a function of wax content in HDPE/20% WF/H1 wax composites	68
Figure 4.21	TGA curves of HDPE, H1 wax, M3 wax and alkali-treated WF	69
Figure 4.22	TGA curves of the HDPE/M3 wax blends	71
Figure 4.23	TGA curves of HDPE/WF composites	71
Figure 4.24	TGA curves of HDPE/10% WF/M3 wax composites	72
Figure 4.25	TGA curves of HDPE/20% WF/M3 wax composites	72
Figure 4.26	TGA curves of the HDPE/H1 wax blends	73
Figure 4.27	TGA curves of HDPE/10% WF/H1 wax PCM composites at various wax contents	74
Figure 4.28	TGA curves of HDPE/20% WF/H1 wax PCM composites at various wax contents	74
Figure 4.29	DMA storage modulus curves for the HDPE/M3 wax blends	76

Figure 4.30	DMA loss modulus curves of HDPE/M3 wax blends	77
Figure 4.31	DMA storage modulus curves for HDPE/WF/M3 wax composites	78
Figure 4.32	DMA loss modulus curves for HDPE/WF/M3 wax composites	79
Figure 4.33	DMA storage modulus curves for the HDPE/H1 wax blends	80
Figure 4.34	DMA loss modulus curves for the HDPE/H1 wax blends	80
Figure 4.35	DMA storage modulus curves for HDPE/WF/H1 wax composites	81
Figure 4.36	DMA loss modulus curves for HDPE/WF/H1 wax composites	82
Figure 4.37	Young's modulus of HDPE/M3 wax blends and HDPE/WF/M3 wax composites as function of wax content	83
Figure 4.38	Stress at break of HDPE/M3 wax blends and HDPE/WF/M3 wax composites as function of wax content	85
Figure 4.39	Elongation at break of HDPE/M3 wax blends and HDPE/WF/M3 wax composites as function of wax content	85
Figure 4.40	Young's modulus of HDPE/WF composites as function of WF content	86
Figure 4.41	Stress at break of HDPE/WF composites as function of WF content	86
Figure 4.42	Elongation at break of HDPE/WF composites as function of WF content	87
Figure 4.43	Young's modulus of HDPE/H1 blends and HDPE/WF/H1 wax composites as function of wax content	90
Figure 4.44	Stress at break of HDPE/H1 wax blends and HDPE/WF/H1 wax composites as function of wax content	91
Figure 4.45	Elongation at break of HDPE/H1 wax blends and HDPE/WF/H1 wax composites as function of wax content	92
Figure 4.46	Water absorption curves of HDPE/WF composites	93
Figure 4.47	Water absorption curves of HDPE/WF/M3 wax composites at 10 wt.% WF and various wax contents	95
Figure 4.48	Water absorption curves of HDPE/WF/M3 wax composites at 20 wt.% WF and various wax contents	95
Figure 4.49	Water absorption curves of HDPE/WF/H1 wax composites at 10 wt.% WF and various wax contents	96
Figure 4.50	Water absorption curves of HDPE/WF/H1 wax composites at 20 wt.% WF and various wax contents	96

Chapter 1: **General introduction**

1.1 Background

Phase change materials are substances with high heat of fusion and have the ability to store energy. Due to this capability, they absorb, store and release large quantities of energy. This is achieved by means of melting and solidifying at certain temperatures [1,2]. They are also known as energy storage materials or latent heat storage materials with considerably higher thermal energy storage densities in comparison with sensible heat storage materials. In order to store and release the heat, phase change materials utilize chemical bonds, and the energy transfer occurs when a material changes phase i.e. solid to liquid, or liquid to solid [3-5]. Phase change materials' capability to absorb, store and release large amounts of energy, are characteristics that form the basis to the various applications of PCMs.

There are desirable characteristics that phase change materials should possess in order to be utilized for thermal storage systems. These are thermo-physical, chemical, kinetic and economic properties. The thermo-physical properties include: high latent heat of fusion per unit volume, high specific heat capacity, high thermal conductivity and small vapour pressure at operation temperatures; chemical properties include: completely reversible freezing or melting cycles, no chemical decomposition, should be non-poisonous, non-flammable and non-explosive; kinetic properties include: high nucleation rate and high rate of crystal growth; and economic properties such as high abundance and low cost [3-6]. For the selection of materials as PCM latent heat storage systems, a careful consideration of these properties is necessary. This gives a more focused and informed choice, since there are numerous materials melting with high heat of fusion in any required temperature range [3]. These numerous materials have different classes each with its own advantages and disadvantages.

Phase change materials are classified into various categories. There are organic and inorganic compounds, as well as eutectic mixtures of these compounds, that all give different phase transition temperatures [3,5,7]. Figure 1.1 gives a schematic representation of the classification of PCMs [5], with the aspects in bold showing the PCM category of interest in this study. The organic compounds include paraffin and non-paraffin compounds, whereas the inorganic category includes salt hydrates, metals and alloys. These organic, inorganic and

eutectics compounds have been a subject of research for the previous forty years [6,7]. Amongst these three classes of PCMs, organic compounds generally are the most broadly studied, and paraffin waxes in particular are of recent research interest due to their promising properties as phase change materials [2,8,9].

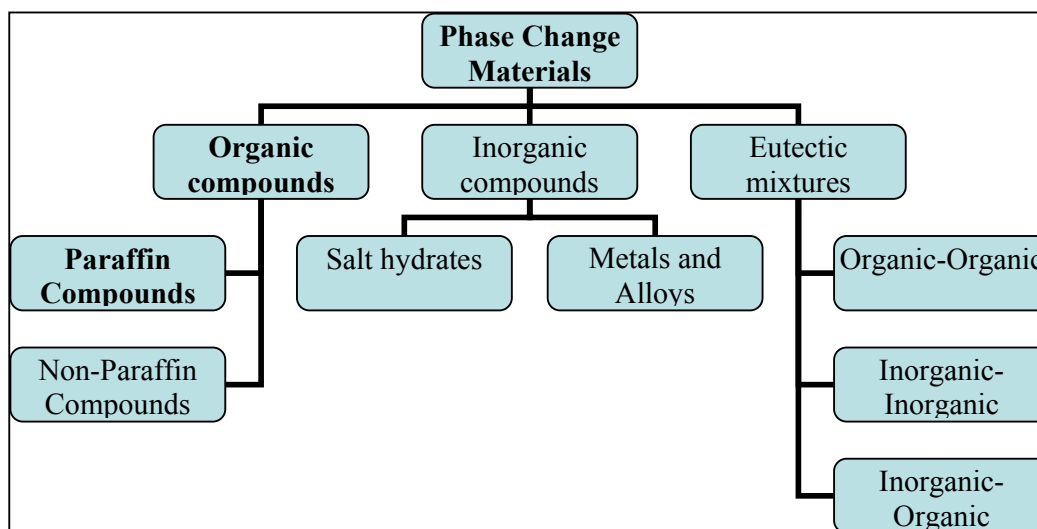


Figure 1.1 Classification of phase change materials (PCMs)

Paraffin waxes are saturated hydrocarbon mixtures that usually consist of a mixture of different alkanes. They are characterized by straight or branched carbon chains with generic formula C_nH_{2n+2} , and have melting temperatures ranging from 23 to 67 °C [9-12]. They are white, semi-transparent, tasteless and odourless solids with common properties such as smooth texture, water repellency, low toxicity, freedom from objectionable odour and colour. They are combustible and have good dielectric properties. They are soluble in benzene, ligroin, warm alcohol, chloroform and carbon disulfide, but insoluble in water and acids. They are used for the preparation of candles, paper coating, protective sealants for food products and beverages, glass cleaning preparations, hot-melt carpet backing, biodegradable mulch, lubricants, and stoppers for acid bottles, as well as electrical insulation [10-15]. They are used as phase change materials for thermal storage application, because they have most of the required properties. They have high latent heat of fusion, negligible super-cooling, low vapour pressure in the molten state, they are chemically inert, have chemical stability, are self-nucleating, commercially available, ecologically harmless, readily available and inexpensive [1,2,9,16]. Their specific heat capacity is about $2.1 \text{ kJ kg}^{-1} \text{ K}^{-1}$, and their enthalpy lies between

180 and 230 kJ kg⁻¹, quite high for organic materials. The combination of these two values results in an excellent energy storage density [1,2]. It is because of these desirable characteristics that paraffin waxes are used as PCMs in this study. Paraffin waxes are said to be conventional solid-liquid PCMs, and therefore not convenient to use directly as phase change materials [17-19]. This means that paraffin waxes need to be encapsulated in order to prevent, for instance, leakage of molten paraffin wax during a phase transition. They have low thermal conductivity [16,19] and large volume change during a phase transition [20]. The application of phase change materials has found importance in various systems from energy storage to thermal protection [1,2].

Phase change materials are of interest in many different applications. They are used as thermal energy storage medium, in areas of space craft, refrigeration and conditioning systems, conservation processes, solar energy systems, energy recovery, heating and cooling of buildings [6,9,16]. Additionally, they are used in thermal protection systems, as well as in active and passive cooling of electric devices [1,2]. To suit a given application, PCMs are selected on the basis of their melting temperature. Materials that melt at temperatures below 15 °C are used for the storage of coolness in air conditioning applications, whereas those melting above 90 °C are used for absorption refrigeration. All materials that melt at temperatures between these two can be applied in solar heating and load leveling applications [6]. Thermal energy storage (TES) is one of the most important areas of application of PCMs [1,2,7].

There are two ways in which heat can be stored. These are described as sensible heat storage (SHS) and latent heat storage (LHS). In sensible heat storage method, the temperature of a storage material varies with the quantity of energy stored. This is due to the rise in temperature of the storage medium without changing its state. It may be categorized, based on the heat storage media, as liquid media storage (water, thermal oil and molten salts) and solid media storage (rocks, bricks, dry and wet earth, and metals) [7,21]. In latent heat storage the energy is stored when a material changes from one state to another i.e. solid to liquid. It has a high-energy storage density and the capacity to store heat as latent heat of fusion at a constant temperature, which is the phase transition temperature of the phase change materials (PCMs) [7].

The phase transitions of the PCMs may be described in terms of changes in internal energy. An increase in internal energy, when energy in the form of heat is added to a material, may result in an increase in temperature (sensible heating) or change in state (latent heating) of a material. Figure 1.2 shows the schematic representation of temperature as a function of time with the accompanying transitions according to stages [3,22].

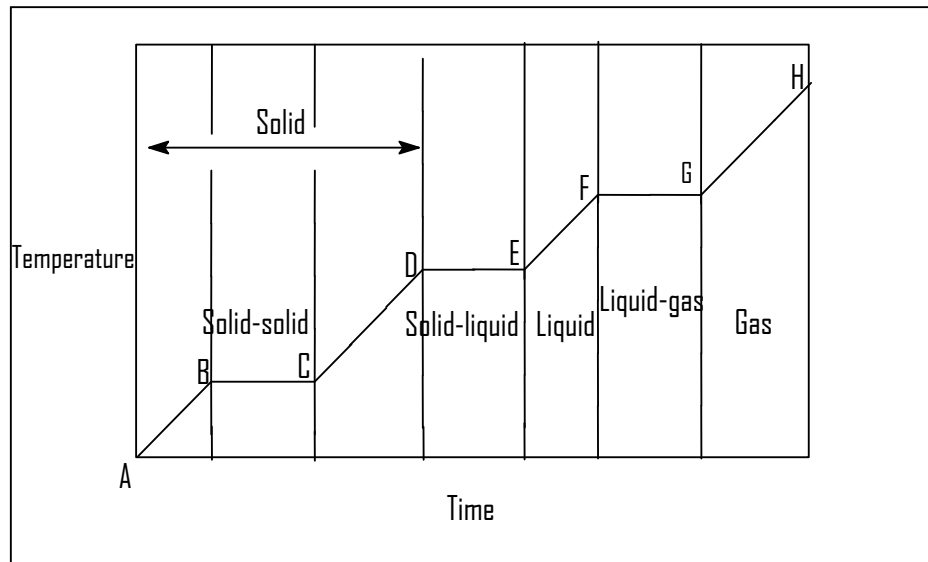


Figure 1.2 Schematic representation of a temperature-time graph

A solid phase is the starting state at point A, where the addition of heat results in a sensible heating of a solid material (A-B) without any change in state, which is followed by a solid-solid phase transition (B-C) that is brought about by a crystalline structural change due to latent heating. Sensible heating is again manifested (C-D) for the solid material, which is then followed by the latent heating given by a solid-liquid phase change (D-E). The material in the liquid state gains energy (sensible heating) and no phase change occurs (E-F), and as energy increases with time another phase change takes place (F-G) i.e. liquid-gas phase transition. This then leads to the stage where the sensible heating of a gaseous material results (G-H) [3,22]. It is clear from this that the energy storage of phase change materials is effected by a temperature change, and this phenomenon brings about the description of PCMs in terms of an increase in specific heat in a temperature range [23].

As seen from the schematic temperature-time representation in Figure 1.2, the latent heat may be categorized into solid-solid, solid-liquid, solid-gas and liquid-gas phase transition processes. Amongst these, the solid-gas and liquid-gas phase changes are not often employed for the storage of energy. This is due to the fact that gases occupy large volumes, thus making the system large, sophisticated and practically impossible. As for the solid-solid phase transition, heat is absorbed and stored as a material changes from one crystalline form to another. Generally, this system has small latent heat and is thus less interesting. Solid-liquid phase change of latent heat storage on the other hand, is of interest due to its high-energy storage density and the capacity to store energy as latent heat of fusion at a constant temperature, and this relates to phase change materials [3,7]. Solid-liquid phase change materials such as paraffin waxes are of particular research interest for latent heat storage. However, it is inconvenient to use them directly as PCMs due to leaking of molten material during a phase change, and they therefore need to be encapsulated to prevent this [1,2,3,7].

There are different ways in which encapsulation of phase change materials can be achieved. The known methods of encapsulation are phase change materials in concrete or gypsum wallboards (*PCM-Concrete/Gypsum Wallboards*), phase change materials in graphite or metal (*PCM-Graphite/Metal*), and phase change materials in polymers (*PCM-Polymer*) [24].

- The *PCM-Concrete/Gypsum Wallboards* encapsulation method can be achieved in several ways, such as encapsulation of a PCM by a polymer first and then mixing it with concrete, the direct impregnation of a concrete with the PCM, and spraying a PCM on a concrete or gypsum wallboard. This could be used to replace thick expensive walls that act as a buffer for temperature variations, as well as in floor panels together with under-floor heating systems in buildings. There are limitations inherent to these ways. A long time is required for the concrete to be immersed into a PCM, loss of some PCM out of the concrete during thermal cycling, and flammability of the storage unit if too much of PCM (e.g. paraffin wax) is contained in a system. However, to avoid flammability and leaking of a PCM out of concrete, macro as well as micro-encapsulations may be applied. Macro-encapsulation is usually done with polymers, whereas micro-encapsulation could be done in tubes or in balls [24].
- The *PCM-Graphite/Metal* encapsulation method is used mainly to achieve high thermal conductivity of a storage unit [16,19]. In using a material such as graphite with a good thermal conductivity ($150 \text{ Wm}^{-1}\text{K}^{-1}$) to encapsulate a PCM with low thermal conductivity such as a paraffin wax ($0.24 \text{ Wm}^{-1}\text{K}^{-1}$), a composite with high

thermal conductivity could result. This is achieved when a porous graphite matrix is impregnated by immersion into molten paraffin wax. The disadvantages of a graphite matrix are high anisotropy with respect to thermal conductivity, and the lowering of the specific latent heat of fusion. A PCM could also be brought into a porous metal matrix and a highly thermal conductive storage unit is formed, since metals are conductive in nature. However, most metals have an unacceptable high density, which then makes them less interesting in this field [24].

- The *PCM-Polymer* containment method has been significantly researched and proves to be a very good encapsulation possibility for all kinds of PCMs, especially paraffin waxes. The rising interest on this kind of encapsulation is primarily due to polymers having low density, not rusting, being easy to manufacturing and less costly. These composites have a high thermal storage capacity and a low density, thus opening the possibility of various applications. They could be used, for instance, in building materials in the form of panels, in fabrics in the form of fibres, as food or beverage containers, and to be mixed into heat transfer fluid in the form of pellets. There are three possibilities of encapsulating a PCM with polymer matrix. The first is the mixing of an inorganic hydrate PCM into a polymer before the latter is cross-linked. A second possibility is the blending of a polymerizable material with an inorganic hydrate, whereby a polymer is then chemically cross-linked in solution, in which both constituents are dissolved. The third one is the formation of a polymer matrix that is cross-linked and capable of absorbing a molten PCM such as paraffin wax. All these possibilities are plagued by cross-linking, which requires significant quantities of energy (in the case of electron beam cross-linking) and a lot of time [24]. Recently, researchers had come up with a simple and straight-forward possibility, where a PCM is encapsulated with a polymer that is not cross-linked. The blending of polymers with PCMs has received research attention due to its ease of recycling, its non-toxic nature, no need for a lot of energy to create blends, and because they are readily available and relatively cheap. The best candidate for this *PCM-Polymer* encapsulating possibility is the blending of polyolefins with paraffin waxes [1,2,16,19].

Blending of existing polymers reduces the need for synthesis of new materials. It is often a quicker and less expensive system than the development of new polymers. A number of blend systems have been developed and commercialized. These may be both mechanical blends of two or more constituents, or a chemical combination of various monomers, grafted

copolymers and others. Amongst all the polymer families, the polyolefins is the widest used family in industry [10]. There are factors that generally influence the final properties of the blends, viz. physical and chemical properties, morphology of pure components, ratios in a blend, processing methods and the interaction amongst the constituents. The blending of polyolefins, especially polyethylenes and polypropylene, with paraffin waxes has been studied over the past years, mostly by Luyt and co-workers [10-14,25]. They concentrated on the determination of the mechanical and thermal properties as function of wax content in these blends. Some work has also been done on the blending of polyolefins with paraffin waxes as PCMs, and their morphology, thermal and thermo-mechanical properties have been investigated, but not much has been done on their mechanical properties (e.g. tensile strength). Polymer matrices such as polyolefins (PP, LDPE and HDPE) and thermoplastic elastomers [poly(styrene-butadiene-styrene)] have been investigated [1,2,16,19]. Amongst the polyolefins, HDPE has shown good quality performance as supporting material for paraffin waxes due to its structural strength and high crystallization [16,26,27]. Generally the mechanical properties and thermal stabilities of polyolefins decrease as the wax content increases. Since the storage capacity of a PCM depends on the wax content, it is necessary to have high wax contents in the polymer matrix, which gives rise to products with unacceptably poor mechanical properties [19,25,28]. This problem could be solved with the inclusion of a natural filler which may improve the strength and thermal stability of the PCMs [29].

A filler is a material that is added to a plastic in order to modify its strength and working properties, or sometimes to lower its cost. It may also give rise to high heat resistance, high mechanical strength, low moisture absorption, and good electrical characteristics. Fillers are abundantly available at low cost. They are required to be compatible with polymers and other additives, and should not have abrasive or chemical action on the mould. They are classified into: cellulosic products (wood and cotton), carbon, inorganic materials (silica), silicates (asbestos and clay), glass, metals, metal oxides (alumina and zinc oxides), and even synthetic fibres (nylon and polyesters). Fillers are normally used in large quantities. Fibrous fillers are said to greatly enhance the mechanical properties of the polymers, since their reinforcement is much more effective than that of spherical fillers. This effect of fibrous filler depends on the fibre length and the interfacial bond between it and the continuous resin matrix [30]. Amongst these categories of fillers, cellulosic products are of particular interest due to the advantages they offer, such as relative good properties and lower costs as well as environmental friendliness [29]. These cellulosic fibres are natural fibres originating from plants, and are

termed plant fibres. Wood fibre is well suited to use as a filler in polymers, especially polyethylene, due to its low density, high specific stiffness and strength, and low cost. It is also recyclable and biodegradable, and composite processing is easy with minimum abrasion of equipment compared to inorganic fillers [31-38]. With this in mind, wood flour was chosen as reinforcing filler in this study. However, there are drawbacks adherent to natural fibre as thermoplastic filler viz. poor interfacial adhesion between the hydrophobic polymer and the hydrophilic wood filler, and high water uptake that could be overcome [31,35].

These drawbacks can be overcome in two ways [31]. These are physical and chemical methods of fibre surface modification. The physical methods include stretching, calendaring, thermo-treatment, and the production of hybrid yarns. The chemical methods include change of surface tension using stearic acids and silane coupling agents, as well as sodium hydroxide, maleic anhydride, urethane derivatives of polypropylene glycol (PPG), permanganate, impregnation of fibre, chemical coupling (graft copolymerization), treatment with compounds containing methanol groups, treatment with isocyanates, and organosilanes as coupling agents [31,32]. Several studies were carried out on polymer-cellulosic fibre composites, especially polyolefins, and biodegradable polymers as matrices [33,36-42].

1.2 Aims and objectives

The aims of this study are (a) to investigate whether the incorporation of natural filler (wood flour) in PCM blends could improve their mechanical properties and thermal stability, and (b) to compare the performance of two types of paraffin wax as PCMs in an HDPE matrix. The objectives are therefore: (i) to develop shape-stabilized PCMs with two different paraffin waxes in HDPE, (ii) to chemically modify wood flour in order to improve interfacial adhesion with the polymer and/or wax, and (iii) to characterize these blend composites in terms of their morphology, as well as thermal, mechanical, thermo-mechanical, and water absorption properties.

1.3 Thesis outline

The outline of this thesis is as follows:

- Chapter 1: General introduction

- Chapter 2: Literature review
- Chapter 3: Experimental
- Chapter 4: Results and discussion
- Chapter 5: Conclusions

1.4 References

1. I. Krupa, G. Miková, A.S. Luyt. Polypropylene as a potential matrix for the creation of shape stabilized phase change materials. *European Polymer Journal* 2007; 43:895-907.
2. I. Krupa, G. Miková, A.S. Luyt. Phase change materials based on low-density polyethylene/paraffin wax blends. *European Polymer Journal* 2007; 43:4695-4705.
3. A.F. Regin, S.C Solanki, J.S. Saini. Heat transfer characteristics of thermal energy storage system using PCM capsules: A review. *Renewable and Sustainable Energy Reviews* 2008; 12:2438-2458.
4. V.V. Tyagi, D. Buddhi. PCM thermal storage in buildings: A state of art. *Renewable and Sustainable Energy Reviews* 2007; 11:1146-1166.
5. A. Sharma, V.V. Tyagi, C.R. Chen, D. Buddhi. Review on thermal energy storage with phase change materials and applications. *Renewable and Sustainable Energy Reviews* 2009; 13:318-345.
6. M.M. Farid, A.M. Khudhair, S.A.K. Razack, S. Al-Hallaj. A review on phase change energy storage: materials and applications. *Energy Conversion and Management* 2004; 45:1597-1615.
7. S.M. Hasnain. Review on sustainable thermal energy storage technologies, Part I: Heat storage materials and techniques. *Energy Conversion and Management* 1998; 39(11):1127-1138.
8. M. Kenisarin, K. Mahkamov. Actual problems in using phase-change materials to store solar energy. Paper presented at NATO Advanced Study Institute Summer School on Thermal Energy Storage for Sustainable Energy Consumption (TESSEC), June 6-17, 2005 Çeşme, Izmir, Turkey.
9. M. Akgün, O. Aydin, K. Kaygusuz. Experimental study on melting/solidification characteristics of a paraffin as PCM. *Energy Conversion and Management* 2007; 48:669-678.
10. I. Krupa, A.S. Luyt. Thermal properties of uncross-linked and cross-linked LLDPE/wax blends. *Polymer Degradation and Stability* 2000; 70:111-117.

11. M.J. Hato, A.S. Luyt. Thermal fractionation and properties of different polyethylene/wax blends. *Journal of Applied Polymer Science* 2007; 104:2225-2236.
12. I. Krupa, A.S. Luyt. Physical properties of blends of LLDPE and an oxidized paraffin wax. *Polymer* 2001; 42:7285-7289.
13. I. Krupa, A.S. Luyt. Thermal properties of polypropylene/wax blends. *Thermochimica Acta* 2001; 372:137-141.
14. T.N. Mtshali, I. Krupa, A.S. Luyt. The effect of cross-linking on the thermal properties of LDPE/wax blends. *Thermochimica Acta* 2001; 380:47-54.
15. J.C. Crause, I. Nieuwoudt. Paraffin wax fractionation: state of the art vs. supercritical fluid fractionation. *Journal of Supercritical Fluids* 2003; 27:39-54.
16. A. Sari. Form-stable paraffin/high density polyethylene composites as solid-liquid phase change material for thermal energy storage: preparation and thermal properties. *Energy Conversion and Management* 2004; 45:2033-2042.
17. L. Xing, L. Hongyan, W. Shujun, Z. Lu, C. Hua. Preparation and thermal properties of form stable paraffin phase change material encapsulation. *Energy Conversion and Management* 2006; 47:2515-2522.
18. L. Xing, L. Hongyan, W. Shujun, Z. Lu, C. Hua. Preparation and thermal properties of form-stable paraffin phase change material encapsulation. *Solar Energy* 2006; 80:1561-1567.
19. M. Xiao, B. Feng, K. Gong. Preparation and performance of shape stabilized phase change thermal storage materials with high thermal conductivity. *Energy Conversion and Management* 2002; 43:103-108.
20. A. Elgafy, K. Lafdi. Effect of carbon nanofiber additives on thermal behavior of phase change materials. *Carbon* 2005; 43:3067-3074.
21. H.E.S. Fath. Technical assessment of solar thermal energy storage technologies. *Renewable Energy* 1998; 14(1-4):35-40.
22. U. Stritih, P. Novak. Thermal storage of solar energy in the wall for building ventilation. IEA, ECES IA Annex 17, Advanced thermal energy storage techniques- Feasibility studies and demonstration projects 2nd Workshop, 3-5 April 2002, Ljubljana, Slovenia.
23. G. Hed. Service life estimation in the design of a PCM based night cooling systems. Doctoral Thesis, Gavle, Sweden, October 2005
24. M. Bader. Microencapsulated paraffin in polyethylene for thermal energy storage. The University of Auckland, New Zealand, February 2002.

25. S.P. Hlangothi, I. Krupa, V. Djoković, A.S. Luyt. Thermal and mechanical properties of cross-linked and uncross-linked linear low-density polyethylene-wax blends. *Polymer Degradation and Stability* 2003; 79:53-59.
26. H. Inaba, P. Tu. Evaluation of thermophysical characteristics on shape-stabilized paraffin as a solid-liquid phase change material. *Heat and Mass Transfer* 1997; 32:307-312.
27. Y. Hong, G. Xin-shi. Preparation of polyethylene-paraffin compound as a form-stable solid-liquid phase change material. *Solar Energy Materials & Solar Cells* 2000; 64:37-44.
28. U. Beginn. Applicability of frozen gels from ultra high molecular weight solid/liquid phase change materials. *Macromolecular Materials and Engineering* 2003; 288:245-251.
29. Y. Zhao, K. Wang, F. Zhu, P. Xue, M. Jia. Properties of poly(vinyl chloride)/wood flour/montmorillonite composites: Effects of coupling agents and layered silicate. *Polymer Degradation and Stability* 2006; 91:2874-2883.
30. P. Bahadur, N.V. Sastry. *Principles of Polymer Science*, 2nd edition, Alpha Science International Ltd. Oxford UK, 2006.
31. A.K. Bledzki, J. Gassan. Composites reinforced with cellulose based fibers. *Progress in Polymer Science* 1999; 24:221-274.
32. P.V. Joseph, K. Joseph, S. Thomas. Effect of processing variables on the mechanical properties of sisal-fiber-reinforced polypropylene composites. *Composites Science and Technology* 1999; 59:1625-1640.
33. J.Z. Lu, Q. Wu, I.I. Negulescu. Wood-fiber/high-density polyethylene composites: coupling agent performance. *Journal of Applied Polymer Science* 2005; 96:93-102.
34. M. Bengtsson, K. Oksman. The use of silane technology in crosslinking polyethylene/wood flour composites. *Composites: Part A* 2006; 37:752-765.
35. J-P. Kim, T-H. Yoon, S-P. Mun, J-M. Rhee, J-S. Lee. Wood-polyethylene composites using ethylene-vinyl alcohol copolymer as adhesion promoter. *Bioresource Technology* 2006; 97:494-499.
36. M. Bengtsson, P. Gatenholm, K. Oksman. The effect of crosslinking on the properties of polyethylene/wood flour composites. *Composites Science and Technology* 2005; 65:1468-1479.

37. S-M. Lai, F-C. Yeh, Y. Wang, H-C. Chan, H-F. Shen. Comparative study of maleated polyolefins as compatibilizers for polyethylene/wood flour composites. *Journal of Applied Polymer Science* 2003; 87:487-496.
38. M. Morreale, R. Scaffaro, A. Maio, F.P. La Mantia. Effect of adding wood flour to the physical properties of a biodegradable polymer. *Composites: Part A* 2008; 39:503-513.
39. A.K. Bledzki, M. Letman, A. Viksne, L. Rence, A comparison of compounding processes and wood type for wood fiber-PP composites. *Composites: Part A* 2005; 36:789-797.
40. X. Colom, F. Carrasco, P. Pagès, J. Cañavate. Effects of different treatments on the interface of HDPE/lignocellulosic fiber composites. *Composites Science and Technology* 2003; 63:161-169.
41. B. Li, J. He. Investigation of mechanical property, flame retardancy and thermal degradation of LLDPE-wood-fiber composites. *Polymer Degradation and Stability* 2004; 83:241-246.
42. N.E. Marcovich, M.A. Villar. Thermal and mechanical characterization of linear low-density polyethylene/wood flour composites. *Journal of Applied Polymer Science* 2003; 90:2775-2784.

Chapter 2: Literature review

2.1 Introduction

A lot of work has been done on the investigation of phase change materials [1-19], polymer-paraffin wax blends [20-29] and polymer-natural fibre composites [30-73]. The most important aspects from these publications are summarized under: (i) preparation and morphology, where the sample preparation methods used by the different authors are summarized and compared, and where the different observed morphologies are presented; (ii) thermal properties, where the melting and crystallization characteristics as well as thermal stability of the samples studied in literature are reported; (iii) mechanical and thermo-mechanical behaviour, in which the tensile and dynamic mechanical properties are reviewed; and (iv) water absorption by natural fibre composites. Each of these sections is sub-divided into sub-sections covering (i) phase change materials, (ii) polyolefin/paraffin wax blends, and (iii) polyolefin/natural fibre composites. The reason for this sub-division is that the work reported in this thesis was done on phase change materials based on polyethylene mixed with wax (PCM) and wood flour (reinforcement).

2.2 Preparation and morphology

2.2.1 Phase change materials (PCMs)

The preparation and characterization of phase change material (PCM) blends and/or composites have been a subject of research for the past four or five decades. The research in this field has led to recent formulations of form-stable or shape-stabilized PCMs. The phase change materials such as paraffin waxes were blended with higher melting temperature polymeric matrices such as polyolefins. The dispersed wax phase within the continuous polymeric phase served as PCM. It was generally found that there was no leakage of molten PCMs from the blends during the melting of the PCM. This was due to the ability of the polymers, with higher melting temperature, to encapsulate the PCMs and keep the form/shape of the blends and/or composites intact. Thus the blends and/or composites were termed form-stable or shape-stabilized PCMs [1-5,8]. These form-stable PCMs fall into two categories: solid-solid (sensible heat storage material) and solid-liquid (latent heat storage material)

PCMs. The first category involves certain molecular crystals that undergo solid state crystal transformations. This is accompanied by the absorption and releasing of enough heat throughout the application temperature range. The second category includes PCMs dispersed into materials with high melting points as supporting materials. The compound material is capable of keeping its shape, even when the PCM transforms from the solid to the liquid state, as long as the operating temperature range of the dispersed material is below the melting point of the supporting material [3,6,8]. These PCMs are encapsulated by various materials, such as polymeric matrices, for possible use as form-stable thermal energy storage blends and/or composites [1,2,9]. This is the focus category of this study due to the use of paraffin waxes as solid-liquid PCMs dispersed in the polyethylene (HDPE) matrix.

There are a variety of polymer matrices for solid-liquid PCM encapsulation, with a broad range of chemical and mechanical characteristics. These include thermoplastics such as polypropylene (PP), high-density polyethylene (HDPE), ultra high molecular weight polyethylene (UHMW-PE), low-density polyethylene (LDPE), as well as thermoplastic elastomers such as styrene-butadiene-styrene (SBS) and styrene-ethylene-butylene-styrene (SEBS) and thermosets such as bisphenol-A epoxy. Solid-liquid PCM-polymer encapsulated blends or composites may be prepared through various methods such as melt-mixing, extrusion and injection moulding for thermoplastics and two-roll mill mixing for thermoplastic elastomers, as well as reaction injection moulding for thermosets [1-7,9]. However, the focus of this review will be primarily on thermoplastics (polyolefin) based PCM blends and/or composites.

Polyolefin/paraffin wax PCMs were investigated as possible shape-stabilized PCMs [1-3,5-7,11-14]. Due to its structural strength and high melting temperature, high density polyethylene (HDPE) was the mostly preferred and studied polymer matrix for the encapsulation of solid-liquid PCMs. Sari [3], Inaba and Tu [5] and Hong and Xin-shi [6] investigated HDPE/paraffin form-stable PCM blends. Sari [3] used two kinds of technical grade paraffin with different melting points; Inaba and Tu [5] used paraffin consisting mainly of pentacosane, whereas Hong and Xin-shi [6] used both refined and semi-refined paraffins of different melting points. In all three studies the blends were prepared by a melt-mixing method. The SEM results of these investigations showed that the paraffin was well dispersed into the net-like crystal structure of HDPE. This net-like crystal structure of HDPE is said to be capable of preventing any leakage of molten paraffin during the heat storage process.

The structure, flame retardant properties and thermal stability of HDPE/paraffin form-stable PCMs and composites were investigated by Cai *et al.* [11-14]. In these studies they used commercial grade paraffins with different melting temperatures and latent heats. In all these cases the samples were prepared by an extrusion method (using a twin-screw extruder) in the temperature range of 120-170 °C. Different flame retardant systems were used with HDPE/paraffin/organophilic montmorillonite (OMT) hybrids [11], HDPE/paraffin/expanded graphite (EG) composites [12], and HDPE/paraffin hybrids [14]. However, the preparation of the HDPE-poly(ethylene-co-vinyl acetate) (EVA)/OMT nano-composites [13] was achieved by an extrusion method as the first step, followed by pelletization and drying. These nano-composites were then mixed with the paraffin through extrusion (using a twin-screw extruder). The SEM results showed that the paraffin, in all these studies, was well dispersed in the net-like crystal structure of the HDPE, the HDPE/expanded graphite composites and the HDPE-EVA/OMT nano-composites. Furthermore, there was no effect on the structure as a result of the additives, and the flame retardants were well dispersed in the matrices with no remarkable observation of agglomerations [11,12,14]. The XRD results of the hybrid composites showed that there was intercalation of the paraffin into the silicate layers of the OMT [11]. Both the XRD and TEM results showed the formation of an ordered intercalated nano-morphology in the HDPE-EVA/OMT nano-composites [13].

Krupa *et al.* [1,2] blended isotactic polypropylene (PP) and low density polyethylene (LDPE) respectively with a soft petroleum wax (Wax S) and a hard oxidized Fischer-Tropsch paraffin wax (Wax FT). In both studies, the blends were prepared by a melt-mixing method. The SEM results from both studies showed that these polyolefin/paraffin wax PCM blends were immiscible. The extent of immiscibility and/or phase separation observed for both waxes with the two polymer matrices differed remarkably in that the Wax FT blends were less immiscible than those containing Wax S.

Luyt and Krupa [18] used an oxidized hard Fischer-Tropsch paraffin wax in an epoxy resin matrix as shape-stabilized PCM. This was prepared by mechanical mixing of the wax powder with the liquid resin at room temperature, followed by curing the samples using UV. The SEM results demonstrated the presence of spherical wax particles in the epoxy resin matrix. These were also observed even after heating the sample to a temperature above the melting point of wax, and cooling. It was concluded that the wax distribution was fairly heterogeneous

at low wax contents, but the homogeneity improved with increased wax content. However, the wax and the epoxy resin had poor interaction.

2.2.2 Polyolefin/paraffin wax blends

Blending of polymers is a promising method of obtaining materials with practical importance for various applications. Since the blended constituents have different chemical compositions and physical properties, materials with improved properties can result. Polyolefin/paraffin wax blends, for instance, have good processability properties compared to pure polyolefins due to wax acting as a processing agent. The preparation of these blends is mostly based on extrusion, mechanical mixing and melt-mixing methods. Each method of preparation gives relatively different characteristics to the final materials [20-29]. To investigate the morphology of polymer blends, methods such as differential scanning calorimetry (DSC), dynamic mechanical thermal analysis (DMTA) and transmission electron microscopy (TEM) may be employed [20]. DSC had been used, *inter alia*, to establish the miscibility properties of the polymer/wax blends.

Several thermoplastic matrices such as polyolefins were blended with various grades of wax. Polyethylenes and polypropylene (PP) belong to the most studied matrices [20-29]. Krupa and Luyt [21,22] prepared blends of normal hard Fischer-Tropsch paraffin wax with PP and LDPE by using melt extrusion. The PP/wax blends [21] (with 5-30% wax content) were homogeneous on a macro-scale only at wax contents of less than 10%. Clear phase separation was observed at higher wax contents. The LDPE/wax blends [22] were found to be miscible at low wax contents (10 and 20%), while phase separation was observed at higher contents. The SEM results showed that at high wax contents the blends had some rupture along different lines.

The influence of different kinds of paraffin wax and processing methods on different types of polyethylenes was also investigated. Krupa and Luyt [23] studied linear low-density polyethylene (LLDPE)/hard oxidized paraffin wax blends. The constituents (in a powder form) were mechanically mixed followed by melt pressing at 160 °C. It was observed that the blends were miscible in the crystalline phase for all the tested compositions. A similar study was conducted by Hato and Luyt [24] who focused on the properties of different polyethylenes (HDPE, LLDPE and LDPE) blended with two different types of paraffin wax.

The blends were prepared by melt mixing using a Brabender Plastograph at 160 °C (HDPE), 150 °C (LLDPE) and 140 °C (LDPE). It was established that the HDPE containing blends were completely miscible up to 20% wax, above which partial miscibility was observed. For the LLDPE and LDPE containing blends the different waxes showed different miscibilities with the polymer. Regardless of the processing methods, LLDPE and hard oxidized paraffin wax showed similar miscibility tendencies in both studies. Mpanza and Luyt [25] studied the influence of different paraffin waxes as processing agents for low density polyethylene (LDPE). The waxes were blended with LDPE through melt mixing at 150 °C using a Brabender Plastograph. The DSC results revealed that the different waxes had different miscibilities with LDPE.

The morphology of polyethylene/wax blends was investigated for both uncross-linked and cross-linked systems. However, this review will only report on uncross-linked systems. Krupa and Luyt [20,26] prepared these systems and investigated their mechanical and thermal properties. These blends were prepared by mechanically mixing LLDPE powder and a hard Fischer-Tropsch paraffin wax. The mixed components were then melt pressed at different temperatures to form sheets. The miscibility of the blends was characterized using the log-additive rule and the fact that the melt flow rate and melt viscosities are related. Calculations based on these results show that the LLDPE/wax blends were mutually miscible in the observed concentration region [20]. Krupa and Luyt [26] reported on the uncross-linked LLDPE/wax blend system and observed miscibility in the crystalline phase. Mtshali *et al.* [27] observed that LDPE/hard Fischer-Tropsch paraffin wax blends were only miscible at low wax contents (up to 10%). Hlangothi *et al.* [28] found that LLDPE/hard Fischer-Tropsch paraffin wax blends showed co-crystallization and therefore miscibility.

2.2.3 Polyolefin/natural fibre composites

Polyolefin/natural fibre composites were generally prepared through solution mixing, extrusion, injection and compression moulding, roll-milling and melt mixing [31-47]. These methods differ in terms of their operating principles and processing parameters, which may lead to relatively different properties of the prepared composite materials. Polyolefins were studied as composite material matrices with a wide range of natural fibres/fillers used as polymer reinforcements. These natural fibres/fillers include abaca, alfa, bagasse, bamboo, banana, cane trash, coir, cotton, flax, hemp, henequen, jute, kapok, kenaf, kraft, maize, olive

stone flour, pineapple, ramie, rice starch, sago, silk, sisal, tapioca, wood (fibres and flour), and wool [36,37,47]. The following section will focus on the non-treated natural fibre composites, whereas the treated composites will be discussed later.

The preparation and morphology analysis of unmodified natural fibre/HDPE composites was carried out by a number of researchers [34,35,38,48-53]. Bengtsson *et al.* [34], Lai *et al.* [35], Wang *et al.* [48] and Lu *et al.* [49,50] investigated composites based on high-density polyethylene (HDPE) and wood flour (WF). These composites were prepared through extrusion (using a co-rotating twin-screw extruder), as well as injection and melt moulding processes. The SEM results of the composites, in all these studies, showed that there is poor interfacial adhesion between WF and HDPE because of weak/low affinity between the polar natural fibre and non-polar thermoplastic matrix. This is informed by the presence of gaps between the HDPE matrix and natural fibre (WF), fibre pull-out producing holes with smooth walls on the polymer matrix, and a relatively smooth surface on the wood filler. Additionally, there was no continuous distribution of WF in the polymer matrix and the fibre particles were in direct contact with each other [50]. However, there was some part of the WF covered with plastic due to mechanical interlocking links [34,50]. Colom *et al.* [38] reported on aspen fibre-reinforced HDPE composites prepared through a Brabender roll mill and compression moulding. The SEM characterization of the non-treated composites suggested the existence of poor interfacial adhesion similar to the other studies [34,35,48-50].

LLDPE was reinforced with natural fibres and the composites were characterized for their morphology. Marcovich and Villar [40] and Kuan *et al.* [54] used WF, whereas Kim *et al.* [55] used saw dust to reinforce LLDPE. The composites were prepared through extrusion methods (a counter-rotating twin-screw [40] and co-rotating twin-screw extruder [54]) as well as melt blending [55]. The SEM results for all the studies showed the existence of fibre pull-outs, gaps and no polymer matrix coating around the filler surfaces. Similar to the previous studies on HDPE [34,35,38,48-50], the authors concluded that these indicated the existence of poor interfacial adhesion for non-treated LLDPE/natural fibre composites.

LDPE was also used as a matrix for natural fibres [45,53,56,57]. Viksne *et al.* [45] investigated the effect of paraffin on the fibre dispersion and mechanical properties of polyolefin-sawdust composites. HDPE, LDPE and recycled polyethylene waste (WPE) were used as matrices. Composites were prepared in a two-roll mill followed by compression and

injection moulding. The SEM results of the LDPE/WF composites showed poor interfacial adhesion between the components, and large WF aggregates were visible. However, the addition of paraffin into the LDPE/WF composites inhibited WF aggregate formation and it was difficult to distinguish WF from the polymer matrix.

PP has also been well studied as a matrix for polyolefin/natural fibre composites. Publications on these composites [46,53,58,59-65] focused on the improvement of interfacial adhesion between natural fibres and the PP matrix with the aid of various coupling agents. However, only non-treated composites are discussed in this section. Nygård *et al.* [58], Nachtigal *et al.* [59], Bengtsson *et al.* [60] and Bledzki *et al.* [63] reported on various natural fibres reinforced PP composites. Wood powder (WP) and wood (pulp and wallboard) [58], wood flour [59], bleached sulphite and kraft cellulose fibres (both from soft wood) [60] and abaca fibres compared with jute and flax reinforced PP composites [63] were used as PP reinforcements. These composite systems were prepared through extrusion [58,60], melt-mixing [59] and high speed cascade mixing with injection moulding [63] methods. The morphology characterization of these composites determined through SEM showed poor interfacial adhesion between natural fibres and thermoplastic PP matrices. Similar to the other polyolefins, the presence of gaps between fibres and PP matrices, fibre pull-outs resulting in voids and cavities and, in addition, a rough porous morphology were observed. Nygård *et al.* [58], however, observed that the WP was well distributed in the PP matrix. Bledzki *et al.* [63] observed fibre pull-outs, debonding as well as micro-cracks, and these were attributed to the local internal stress. Contrary to some of the studies [58-60], these authors observed strong adhesion between the abaca fibre and PP matrix for non-treated composite systems. However, they could not give an explanation for this behaviour which is normally only observed for coupled/treated composites [46,53,58-65]. Generally, most non-coupled/untreated natural fibres-polyolefin composites have poor interfacial adhesion, except for a rare case such as that of Bledzki *et al.* [63]. It is therefore necessary to review the treated composite systems and compare them with these.

Modified natural fibre-thermoplastic composites offer improved properties relating to morphology compared to non-coupled/untreated composites. The modification may be either fibre surface or polymer treatment, and gives enhanced interfacial adhesion between the polymer matrix and fibre, good fibre dispersion within the matrix and good fibre covering by the polymer. However, the degree of interfacial adhesion of the composite components

depends largely on the chemical nature of the chosen coupling agent [49]. Different coupling agents such as silane, organosilanes, maleic anhydride, maleic anhydride grafted polyolefins, acrylic acid grafted polyolefins, organic peroxide, and ethylene-vinyl alcohol copolymer (EVAL) were used to enhance the compatibility between natural fibres and polyolefins [34,35,38,40,48,54,55,58-60,63]. The SEM observations from these authors confirmed good compatibility and interfacial adhesion between the polyolefin matrices and the various natural fibres after modification of the composites. This was gathered from the absence of gaps between fibres and matrices, reduction in fibre pull-outs resulting in small voids and few cavities, improved fibres dispersion within polymer matrices, good fibre covering by polymers and less fibres agglomeration.

2.3 Thermal properties

2.3.1 Melting and crystallization

2.3.1.1 Phase change materials (PCMs)

The thermal properties of HDPE encapsulated paraffin wax PCM blends were reported by Sari [3], Inaba and Tu [5] and Hong and Xin-shi [6]. The used paraffins were of different grades and melting points. In all these studies, with the aid of differential scanning calorimetry (DSC) method of analysis, it was found that HDPE and paraffin interacted physically rather than chemically. This stems from observations such as independent melting of blends components; little influence on thermal properties by one component to the other after compounding; and the dependence of thermal properties (transition and melting temperatures as well as latent heat) on the mass fraction of the dispersed paraffin. Hong and Xin-shi [6] found that the latent heat of PCM blends also included the sensible heat of HDPE in the phase change transition range. This was based on the fact that the calculated percentage values of the ratio of latent heats for the form-stable PCMs to that of the paraffin were a little higher than the mass percentage of paraffin.

Beginn [7] determined the thermal properties (using DSC) of PCM gels made of ultra high molecular weight polyethylene (UHMW-PE) and paraffin waxes of various melting points. It was found that PCM gels could store and release enthalpies of up to 200 J g^{-1} at the melting temperature of wax. These PCM gels were homogeneous on a macroscopic level, but had a

large degree of phase segregation. Although some degree of shape stabilization was reported, but there was a leakage of molten paraffin waxes at high temperatures. This was due to poor formation of a network by PE gel to contain molten wax.

Cai *et al.* [11-14] reported on the thermal characteristics of HDPE/paraffin PCM composites with different flame retardants. In all these studies, it was reported that the introduction of flame retardants had no remarkable influence on latent heat of form-stable PCM. Similar to other studies [3,5,6], it was observed that thermal properties of PCMs were dependant on the mass ratio of paraffin in the PCM composites, but latent heats of PCM composites were slightly less than those of pure paraffins. For HDPE-EVA/OMT/paraffin PCM nano-composites [13], the latent heat of paraffin decreased with an increase in silicate layers of the OMT. However, this behaviour was not explained.

Krupa *et al.* [1,2] evaluated the thermal behaviour of polyolefin/paraffin wax PCM blends using DSC. Both Wax S and Wax FT blended with isotactic polypropylene (iPP) and low density polyethylene (LDPE) respectively, displayed multiple endothermic melting peaks. These were referred to as solid-solid (first peak) and solid-liquid (second one) transitions. However, these were clearly defined for Wax S but overlapped for Wax FT. In a quest to clarify this difference in behaviour of waxes, Krupa and Luyt [16] conducted a separate study by investigating changes in the crystalline structure of waxes with an increase and a decrease in temperature. This study confirmed the presence of both solid-solid and solid-liquid (melting of crystallites) in the case of Wax S, but for Wax FT there was no evidence for solid-solid transition. The authors concluded that the multiple endothermic peaks for Wax FT were due to melting of crystalline fractions with different molecular weight distributions. Krupa *et al.* [1] found that both waxes plasticized the PP matrix. There was inhomogeneity of the samples and an apparent leakage of paraffin wax from the matrix during sample preparation. It was concluded that the specific melting enthalpy of paraffin waxes were relatively too low to effectively absorb large amounts of energy. This was due to low experimental specific melting enthalpy values than the theoretically expected ones. On the other hand, LDPE/wax PCM blends [2] showed correspondence between the mass fraction of wax in the blends and theoretically calculated portion implying that there was no leakage of wax from the matrix during preparation.

In other studies, such as those by Xiao *et al.* [4,17], Peng *et al.* [9] and Luyt and Krupa [18], various grades of paraffin waxes were respectively encapsulated by poly(styrene-butadiene-styrene) (SBS), room temperature cured bisphenol epoxy and styrene-ethylene-butylene-styrene (SEBS), and UV cured epoxy. It was generally found that, in all these studies, PCM blends and/or composites exhibited the same phase transition characteristics as paraffin waxes and their latent heats were equal to the mass fraction of the dispersed paraffin in the blends and/or composites. This observation clearly indicated the absence of any chemical interaction, but the presence of physical interaction between paraffin waxes and respective polymer matrices, similar to other reviewed studies [3,5,6,11-14].

2.3.1.2 Polyolefins/wax blends

The thermal properties of normal hard Fischer-Tropsch paraffin wax blended with polypropylene (PP) and LLDPE respectively were determined by Krupa and Luyt [21,22]. In both studies it was found that both onset temperature of melting and melting temperature decreased with an increase in wax portion. The specific enthalpies of melting for both blend systems increased with an increase in wax content due to bigger value for wax than polymer matrices. In both systems, an increase in wax content resulted into a decrease in crystallization temperatures. In a study where LLDPE was blended with an oxidized hard wax, Krupa and Luyt [23] found that an increase in wax portion did not influence the onset temperature of melting; melting temperature; crystallization temperature; and enthalpies of crystallization, but did insignificantly influence the specific enthalpies of melting. This insignificance was due to the high similarity of specific melting enthalpies for both wax and LLDPE.

Hato and Luyt [24] reported the thermal properties of both H1 and A1 waxes, each blended with HDPE, LLDPE and LDPE matrices respectively. It was found that, for H1 wax containing blends (with all matrices) there was an increase in enthalpies as a function of wax content showing an increase in crystallinity of the blends. This was attributed to several reasons such as the higher melting enthalpy of H1 wax compared to those for various polymer matrices; partial miscibility of LLDPE and wax; and co-crystallization of wax with LDPE. For A1 wax containing blends, it was reported that the melting enthalpies of the blends were lower than that of pure HDPE. These increased as a function of wax content for HDPE blends, but decreased with an increase in wax portion for LLDPE and LDPE blends. This was

attributed to lower enthalpy values of A1 wax with respect to pure polymer matrices (HDPE and LLDPE); probable co-crystallization of wax and LDPE; and the simultaneous crystallization of A1 wax and LDPE. Furthermore, Mpanza and Luyt [25] blended LDPE with Enhance, H1 and M3 waxes respectively. It was found that both Enhance and H1 waxes increased the melting enthalpies of the blends with an increase in wax portion. This showed an increase in crystallinity of the blends due to high enthalpies of the waxes than that of pure polymer matrix. However, Enhance wax containing blends gave higher enthalpy values than H1 wax containing ones due to differences in enthalpies of pure waxes. There was also a slight increase in lamellar thickness for both blend systems. M3 wax containing blends showed a decrease in crystallinity by giving a decrease in enthalpy, and there was a decrease in both onset temperature of melting and melting temperature as a function of wax. This was due to the fact that M3 wax does not co-crystallize with LDPE, but inhibits the crystallization of LDPE by acting as a plasticizer.

The thermal properties of the uncross-linked and cross-linked polyolefin/wax blends systems were reported, however this study will only report on the uncross-linked systems. Krupa and Luyt [26] found that the wax content had no influence on the melting point and onset temperature of melting of LLDPE/hard normal paraffin wax blends. The enthalpy of the blends increased with an increase in wax portion. On the other hand, Mtshali *et al.* [27] reported that the specific melting enthalpy values of LDPE/hard normal wax, for both experimentally and theoretically determined, were in good agreement. Hlangothi *et al.* [28] found that the melting temperature of LLDPE/hard normal wax blends decreased as a function of wax content. This was due to possible co-crystallization of PE and more wax shorter chains that reduced the lamellae thickness. It was found that the enthalpy of blends increased with wax content due to incorporation of short and linear wax chains into the crystal lattice during crystallization. This suggested an increase in crystallinity of the materials.

2.3.1.3 Polyolefins/natural fibre composites

Various authors reported on the thermal properties of natural fibre-reinforced polyolefin composites and different characteristics were found [40,45,46,57,65,66]. These characteristics were influenced by the nature of polyolefin matrix, fibre or filler and coupling agent used. Marcovich and Villar [40] and Luyt and Malunka [57] found a decrease in crystallinity of natural fibre-reinforced polyethylene in the presence of organic peroxide and maleic

anhydride. This was due to the contribution of modifications in decreasing the initial order of PE molecules. A slight increase in crystallinity of LLDPE/WF composites with wood flour loading [40], but a decrease in crystallinity of LDPE/sisal fibre composites [57] was observed. The sisal fibre loading led to a significant decrease in melting temperature of peroxide treated composites, but the extent of decrease was reduced in the presence of wax, which also increased the crystallinity of PE [57]. These observations were attributed to nucleation effect of WF acting as sites for heterogeneous nucleation as well as grafting and epitaxial crystallization of LDPE-sisal fibre, which were limited in presence of wax as a result of wax covering the sisal fibre surface. Marcovich and Villar [40] concluded that the increase in crystallinity was independent of the degree of compatibility between PE matrix and the filler since this character was exhibited by all the investigated composites. Viksne *et al.* [45] found that when wood flour was treated with paraffin, the moisture absorption of WF was reduced. This was due to the disappearance of the low temperature peak of WF after paraffin treatment.

Authors such as Albano *et al.* [46], Dikobe and Luyt [65] and Salemane and Luyt [66] reported on polypropylene-natural fibre composites. It was found that gamma radiation treatment of PP-lignocellulosic fibre composites showed no change in crystallization temperature, but their fusion temperature decreased with an increase in gamma radiation doses. This decrease was attributed to the oxidative degradation of PP matrix [46]. Dikobe and Luyt [65] observed that wood powder influenced the crystallization behaviour of EVA in PP/EVA blends. The authors concluded that WP was primarily concentrated on the EVA phase, but not PP. Salemane and Luyt [66] reported that the WP increased the crystallinity, but reduced the lamellar thickness of PP/WP composites (with and without a coupling agent). This was attributed to formation of new crystallization zones around WP particles through epitaxial crystallization on their surfaces. However, the coupling agent had no significant influence on melting and crystallization properties of the composites.

2.3.2 Thermal stability

2.3.2.1 Phase change materials (PCMs)

Cai *et al.* [11-14] reported the thermal stability of HDPE/paraffin PCMs with various flame retardants. It was found that some PCM composites [11,14] gave lower onset temperature of degradation in comparison to their HDPE/paraffin hybrids. In all these studies, PCM

composites displayed two-step degradation with large amount of char residue at high temperatures (700 °C) with an increase in flame retardants contents. It was further shown that the addition of suitable amount of OMT [13] and flame retardants [11-14] into the form-stable PCMs improved the thermal stability of PCM composites.

In general, it was found that the paraffin waxes (Wax S and Wax FT) reduced the thermal stability of polyolefins (PP and LDPE) based PCM blends [1,2]. This continued to lower with an increase in wax mass fraction in the blends. The behaviour was attributed to low thermal stability of paraffin waxes. However, Wax FT containing blends showed a higher thermal stability than those of Wax S at the same wax content. There was one-step degradation for Wax FT blends, whereas Wax S blends showed two-step degradation. This behaviour was used to confirm the immiscibility of Wax S blends and the miscibility of Wax FT containing blends complementing the results found from SEM and DSC analysis. No char yield was reported at high temperatures in both studies.

Similar to polyolefin matrices based PCM blends in [1,2], when oxidized hard Fischer-Tropsch paraffin wax is blended with epoxy resin matrix, the thermal stability decreased with an increase in wax content [18]. Only one-step degradation was found which is typical of miscible blends. This, however, does not complement SEM and DSC results which showed the existence of immiscibility character for this PCM system. This behaviour was explained in terms of epoxy resin acting as a heat isolator for wax degradation together with the wax free radicals that accelerated the degradation of epoxy.

2.3.2.2 Polyolefin/wax blends

The thermal stability of polyolefin/wax blends showed large dependence on wax content in the blend systems. This comes from various authors [21,23,25-28] who generally found that an increase in wax mass fraction in the blends led to a decrease in thermal stability of the blends. This behaviour did not matter of the kind of paraffin wax (H1, A1, Enhance or M3 wax) and polyolefin matrix (LLDPE, LDPE or PP) used and was similar for these different studies. This was mainly attributed to the low thermal stability of waxes compared to polyolefin matrices. In some case it was found that the blends were more thermally stable than pure waxes [21,25] due to the presence of polymer matrices, whereas in other cases they were stable than the pure polymer [25].

2.3.2.3 Polyolefins/natural fibre composites

Thermal stability of natural fibre-reinforced polyolefin composites seems to generally depend on the extent to which polymers and fibres interact. This interaction is influenced by the method of modification employed. Generally the thermal stability of natural fibres is significantly lower than that of polyolefins, yet their introduction into polyolefins may lead to either lowering or raising of the composites thermal stability [40,46,54,57,59,65-67,73]. Marcovich and Villar [40], Albano *et al.* [46], Luyt and Malunka [57] and Nachtigal *et al.* [59] found that natural fibres decreased thermal stability of the composites in either untreated or organic peroxide, wax, or gamma radiation treated systems with the residual char increasing with fibre content. This was attributed to polymers with more weak links due to organic peroxide and an increase in concentration of radicals. Luyt and Malunka [57] further reported that wax addition in peroxide treated LDPE/sisal composites reduced the interaction between matrix and fibre by covering the fibres and accelerating their decomposition.

In other studies [54,59,65-67,73] it was reported that thermal stability increased with the inclusion of fibres as well as modification. This was attributed to water-cross-linking reaction [54], higher crystallinity in the presence of fibres [66] and greater polymer-fibre interaction because of improved compatibility due to composites treatment (maleic anhydride grafted polyolefin or acetylation) [59,65,67,73]. In some cases composites degraded in two or three distinguishable steps corresponding to constituents [40,46,65]. Dikobe and Luyt [65] observed this and found that the presence of wood powder in PP/EVA blends reduced the thermal stability of the first degradation step yet improved the second one. This was attributed to strong interaction between WP and EVA together with retardation of evolution of volatile products. Doan *et al.* [73] reported high thermal stability for jute fibre/PP composites than neat PP and fibres in both nitrogen and air atmospheres, and this was due to fibre/matrix interaction.

2.4 Thermo-mechanical and mechanical properties

2.4.1 Thermo-mechanical properties

2.4.1.1 Phase change materials (PCMs)

The dynamic mechanical analysis (DMA) for shape-stabilized PCMs where paraffin waxes were used as energy storage materials was reported by few researchers [1,2,9,18]. Krupa *et al.* [1,2] reported the viscoelastic features of PP and LDPE matrices blended separately with both soft (Wax S) and hard oxidized (Wax FT) paraffin waxes. It was found that Wax S loading led to decreased storage modulus of Wax S/PP blend PCMs throughout the temperature range of investigation [1], whereas in Wax S/LDPE PCM blends high elastic modulus was observed [2] below wax melting point. However, above this wax melting a remarkable decrease in elastic modulus at high wax contents was observed. These were said to suggest plasticising effect of wax on polyolefin matrices, but also that wax could act as highly crystalline filler that immobilized the LDPE chains at the crystal surface. The authors further reported that LDPE formed a continuous phase and Wax S discontinuous phase up to 50% weight Wax S, above which (i.e. 60% weight) there was phase exchange and the blend PCMs collapsed around wax melting. Wax FT containing polyolefin (PP and LDPE) PCM blends systems showed more compact and stronger materials by exhibiting high elastic modulus in its solid state. In its molten state high wax contents showed modulus break. In this regard authors could not confirm which phase of the system was continuous and/or discontinuous due to a very small difference between LDPE and Wax FT melting temperatures. It was therefore unclear whether the structural failure of blend PCMs should be assigned to Wax FT melting or to lower LDPE melting. The conclusions made were that Wax S blends exhibited lower elastic modulus than pure PP and that these LDPE/paraffin wax blends are poor strength materials, especially at temperatures above those of waxes melting.

Other authors such as Peng *et al.* [9] and Luyt and Krupa [18] subjected paraffin/epoxy and paraffin/styrene-ethylene-butylene-styrene (SEBS) systems to DMA technique. Peng *et al.* [9] found that, for paraffin/epoxy PCMs, the system showed a decrease in storage moduli with an increase in temperature. The loss moduli for the same system implied that the interaction between the components was enough to provide the adequate thermal and mechanical performance. For paraffin/SEBS system, the storage moduli were decreasing with an increase

in temperature. Their loss moduli, on the other hand were a combination of both paraffin and SEBS since the blends behaviour is between the two constituents. It was concluded that the paraffin/SEBS system showed excellent thermal and mechanical performance. Furthermore, Luyt and Krupa [18] used epoxy with Wax FT and showed that the elastic modulus of the system decreased sharply with an increase in temperature relative to pure epoxy. The loss modulus demonstrated an eventual disappearance of the epoxy glass transition as wax content increases due to reduction in amount of epoxy (relaxing phase). At high temperatures, there was a remarkable decrease in loss modulus due to wax melting and the consequent softening effect on the blends. The conclusion made is that the epoxy-wax interaction seemed weak, and both solid and molten wax had observable influence on the samples.

2.4.1.2 Polyolefins/natural fibre composites

Different authors investigated and reported on the thermo-mechanical properties of polyolefins/natural fibre composites [34,35,43,49,65,68,69,73]. These researchers observed that the incorporation of natural fibres into polyolefins resulted into composite materials exhibiting high stiffness, with some interfacial adhesion/interaction between fibres and matrices, and less viscous behaviour. This was due to the observed increase in both storage and loss modulus together with a decrease in damping factor ($\tan \delta$) peak amplitude and its shift towards high temperatures. These properties were found to be highly improved by the modification of composites. They were mainly influenced by fibre content and coupling agent (both content and type) involved [34,35,43,49,68,69,73]. In HDPE-natural fibre composites, Bengtsson *et al.* [34] found that the silane cross-linked composites system showed two major transitions corresponding to HDPE γ -relaxation (around -128 °C) and α -relaxation (around 113 °C). They observed that there was no shift in γ -transition peak position to higher temperatures, but an increase in storage modulus with fibre loading indicative of higher stiffness interface. This was attributed to low cross-link density of the composites. However, Behzad *et al.* [68] and Tajvidi *et al.* [69] found that only α -relaxation (around $40-50$ °C) was the major detectable transition of HDPE for both nontreated and treated (with maleated polyethylene). Authors reported that the energy loss became more pronounced above this α -relaxation at high fibre loading. It was shown that compatibilization effect became more pronounced on the viscoelastic properties of these composites at high temperatures and high fibre contents. In general, natural fibres and coupling agents have a considerable effect on the viscoelastic properties of polyolefins/natural fibre composites.

2.4.2 Mechanical properties

2.4.2.1 Phase change materials (PCMs)

Published work on mechanical properties of PCMs in general based on tensile testing specifically is limited. A few authors, Krupa *et al.* [2], Beginn [7] and Meingjin *et al.* [19] have reported on these properties based on DMA in a tensile mode and tensile testing. Krupa *et al.* [2] found that an increase in wax portion in LDPE/soft petroleum wax blends led to a decrease in ultimate strength and elongation properties. This was attributed to shortage of tie molecules responsible for the mechanical transfer in the wax structure. Beginn [7] tested the ultra-high molecular weight polyethylene (UHMW-PE)/paraffin PCMs below and above the melting point of paraffin. The author reported high modulus and low elongation at break below the melting point of paraffin for high polymer content. But above the paraffin melting point, soft gels resulted in low modulus and high elongation at break. The maximum tensile strength decreased remarkably by more than a half. For low polymer content PCMs, the opposite behaviour was reported. Below paraffin melting point there was high elongation at break. It decreased above this temperature and the maximum tensile strength increased. It was explained that the actual mechanical behaviour of the composites depended on the interaction of paraffin crystals and polymer network. Therefore the average alkane crystalline domains will be affected by the concentration of polymer fibres, while on the other hand the crystals may act as additional net points that can join together spatially separated regions of the polymer network. Based on this, it was concluded that it is not simple to predict and/or explain the mechanical properties of such paraffin/polymer fibre composites. Meingjin *et al.* [19] reported the relationship between heat treatment time and mechanical property of thermal regulating fibres based on paraffin and polyvinyl alcohol (PVA). It was found that the modulus of these fibres increased uniformly with an increase in heat treatment time, but elongation at break decreased. The authors gave no explanation for this behaviour.

2.4.2.2 Polyolefin/paraffin wax blends

Mechanical behaviour of polyolefin/wax blends was mainly reported by one group of Luyt *et al.* [22-25,28]. In these different studies it was generally found that the Young's moduli of blends were dependent on wax content. The property (Young's modulus) showed an increase with wax portion in the blends. This was associated with high degree of crystallinity of

paraffin waxes compared to respective polyolefin matrices and the probable co-crystallization of waxes with polymers. Both yield (elongation and stress) and ultimate (elongation and stress) properties did not show a similar general trend but varied according to specific blend systems. A number of studies [22,24,25,28] reported a reduction in elongation at yield with an increase in wax portion. This was attributed to the crystallization of wax in the amorphous part of the polymer matrices restricting the polymer chain mobility, an increase in crystallinity of the blends and the hardness of waxes in comparison with the polymer matrices. However, other authors found that wax content had no influence on elongation at yield [23]. The stress at yield varied from one system to another. Three observations were made with an increase in wax content in various studies: (i) no change/influence [23] was observed; (ii) stress at yield increased with wax content due to an increase in crystallinity of the blends [24,25,28]; and (iii) a decrease in stress at yield with an increase in wax content which showed a reduction in strain hardening of the blends [22,24]. The elongation at break in all these studies showed a decrease with wax content increase. This meant that the materials had lost their draw-ability. This was due to wax molecules that are too short to form tie chains thus increasing the number of chain ends, but lowering number of tie molecules. Generally, it was found that the tensile strength (stress at break) of these polyolefin/wax blends decreased with an increase in wax content. The behaviour indicated a possible decrease in strain hardening and it was due to a decrease in number of average tie chains.

2.4.2.3 Polyolefins/natural fibre composites

Significant work has been done on the mechanical properties of natural fibre-reinforced polyolefin composites [35,38,40,43,46,49,53-56,58,59,62,63,65,66,68,74]. In all these studies it was clear that these properties were mainly affected by fibre/filler dispersion within polymer matrices; compatibility/interfacial adhesion between matrices and fibres; and the nature and content of coupling agent used to enhance compatibility. It was found that non-modified polyolefin/natural fibre composites generally showed poor mechanical properties such as tensile, impact and flexural strength, tensile and flexural modulus. This was attributed to poor fibre-matrix compatibility, poor stress transfer between the composites constituents as well as poor fibre dispersion [38,49,53,58,59,65,66,68,74]. However, Bledzki *et al.* [63] reported improved mechanical properties of abacca fibre/PP composites without any coupling agent and this was explained as due to better fibre distribution in the PP matrix and less fibre fracture.

The treatment of composites varied from the use of coupling agents (mainly maleated polyolefins, silanes), organic peroxide, and water-cross-linking to gamma irradiation methods. The resultant composites showed improved mechanical properties in comparison to nontreated composites. This observation was due to enhanced compatibility between fibres and polyolefin matrices and good fibre dispersion. These were said to have resulted into effective reinforcing effect and stress transfer between the fibres and matrices [35,38,40,43,46,49,53-56,58,59,62,63,65,66,68,74]. To show the variation of coupling agent nature, Kim *et al.* [55] reported that ethylene vinyl alcohol, as a compatibilizer in saw-dust-reinforced LLDPE composites, led to better mechanical properties than ethylene vinyl acetate that led to poor properties. This behaviour increased with an increase in coupling agent's content, and it was attributed to the compatibilizers' ability to chemically bond with saw-dust. Viksne *et al.* [45] found that an increase of paraffin content in saw-dust reinforced polyethylene [HDPE, LDPE and recycled waste PE (WPE)] composites gave improved properties up to a certain level after which a decrease was observed for LDPE and WPE matrices, but a steady drop for HDPE involving composites. This was due to the plasticization effect of paraffin on the matrices as a function of paraffin. Similarly, Albano *et al.* [46] found that an increase in gamma radiation doses on PP/fibre composites resulted into decreased tensile strength, elongation at break and Young's modulus, whereas at low radiation these were increased. The authors explained this as due to formation degradation caused by radicals in the amorphous regions.

2.5 Water absorption

2.5.1 Polyolefin/natural fibre composites

The water absorption behaviour of natural fibre reinforced polyolefin matrices has been a subject of research and discussion. Natural fibres such as wood flour; wood fibre; sago starch; rice hulls and flax fibres with polyolefins (HDPE, LLDPE, LDPE and PP) were studied by various researchers [45,53,59,70-73]. It was mainly found that the natural fibre-polyolefin composites had high water uptake compared to neat polyolefin matrices, which showed total negligible water absorption effect. Yang *et al.* [53] used lignocellulosic materials as control and found that their water uptake was higher than the composites. It is well known that thermoplastics are hydrophobic in nature and therefore would reduce water uptake in the

composites. The water absorption effect on composites increased with an increase in fibre content. This was attributed to the hydrophilic nature of the natural fibres resulting into poor interfacial bonding with hydrophobic thermoplastics thus allowing water penetration through the composite materials. An increase in hydrophilic natural fibre content results into a less hydrophobic thermoplastic material to encapsulate fibres and therefore increased water uptake. However, chemical modification, with the aid of maleic anhydride [53,59,71-73] and paraffin [45], of these composites results into lowered water uptake. This is due to improved compatibility between polyolefin matrices and natural fibres and low viscosity property of paraffin allowing it to penetrate into the pores of WF thus blocking part of internal hydroxyl groups of WF.

2.6 References

1. I. Krupa, G. Miková, A.S. Luyt. Polypropylene as a potential matrix for the creation of shape stabilized phase change materials. *European Polymer Journal* 2007; 43:895-907.
2. I. Krupa, G. Miková, A.S. Luyt. Phase change materials based on low-density polyethylene/paraffin wax blends. *European Polymer Journal* 2007; 43:4695-4705.
3. A. Sari. Form-stable paraffin/high density polyethylene composites as solid-liquid phase change material for thermal energy storage: preparation and thermal properties. *Energy Conversion and Management* 2004; 45:2033-2042.
4. M. Xiao, B. Feng, K. Gong. Preparation and performance of shape stabilized phase change thermal storage materials with high thermal conductivity. *Energy Conversion and Management* 2002; 43:103-108.
5. H. Inaba, P. Tu. Evaluation of thermophysical characteristics on shape-stabilized paraffin as a solid-liquid phase change material. *Heat and Mass Transfer* 1997; 32:307-312.
6. Y. Hong, G. Xin-shi. Preparation of polyethylene-paraffin compound as a form-stable solid-liquid phase change material. *Solar Energy Materials and Solar Cells* 2000; 64:37-44.
7. U. Beginn. Applicability of frozen gels from ultra high molecular weight solid/liquid phase change materials. *Macromolecular Materials and Engineering* 2003; 288:245-251.

8. W. Wang, X. Yang, Y. Fang, J. Ding. Preparation and performance of form-stable polyethylene glycol/silicon dioxide composites as solid-liquid phase change materials. *Applied Energy* 2008 (in press).
9. S. Peng, A. Fuchs, R.A. Wirtz. Polymeric phase change composites for thermal energy storage. *Journal of Applied Polymer Science* 2004; 93:1240-1251.
10. A. Mills, M. Farid, J.R. Selman, S. Al-Hallaj. Thermal conductivity enhancement of phase change materials using a graphite matrix. *Applied Thermal Engineering* 2006; 26:1652-1661.
11. Y. Cai, Y. Hu, L. Song, Q. Kong, R. Yang, Y. Zhang, Z. Chen, W. Fan. Preparation and flammability of high density polyethylene/paraffin/organophilic montmorillonite hybrids as a form stable phase change material. *Energy Conversion and Management* 2007; 48:462-469.
12. Y. Cai, Q. Wei, F. Huang, W. Gao. Preparation and properties studies of halogen-free flame retardant form-stable phase change materials based on paraffin/high density polyethylene composites. *Applied Energy* 2008; 85:765-775.
13. Y. Cai, L. Song, Q. He, D. Yang, Y. Hu. Preparation, thermal and flammability properties of a novel form-stable phase change materials based on high density polyethylene/poly(ethylene-co-vinyl acetate)/organophilic montmorillonite nanocomposites/paraffin compounds. *Energy Conversion and Management* 2008; 49:2055–2062.
14. Y. Cai, Y. Hu, L. Song, Y. Tang, R. Yang, Y. Zhang, Z. Chen, W. Fan. Flammability and thermal properties of high density polyethylene/paraffin hybrid as a form-stable phase change material. *Journal of Applied Polymer Science* 2006; 99:1320-1327.
15. Q. Song, Y. Li, J. Xing, J.Y. Hu, Y. Marcus. Thermal stability of composite phase change material microcapsules incorporated with silver nano-particles. *Polymer* 2007; 48:3317-3323.
16. A.S. Luyt, I. Krupa. Thermal behaviour of low and high molecular weight paraffin waxes used for designing phase change materials. *Thermochimica Acta* 2008; 467:117-120.
17. M. Xiao, B. Feng, K. Gong. Thermal performance of high conductive shape-stabilized thermal storage material. *Solar Energy Materials and Solar Cells* 2001; 69:293-296.
18. A.S. Luyt, I. Krupa. Phase change materials formed by uv curable epoxy matrix and Fischer-Tropsch paraffin wax. *Energy Conversion and Management* 2008 (in press).

19. J. Mengjin, S. Xiaoqing, X. Jianjun, Y. Guangdou. Preparation of a new thermal regulating fibre based on PVA and paraffin. *Solar Energy Materials and Solar Cells* 2008; 92:1657-1660.
20. I. Krupa, A.S. Luyt. Mechanical properties of uncrosslinked and crosslinked linear low-density polyethylene/wax blends. *Journal of Applied Polymer Science* 2001; 81:973-980.
21. I. Krupa, A.S. Luyt. Thermal properties of polypropylene/wax blends. *Thermochimica Acta* 2001; 372:137-141.
22. I. Krupa, A.S. Luyt. Thermal and mechanical properties of extruded LLDPE/wax blends. *Polymer Degradation and Stability* 2001; 73:157-161.
23. I. Krupa, A.S. Luyt. Physical properties of blends of LLDPE and an oxidized paraffin wax. *Polymer* 2001; 42:7285-7289.
24. M.J. Hato, A.S. Luyt. Thermal fractionation and properties of different polyethylene/wax blends. *Journal of Applied Polymer Science* 2007; 104:2225-2236.
25. H.S. Mpanza, A.S. Luyt. Comparison of different waxes as processing agents for low-density polyethylene. *Polymer Testing* 2006; 25:436-442.
26. I. Krupa, A.S. Luyt. Thermal properties of uncross-linked and cross-linked LLDPE/wax blends. *Polymer Degradation and Stability* 2000; 70:111-117.
27. T.N. Mtshali, I. Krupa, A.S. Luyt. The effect of cross-linking on the thermal properties of LDPE/wax blends. *Thermochimica Acta* 2001; 380:47-54.
28. S.P. Hlangothi, I. Krupa, V. Djoković, A.S. Luyt. Thermal and mechanical properties of cross-linked and uncross-linked linear low-density polyethylene-wax blends. *Polymer Degradation and Stability* 2003; 79:53-59.
29. A.S. Luyt, V.G. Geethamma. Effect of oxidized paraffin wax on the thermal and mechanical properties of linear low-density polyethylene-layered silicate nanocomposites. *Polymer Testing* 2007; 26:461-470.
30. P.V. Joseph, K. Joseph, S. Thomas. Effect of processing variables on the mechanical properties of sisal-fibre-reinforced polypropylene composites. *Composites Science and Technology* 1999; 59:1625-1640.
31. J.Z. Lu, Q. Wu, I.I. Negulescu. Wood-fibre/high-density polyethylene composites: coupling agent performance. *Journal of Applied Polymer Science* 2005; 96:93-102.
32. M. Bengtsson, K. Oksman. The use of silane technology in crosslinking polyethylene/wood flour composites. *Composites: Part A* 2006; 37:752-765.

33. J.-P. Kim, T.-H. Yoon, S.-P. Mun, J.-M. Rhee, J.-S. Lee. Wood–polyethylene composites using ethylene–vinyl alcohol copolymer as adhesion promoter. *Bioresource Technology* 2006; 97:494-499.
34. M. Bengtsson, P. Gatenholm, K. Oksman. The effect of crosslinking on the properties of polyethylene/wood flour composites. *Composites Science and Technology* 2005; 65:1468-1479.
35. S.-M. Lai, F.-C. Yeh, Y. Wang, H.-C. Chan, H.-F. Shen. Comparative study of maleated polyolefins as compatibilizers for polyethylene/wood flour composites. *Journal of Applied Polymer Science* 2003; 87:487-496.
36. M. Morreale, R. Scaffaro, A. Maio, F.P. La Mantia. Effect of adding wood flour to the physical properties of a biodegradable polymer. *Composites: Part A* 2008; 39:503-513.
37. A.K. Bledzki, M. Letman, A. Viksne, L. Rence. A comparison of compounding processes and wood type for wood fibre-PP composites. *Composites: Part A* 2005; 36:789-797.
38. X. Colom, F. Carrasco, P. Pagès, J. Cañavate. Effects of different treatments on the interface of HDPE/lignocellulosic fibre composites. *Composites Science and Technology* 2003; 63:161-169.
39. B. Li, J. He. Investigation of mechanical property, flame retardancy and thermal degradation of LLDPE-wood-fibre composites. *Polymer Degradation and Stability* 2004; 83:241-246.
40. N.E. Marcovich, M.A. Villar. Thermal and mechanical characterization of linear low-density polyethylene/wood flour composites. *Journal of Applied Polymer Science* 2003; 90:2775-2784.
41. H.-T. Liao, C.-S. Wu. Study on the properties of polyethylene-octene-elastomer/wood flour blends. *Journal of Applied Polymer Science* 2003; 88:1919-1924.
42. P.W. Balasuriya, L. Ye, Y.-W. Mai. Mechanical properties of wood flake-polyethylene composites. Part I: Effects of processing methods and matrix melt flow behaviour. *Composites: Part A* 2001; 32:619-629.
43. N.M. Stark, L.M. Matuana. Surface chemistry and mechanical property changes of wood-flour/high-density-polyethylene composites after accelerated weathering. *Journal of Applied Polymer Science* 2004; 94:2263-2273.

44. B. Xu, J. Simonsen, W.E. (S.) Rochefort. Creep resistance of wood-filled polystyrene-high-density polyethylene blends. *Journal of Applied Polymer Science* 2001; 79:418-425.
45. A. Viksne, L. Rence, M. Kalnins, A.K. Bledzki. The effect of paraffin on fibre dispersion and mechanical properties of polyolefin-sawdust composites. *Journal of Applied Polymer Science* 2004; 93:2385-2393.
46. C. Albano, J. Reyes, M. Ichazo, J. González, M. Brito, D. Moronta. Analysis of the mechanical, thermal and morphological behaviour of polypropylene compounds with sisal fibre and wood flour, irradiated with gamma rays. *Polymer Degradation and Stability* 2002; 76:191-203.
47. M.J. John, R.D. Anandjiwala. Recent developments in chemical modification and characterization of natural fibre-reinforced composites. *Polymer Composites* 2008; volume: 187-207 (DOI 10.1002/pc.20461).
48. Y. Wang, F.-C. Yeh, S.-M. Lai, H.-C. Chan, H.-F. Shen. Effectiveness of functionalized polyolefins as compatibilizers for polyethylene/wood flour composites. *Polymer Engineering and Science* April 2003; 43(4).
49. J. Z. Lu, Q. Wu, I.I. Negulescu. Wood-fibre/high-density-polyethylene composites: Coupling agent performance. *Journal of Applied Polymer Science* 2005; 96:93-102.
50. J. Z. Lu, I.I. Negulescu, Q. Wu. Maleated wood-fibre/high-density-polyethylene composites: Coupling mechanisms and interfacial characterization. *Composite Interfaces* 2005; 12(1-2):125-140.
51. T. Li, N. Yan. Mechanical properties of wood flour/HDPE/ionomer composites. *Composites: Part A* 2007; 38:1-12.
52. Y. Geng, K. Li, J. Simonsen. Effects of a new compatibilizer system on the flexural properties of wood-polyethylene composites. *Journal of Applied Science* 2004; 91:3667-3672.
53. H.-S. Yang, H.-J. Kim, H.-J. Park, B.-J. Lee, T.-S. Hwang. Water absorption behavior and mechanical properties of lignocellulosic filler-polyolefin bio-composites. *Composite Structures* 2006; 72:429-437.
54. C.-F. Kuan, H.-C. Kuan, C.-C. M. Ma, C.-M. Huang. Mechanical, thermal and morphological properties of water-crosslinked wood flour reinforced linear low-density polyethylene composites. *Composites: Part A* 2006; 37:1696-1707.

55. J.-P. Kim, T.-H. Yoon, S.-P. Mun, J.-M. Rhee, J.-S. Lee. Wood-polyethylene composites using ethylene-vinyl alcohol copolymer as adhesion promoter. *Bioresource Technology* 2006; 97:494-499.
56. K. Joseph, S. Thomas, C. Pavithran. Effect of aging on the physical and mechanical properties of sisal-fibre-reinforced polyethylene composites. *Composites Science and Technology* 1995; 53:99-110.
57. A.S. Luyt, M.E. Malunka. Composites of low-density polyethylene and short sisal fibres: the effect of wax addition and peroxide treatment on thermal properties. *Thermochimica Acta* 2005; 426:101-107.
58. P. Nygård, B.S. Tanem, T. Karisen, P. Brachet, B. Leinsvang. Extrusion-based wood fibre-PP composites: Wood powder and pelletized wood fibres – a comparative study. *Composites Science and Technology* 2008; 68:3418-3424.
59. S.M.B. Nachtigal, G.S. Cerveira, S.M.L. Rosa. New polymeric-coupling agent for polypropylene/wood-flour composites. *Polymer Testing* 2007; 26:619-628.
60. M. Bengtsson, M. Le Baillif, K. Oksman. Extrusion and mechanical properties of highly filled cellulose fibre-polypropylene composites. *Composites: Part A* 2007; 38:1922-1931.
61. J.S. Fabiyi, A.G. McDonald, M.P. Wolcott, P.R. Griffiths. Wood plastic composites weathering: Visual appearance and chemical changes. *Polymer Degradation and Stability* 2008; 93:1405-1414.
62. K.L. Fung, X.S. Xing, R.K.Y. Li, S.C. Tjong, Y.-W. Mai. An investigation on the processing of sisal fibre reinforced composites. *Composites Science and Technology* 2003; 63:1255-1258.
63. A.K. Bledzki, A.A. Mamun, O. Faruk. Abaca fibre reinforced PP composites and comparison with jute and flax fibre PP composites. *Express Polymer Letters* 2007; 1(11):755-762.
64. M. Zampaloni, F. Pourboghrat, S.A. Yankovich, B.N. Rodgers, J. Moore, L.T. Drzal, A.K. Mohanty, M. Misra. Kenaf natural fibre reinforced polypropylene composites: A discussion on manufacturing problems and solutions. *Composites: Part A* 2007; 38:1569-1580.
65. D.G. Dikobe, A.S. Luyt. Morphology and properties of polypropylene/ethylene vinyl acetate copolymer/wood powder blend composites. *Express Polymer Letters* 2009; 3(3):190-199.

66. M.G. Salemane, A.S. Luyt. Thermal and mechanical properties of polypropylene-wood powder composites. *Journal of Applied Polymer Science* 2006; 100:4173-4180.
67. C. Albano, J. González, M. Ichazo, D. Kaiser. Thermal stability of blends of polyolefins and sisal fiber. *Polymer Degradation and Stability* 1999; 66:179-190.
68. M. Behzad, M. Tajvidi, G. Ehrahimi, R.H. Falk. Dynamic mechanical analysis of compatibilizer effect on the mechanical properties of wood flour - high-density polyethylene composites. *IJE Transactions B: Applications* 2004 April; 17(1):95-104.
69. M. Tajvidi, R.H. Falk, J.C. Hermanson, C. Felton. Influence of natural fibres on the phase transitions in high-density polyethylene composites using dynamic mechanical analysis. *Seventh International Conference on Woodfiber-Plastic Composites (and other natural fibres)* May 19-20, 2003 Monona Terrace Community & Convention Center, Madison, Wisconsin, USA.
70. I.D. Danjaji, R. Nawang, U.S. Ishiaku, H. Ismail, Z.A.M. Mohd Ishak. Degradation studies and moisture uptake of sago-starch-filled linear low-density polyethylene composites. *Polymer Testing* 2002; 21:75-81.
71. W. Wang, M. Sain, P.A. Cooper. Study of moisture absorption in natural fibre plastic composites. *Composites Science and Technology* 2006; 66:379-386.
72. A. Arbelaiz, B. Fernández, J.A. Ramos, A. Retegi, R. Llano-Ponte, I. Mondragon. Mechanical properties of short flax fibre bundle/polypropylene composites: Influence of matrix/fibre modification, fibre content, water uptake and recycling. *Composites Science and Technology* 2005; 65:1582-1592.
73. T-T-L. Doan, H. Brodowsky, E. Mäder. Jute fibre/polypropylene composites II. Thermal, hydrothermal and dynamic mechanical behaviour. *Composites Science and Technology* 2007; 67:2707-2714.
74. S. Mohanty, S.K. Verma, S.K. Nayak. Dynamic mechanical and thermal properties of MAPE treated jute/HDPE composites. *Composites Science and Technology* 2006; 66:538-547.

Chapter 3: Experimental

3.1 Materials

3.1.1 High density polyethylene (HDPE)

HDPE was supplied in pellet form by DOW Chemicals, Republic of South Africa. It has an MFI of 8 g/10 min (ASTM D-1238), a molecular weight of $168\,000\text{ g mol}^{-1}$, a melting point of $130\text{ }^{\circ}\text{C}$, and a density of 0.954 g cm^{-3} .

3.1.2 Waxes

Hard paraffin wax (H1 wax) is a white powdered substance supplied by Sasol Wax, Sasolburg, Republic of South Africa. It is a normal straight chain hydrocarbon compound with an average molecular weight of 785 g mol^{-1} and a density of 0.94 g cm^{-3} at $25\text{ }^{\circ}\text{C}$. It has a softening point of $107\text{ }^{\circ}\text{C}$, congealing point of $98\text{ }^{\circ}\text{C}$ and a drop melting point of about $112\text{ }^{\circ}\text{C}$.

Soft paraffin wax (M3 wax) was supplied in powder form by Sasol Wax. It is a paraffin wax consisting of approximately 99% of straight short-chain hydrocarbons and few branched chains, and is primarily used in the manufacturing of candles. It has an average molar mass of 440 g mol^{-1} and a carbon distribution of C15-C78. It has a density of 0.90 g cm^{-3} at $25\text{ }^{\circ}\text{C}$ and a melting point range of $40\text{-}60\text{ }^{\circ}\text{C}$.

3.1.3 Wood flour (WF)

Pine wood flour was a cream-white powder supplied by Taurus furniture manufacturers, Phuthaditjhaba, Republic of South Africa. This wood flour has particle sizes $<150\text{ }\mu\text{m}$ and a density of 1.5 g cm^{-3} .

3.1.4 Other chemicals

Sodium hydroxide was supplied in pellet form by Associated Chemical Enterprises (ACE) (Pty) Ltd., Republic of South Africa. It was a chemically pure (CP) grade with an assay of 97%.

A chemically pure (CP) grade glacial acetic acid with an assay of 99.8% and a density of 1.05 g cm⁻³ was supplied by Laboratory Consumables & Chemical Supplies, Durban, Republic of South Africa.

3.2 Methods

3.2.1 Wood flour treatment

The received wood flour was pre-treated with a NaOH solution before preparing the natural fibre reinforced HDPE composites. It was immersed in 10% NaOH solution for 60 min., followed by washing with de-ionised water several times, and finally with a 0.25 M CH₃COOH solution [1]. The washings were continuously tested with a red litmus paper until they were neutral. It was then filtered under vacuum with a sintered glass funnel and dried in an oven at 105 °C for 24 hours. The dried agglomerated WF was then ground with a mortar and pestle to a fine powder and sieved with a 150 µm pore size sieve.

3.2.2 Blends and composites preparation

The sample ratios are shown in Table 3.1. All the samples were prepared by a melt mixing process using a Brabender Plastograph 50 mL internal mixer at 160 °C and 35 r.p.m. for 15 min. For the blends, the dry components were physically pre-mixed then fed into the heated mixer, whereas for the composites the WF was added into the Brabender mixing chamber within a minute after adding the pre-mixed HDPE/wax blends. The samples were then melt-pressed at 170 °C for 10 min under 100 kPa pressure using a hydraulic melt-press to form 14.7x14.7 cm² square sheets. Test samples were then cut from the sheets for various analyses.

Table 3.1 Sample ratios used for the preparation of the different blends and composites

HDPE (w/w)	HDPE/M3 wax (w/w)	HDPE/H1 wax (w/w)
100	80/20	80/20
-	70/30	70/30
-	60/40	60/40
-	50/50	50/50
-	40/60	40/60
HDPE/WF (w/w)	HDPE/WF/M3 wax (w/w)	HDPE/WF/H1 wax (w/w)
90/10	80/10/10	80/10/10
80/20	70/20/10	70/20/10
-	60/10/30	60/10/30
-	50/20/30	50/20/30
-	40/10/50	40/10/50
-	30/20/50	30/20/50

3.3 Analysis techniques

3.3.1 Scanning electron microscopy (SEM)

SEM is primarily a technique for the examination of surfaces in order to obtain crystallographic information from macroscopic crystals, in the form of electron channelling patterns. It uses a fine beam of electrons that is scanned across the sample surface. The instrument is fitted with a detector that collects the electrons emitted from each point of the surface. The developed current from the detector is then displayed on a cathode-ray tube that is scanned simultaneously with the electron probe. In this way the sample image is created line by line. The sample preparation depends on the nature of the sample, since appropriate samples may be examined directly with little or no prior preparation. Unfortunately, most polymers are not appropriate samples as they present specific problems. Firstly, they are poor conductors of electricity and therefore allow rapid charge build-up, resulting into image distortion. Secondly, there are molecular changes induced in the sample by the impinging electrons, resulting into radiation damages. Thus most polymers require prior preparations. These include: (i) conductive coatings, where suitable conducting films are used (gold, gold-palladium alloy or carbon) for good path to earth charge leakage, and is achieved by either evaporation or, more conveniently, sputtering; (ii) general chemical etching methods (solvent etching, degradation techniques and true etching) used to develop a relief related to the

underlying microstructure for enhanced surface topography; and (iii) plasma etching, used in connection with technological applications such as lithography and polymeric resist in electronics applications [2].

SEM analyses for this study were carried out using a Shimadzu ZU SSX-550 Superscan scanning electron microscope. Samples were frozen in liquid nitrogen, fractured by simply breaking the specimen into an appropriate size to fit the specimen chamber, and then mounted onto the holder. Conductive coating onto the sample surfaces was performed using gold by a sputtering method before recording the SEM micrographs.

3.3.2 Differential scanning calorimetry (DSC)

DSC is an analysis technique in which quantitative information on thermal transitions in materials may be obtained. In DSC, the difference in heat flow (power) to a sample and to a reference is monitored against time or temperature, while the temperature of the sample, in a specified atmosphere, is programmed. There are two recognized types of DSC. These are: (i) power-compensated DSC, where the sample and reference are heated by separate individual heaters, and the temperature difference is kept close to zero, while the difference in electrical power needed to maintain equal temperatures is measured; and (ii) heat flux DSC, where the sample and the reference are heated from the same source and the temperature difference is measured. This signal is converted to a power difference using the calorimetric sensitivity. The DSC may be used to measure: (i) physical transitions, including melting, crystalline phase changes, changes in liquid and crystalline states in polymers, phase diagrams, heat capacity, glass transitions, thermal conductivity, diffusivity and emissivity; and (ii) chemical reactions, including dehydration, decomposition, polymer curing, glass formation and oxidative attack [2-6].

In this study, two DSC instruments were used. DSC analyses for all the M3 wax containing PCM blends and composites were done in a Perkin-Elmer Pyris-1 differential scanning calorimeter, whereas the H1 wax PCM blends and composites were analysed on a Perkin-Elmer DSC7 differential scanning calorimeter. In both cases, the samples were run under nitrogen flow (flow rate 20 mL min⁻¹). The instruments were computer controlled and calculations were done using Pyris software. They were both calibrated using the onset temperatures of melting of indium and zinc standards, as well as the melting enthalpy of

indium. Samples (mass range 5-10 mg) were sealed in aluminium pans. All the M3 wax containing PCM blend and composite samples were heated from -40 to 160 °C, and those containing H1 wax were heated from 0 to 160 °C, both at a heating rate of 10 °C min⁻¹, and cooled at the same rate. For the second scan, the samples were heated and cooled under the same conditions. The peak temperatures of melting and crystallization, as well as melting and crystallization enthalpies, were determined from the second scans to eliminate any thermal history effects. All the DSC measurements were repeated three times on different samples for each composition. The melting and crystallization temperatures, as well as enthalpies, are reported as average values with standard deviations.

3.3.3 Thermogravimetric analysis (TGA)

TGA is technique whereby the mass of the sample is monitored against time or temperature while the temperature of the sample, in a specified atmosphere, is programmed. It is not all thermal events that lead to a change in mass of the sample (e.g. melting, crystallization or glass transition), but there are important exceptions that include desorption, absorption, sublimation, vaporization, oxidation, reduction and decomposition. TGA is mainly used to characterize the decomposition and thermal stability of materials under a variety of conditions, and to examine the kinetics of the physico-chemical processes occurring in the sample. The mass change features of a material depend on the experimental conditions employed. The following factors influence the characteristics of the recorded TG curve: (i) sample mass; (ii) sample volume; (iii) physical form of a sample; (iv) the shape and nature of the sample holder; and (v) the scanning rate [2-6].

The TGA analyses were carried out on a Perkin-Elmer TGA7 thermogravimetric analyser. The samples (mass range 5-10 mg) were heated from 30 to 650 °C at a heating rate of 20 °C min⁻¹ under flowing nitrogen (flow rate 20 mL min⁻¹). The mass-temperature profile was analysed for the amount or percent mass loss at any given temperature, for any non-combusted residue at the final temperature, and for temperatures of various sample degradation processes. The maximum analysis temperature was selected so that the specimen mass was stable at the end of the experiment for all chemical reactions to be completed. In this study, the TGA technique was mainly used to examine the thermal stability of the samples.

3.3.4 Dynamic mechanical analysis (DMA)

DMA is a technique in which the storage and loss modulus of the sample, under oscillating load, are monitored against time, temperature or frequency of oscillation, while the temperature of the sample in a specified atmosphere is programmed. It requires that the applied stress or strain is varied in a periodic way. The deformation can be applied sinusoidally, in a constant (or step fashion), or at a fixed rate. DMA determines changes in sample properties that result from changes in temperature, time, frequency, force and strain. It uses samples that are in bulk solid, film, fibre, gel, or viscous liquid form. Interchangeable clamps of a DMA instrument are employed to allow measurements of many properties including modulus, damping, creep, stress relaxation, glass transitions, and softening points of materials. In DMA the sample is clamped between the ends of two parallel arms with adjustable distance to accommodate a wide range of sample lengths. The design of the instrument may allow a fixed frequency mode, where the frequency and amplitude are selected by the operator, or a resonant frequency mode, where the instrument allows the sample to oscillate at its natural resonant frequency. DMA has a range of applications extending from the measurement of solid-solid transitions, relaxation kinetics, film formation to helping define the morphology of complex, phase separated polymer systems, and characterising cross-linking behaviour [2-7].

The dynamic mechanical properties of the blends and composites in this project were investigated using a Perkin Elmer Diamond DMA. The settings for the analyses were as follows:

Frequency	1 Hz
Amplitude	20 μm
Temperature range	-140 to +100 $^{\circ}\text{C}$
Temperature program mode	Ramp
Measurement mode	Bending (dual cantilever)
Heating rate	5 $^{\circ}\text{C min}^{-1}$
Preloading force	0.02 N
Sample length	20 mm
Sample width	12.0 – 12.5 mm
Sample thickness	1.0 – 1.3 mm

3.3.5 Tensile testing

Tensile testing is the mechanical or physical testing of polymer materials carried out under an extension force. These tests are also used to assess the ageing or chemical resistance of materials. They are, however, of limited use in predicting material performance due to limited information provided by the tests. Tensile properties are useful indicators for quality control purposes. The following factors should be taken into consideration whenever a test is carried out: (i) Polymers are viscoelastic materials, therefore their properties are dependent on temperature, humidity, stretching speed or timescale of the test, and the history of the sample; (ii) Tensile testing provides limited information, and therefore no accurate prediction of performance can be made without extensive product testing; and (iii) Variability in the test results will be found due to variation in the sample material, sample preparation, test procedure and test machine accuracy [2].

A Hounsfield H5KS universal testing machine was used for tensile analysis of the samples. The dumb-bell shaped samples (Figure 3.1) were tested at a speed of 50 mm min^{-1} under a load-cell force of 250.0 N. About five test specimens for each sample were analysed, and the averages and standard deviations of the different tensile properties reported.

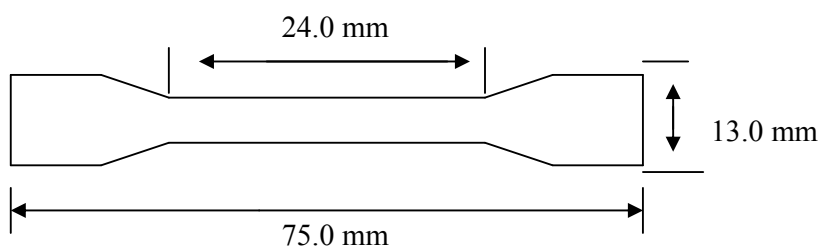


Figure 3.1 Dumb-bell shaped tensile testing sample

3.3.6 Water absorption

Water absorption analysis is a technique designed to assess the performance of fibre-reinforced polymer matrices in applications of hot-wet environments. Since structural composites are exposed to a range of hygrothermal conditions through their design life, it is necessary to determine their mechanics of degradation and levels of performance retention.

Composites with common structural polymer matrices often absorb moisture and this has profound effects on their mechanical, thermal, dielectric and barrier property performance. There are recognized ways in which water could penetrate these fibre-reinforced polymer composites. They are: (i) partly conduction by diffusion, which involves transportation of water molecules into the matrix and, in some cases, into the fibres; (ii) rapid conduction by diffusion (i.e. water wicking), which is transportation of the water molecules along the fibre-matrix interface; and (iii) percolating flow and storage of water molecules in micro-cracks. The latter two are said to be damage-dependent mechanisms that increase both the rate and maximum capacity of moisture absorption [8].

Test samples were initially weighed while dry, and then placed in de-ionised water at room temperature. The samples' water absorption was monitored for about 4 days at 10 and 14 hours intervals. At every interval the samples were removed from the water, dried with a water absorbent paper towel and weighed, and then replaced in the water. The percentage water absorption was calculated using Equation 3.1.

$$\%W_a = \frac{W_f - W_i}{W_i} \times 100 \quad (3.1)$$

where W_a is the total water absorbed, W_f is the final weight of the sample after a certain time t of water immersion, and W_i is the initial sample mass.

3.4 References

1. P.V. Joseph, K. Joseph, S. Thomas. Effect of processing variables on the mechanical properties of sisal-fibre-reinforced polypropylene composites. *Composites Science and Technology* 1999; 59:1625-1640.
2. B.J. Hunt, M.I. James. *Polymer Characterization*, 1st edition. Blackie Academic & Professional, London, 1997.
3. P.J. Haines. *Thermal Methods of Analysis: Principles, Applications and Problems*, 1st edition. Blackie Academic & Professional, London, 1995.
4. E.L. Charsley, S.B. Warrington. *Thermal Analysis - Techniques and Applications*, Royal Society of Chemistry, Leeds, 1992.

5. T. Hatakeyama, F.X. Quinn. Thermal Analysis: Fundamentals and Applications to Polymer Science. John Wiley & Sons, Chichester, 1994.
6. M.E. Brown. Introduction to Thermal Analysis: Techniques and Applications, 1st edition. Chapman & Hall, London, 1988.
7. <http://www.mrl.ucsb.edu/mrl/centralfacilities/polymer/DMA.html>
8. C.J. Tsenoglou, S. Pavlidou, C.D. Papaspyrides. Evaluation of interfacial relaxation due to water absorption in fibre-polymer composites. Composites Science and Technology 2006; 66:2855-2864.

Chapter 4: Results and discussion

4.1 Scanning electron microscopy (SEM)

The SEM micrographs of various alkali treated wood flour (WF) composite systems are shown in Figures 4.1 to 4.3. In Figure 4.1 the SEM micrographs, at two different magnifications, of the 80/20 w/w HDPE/WF composite are shown. The images show no visible WF fractures. The crystalline structure of the HDPE matrix is clearly visible in the areas around the WF particles. The WF particles seem clustered (A in Figure 4.1a) within the polyethylene matrix, indicating poor filler dispersion. There are some gaps (B in Figure 4.1a) between the WF particles and the HDPE matrix, as well as some fibre pull-outs creating holes with smooth walls in the polymer matrix (C in Figure 4.1a). There is, however, evidence of some intimate contact between WF and HDPE (D in Figure 4.1b), probably as a consequence of the alkali treatment of the WF that resulted into a rough surface allowing the polymer to adhere onto it through mechanical interlocking [1,2]. Aziz and Ansell [8] reported on the surface topography of untreated and alkaliized fibres. They found that the treatment of hemp and kenaf with 6% NaOH removed the wax, oil and impurities and roughened the surface of the fibre bundles. Although there may be improved interaction between the WF and HDPE due to the WF pre-treatment with an alkali, there was clearly still a poor interfacial adhesion between the HDPE matrix and the WF. This is in agreement with other published work on natural fibre reinforced HDPE composites [3-7].

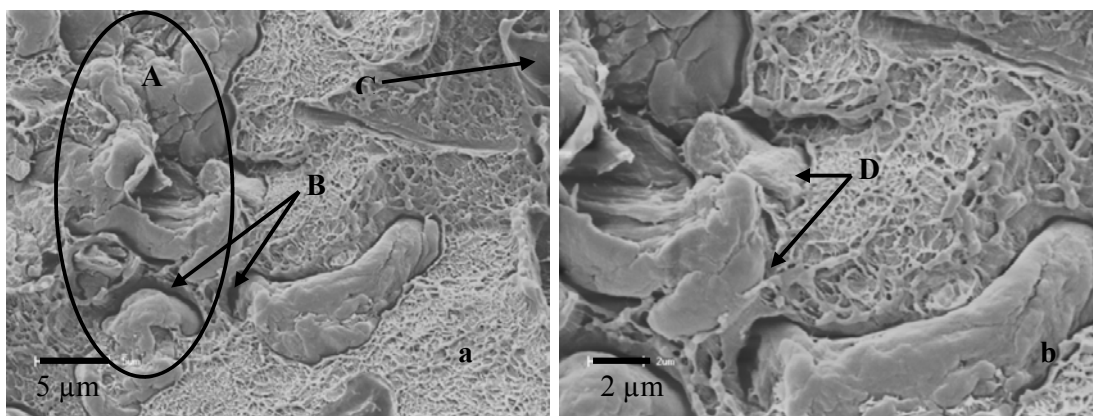


Figure 4.1 SEM micrographs of 80/20 w/w HDPE/WF (alkali-treated) composite

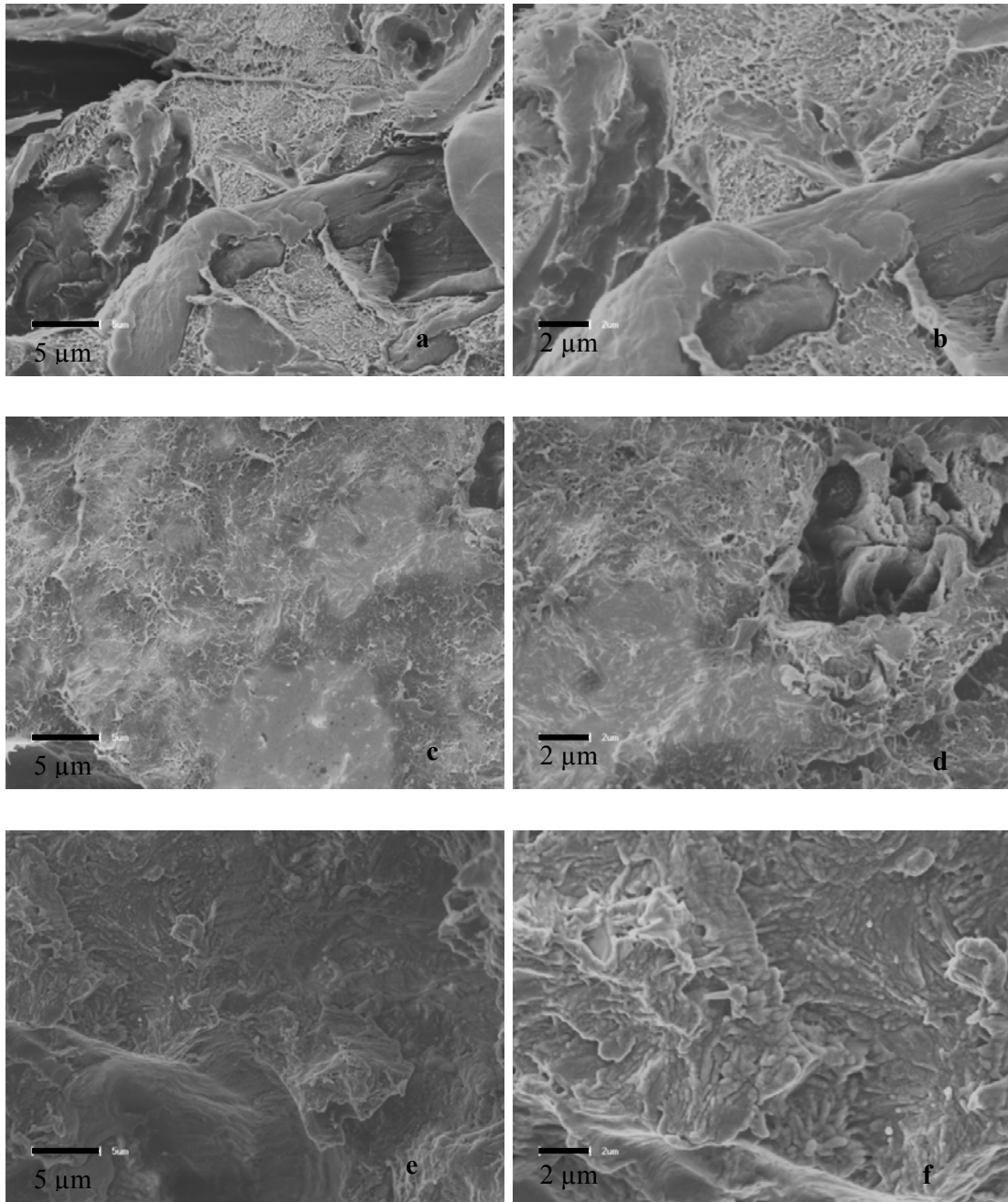


Figure 4.2 SEM micrographs of 70/20/10 w/w HDPE/WF/M3 wax (a & b), 50/20/30 w/w HDPE/WF/M3 wax (c & d), and 30/20/50 w/w HDPE/WF/M3 wax (e & f) composites

Figure 4.2 presents the micrographs of HDPE/20% WF (alkali treated) and various contents of M3 wax. It seems as if the M3 wax crystallized separately from the HDPE matrix. This separate crystallization behaviour of M3 wax may be the result of its low molecular weight, and therefore lower viscosity. Therefore it is easy for the M3 wax to separate from the blends [10]. Figures 4.2a and 4.2b clearly show a much more intimate contact between WF and the matrix, although it seems as if the WF is primarily covered by the wax. As the wax content increases, it becomes more difficult to observe individual WF particles, and to distinguish between the HDPE and wax phases (Figure 4.2 (c-f)). This is probably the consequence of higher affinity between WF and the wax, as well as the wax crystallizing separately in the amorphous phase of the HDPE. The WF is most likely to be situated in this amorphous phase. Prior to the alkali treatment, the WF was covered by its natural wax and other components as described by Aziz and Ansell [8], which were removed in the treatment process. Therefore it seems favourable for M3 wax to be attracted to the rough WF surfaces, also because of its shorter chains that will more easily penetrate the pores left after the alkali treatment of the WF.

Figure 4.3 shows the SEM micrographs of the fractured surfaces of HDPE/WF (20 wt.%) (alkali treated) and various contents of H1 wax. It can be seen that the crystalline structure of HDPE is clearly visible in the composites, but it varies with wax content. This may be the consequence of the miscibility of the H1 wax with the HDPE matrix as observed in the DSC results (discussed later in section 4.2). It is clear that the WF particles are covered by the H1 wax, indicating a fairly good affinity between the WF and the paraffin wax. All the photos show gaps around the WF particles, and in some photos there is evidence of fibre pull-out during fracture. For the highest wax content composite samples, a small portion of the wax that has crystallized separately from the polymer matrix is seen, and this is also observed in the DSC results (discussed later in section 4.2).

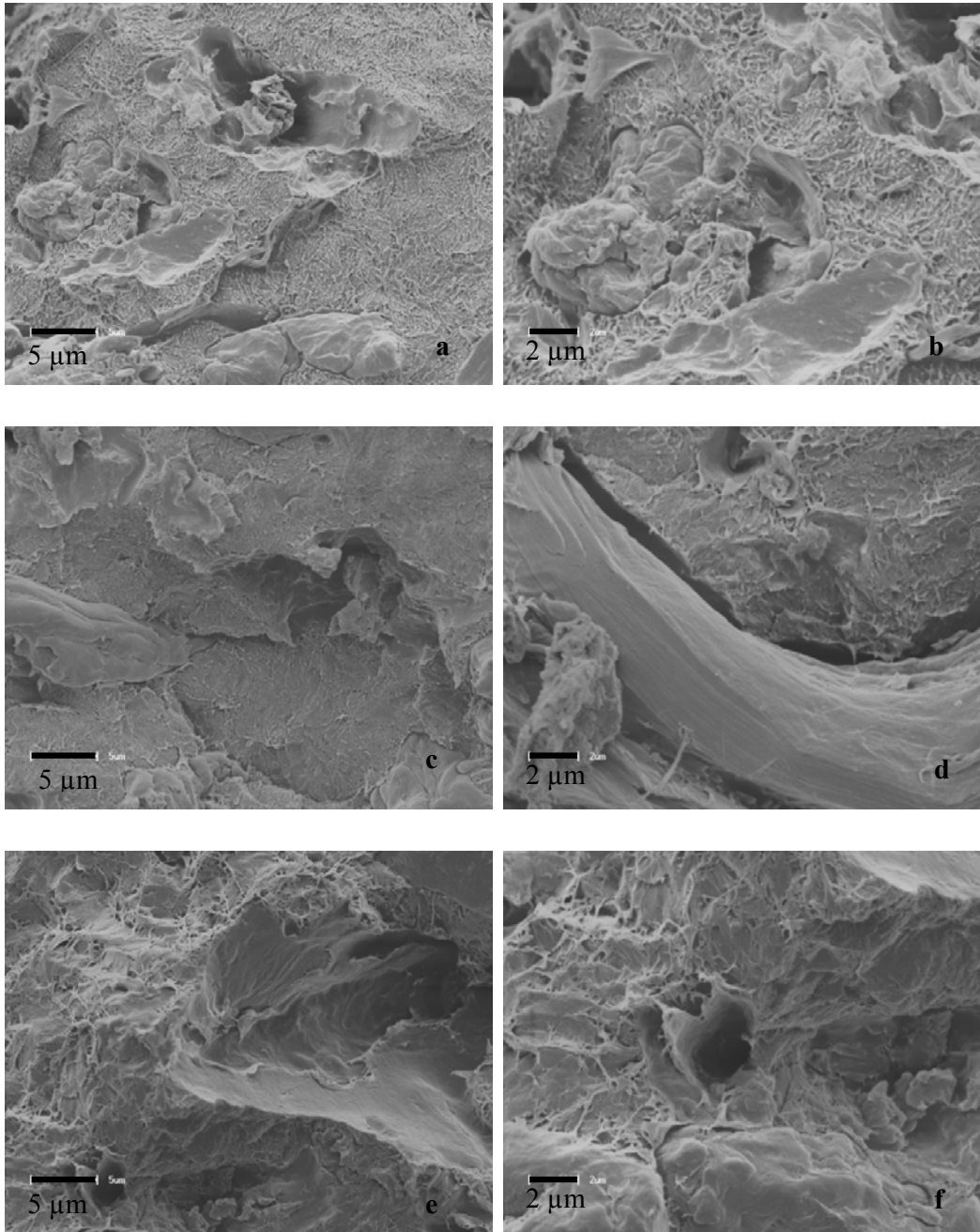


Figure 4.3 SEM micrographs of 70/20/10 w/w HDPE/WF/H1 wax (a & b), 50/20/30 w/w HDPE/WF/H1 wax (c & d), and 30/20/50 w/w HDPE/WF/H1 wax (e & f) composites

4.2 Differential scanning calorimetry (DSC)

The DSC results for the HDPE/paraffin wax blends and the HDPE/WF/paraffin wax composites are summarized in Figures 4.4 to 4.12. The peak temperatures of melting, melting enthalpies and the calculated melting enthalpies are summarized in Table 4.1 for the M3 wax containing systems and in Table 4.2 for the H1 wax systems. All the reported DSC heating results were obtained from the second scan to eliminate the effect of thermal history. The calculated melting enthalpy values were determined according to Equation 4.1.

$$\Delta H_m^{add} = \Delta H_{m,PE} w_{PE} + \Delta H_{m,w} w_w \quad (4.1)$$

where $\Delta H_{m,PE}$, $\Delta H_{m,w}$, ΔH_m^{add} are respectively the specific melting enthalpies of PE, wax and blends, and w_{PE} , w_w are the weight fractions of PE and wax in the blends.

4.2.1 HDPE/M3 wax PCM blends and HDPE/WF/M3 wax composites

The DSC heating results of the HDPE and the M3 paraffin wax are shown in Figure 4.4. The HDPE has only one endothermic peak, while the paraffin wax shows multiple peaks. The HDPE has a peak maximum at 136 °C with an enthalpy of 158 J g⁻¹, whereas the M3 wax has two peaks at 33 °C (peak shoulder) and 59 °C (peak maximum). Its observed melting enthalpy is 150 J g⁻¹, which is lower than that of HDPE. It is observed that the M3 paraffin wax melts over a broad temperature range. The two endothermic peaks may be referred to as a solid-solid transition (at the peak shoulder) and melting [9-11]. In the case of HDPE/M3 wax blends, there are two separate endothermic peaks that are related to the melting peaks of the M3 wax and the HDPE. This behaviour indicates that the HDPE is immiscible with the M3 wax at all the investigated compositions. This was also reported by Mpanza and Luyt [12] for LDPE/M3 wax blends. They found that the LDPE and M3 wax are only miscible up to 5 wt% M3 wax content. Above this wax content there was partial immiscibility, and a portion of the M3 wax probably crystallized in the amorphous phase of LDPE. This was also observed in our SEM results (discussed in section 4.1), where the M3 wax was observed to crystallize separately from the HDPE.

The melting peak temperatures of the blends are shown in Table 4.1. It is observed that the melting temperatures of M3 wax remained fairly constant within experimental error with increasing wax content. However, an increase in wax content resulted into a decrease in the melting peak temperatures of HDPE. This is probably the result of the plasticization effect of the M3 wax on the HDPE matrix. This behaviour was also reported by Krupa *et al.* [9] and Mpanza and Luyt [12] in their studies of PP/paraffin wax shape stabilized phase change materials and LDPE/paraffin wax blends. Krupa *et al.* [9] observed that the melting temperature of the PP component in the blends decreased with an increase in Wax S content. They explained this in terms of the plasticization of the PP matrix by wax. Mpanza and Luyt [12] found that an increase in M3 wax content resulted to a very slight decrease in the onset and peak temperatures of melting of the LDPE/M3 wax blends. Since M3 wax has a higher crystallinity than LDPE, this was attributed to M3 wax that inhibited the crystallization of LDPE by acting as a plasticizer.

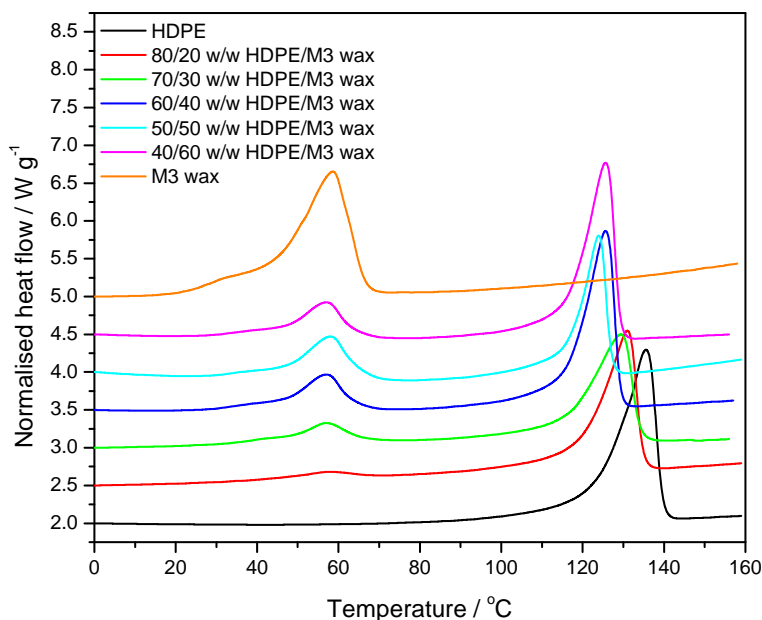


Figure 4.4 DSC heating curves of HDPE, M3 wax and the HDPE/M3 wax blends

Table 4.1 Summary of DSC results for HDPE/M3 wax blends and HDPE/WF/M3 wax composites

Samples	$T_{p,m} \pm sT_{p,m} / ^\circ\text{C}$	$\Delta H_m^{\text{obs}} \pm s\Delta H_m^{\text{obs}} / \text{J g}^{-1}$	$\Delta H_m^{\text{calc}} / \text{J g}^{-1}$
HDPE	135.9 ± 2.6	157.6 ± 13.2	-
M3 wax	$58.8^{\text{a}} \pm 1.9$ $33.0^{\text{b}} \pm 1.0$	149.5 ± 4.1	-
HDPE/M3 wax (w/w)			
80/20	55.9 ± 1.9	6.4 ± 1.6	29.9
	131.4 ± 2.0	102.2 ± 1.1	126.1
70/30	57.7 ± 0.8	13.6 ± 5.3	44.9
	130.4 ± 0.9	86.9 ± 2.5	110.3
60/40	57.3 ± 1.5	23.4 ± 1.2	59.8
	126.0 ± 1.5	93.3 ± 11.9	94.6
50/50	56.8 ± 1.3	32.7 ± 21.8	74.8
	124.7 ± 1.8	89.9 ± 15.4	78.8
40/60	56.9 ± 1.8	32.2 ± 23.1	89.7
	125.1 ± 2.5	82.8 ± 32.5	63.0
HDPE/WF (w/w)			
90/10	138.1 ± 0.5	156.7 ± 8.2	141.8
80/20	135.8 ± 1.9	121.9 ± 11.0	126.1
HDPE/WF/M3 wax (w/w)			
80/10/10	55.5 ± 0.6	1.5 ± 0.1	15.0
	132.9 ± 0.6	135.6 ± 3.0	126.1
60/10/30	56.9 ± 0.1	20.7 ± 1.8	44.9
	127.9 ± 0.7	105.2 ± 7.8	94.6
40/10/50	57.9 ± 0.3	55.6 ± 4.1	74.8
	123.4 ± 0.4	75.6 ± 2.6	63.0
70/20/10	55.2 ± 0.5	1.9 ± 0.3	15.0
	132.6 ± 0.9	121.4 ± 5.3	110.3
50/20/30	58.7 ± 1.4	23.5 ± 2.2	44.9
	129.0 ± 2.3	85.2 ± 3.4	78.8
30/20/50	58.7 ± 0.1	58.5 ± 4.7	74.8
	122.4 ± 0.3	53.8 ± 2.7	47.3

$T_{p,m}$, ΔH_m^{obs} , ΔH_m^{add} and s are respectively the peak temperature of melting, observed melting enthalpy, calculated melting enthalpy and standard deviation, while a and b respectively indicate the first (maxima) and second (shoulder) peaks in the wax melting curve.

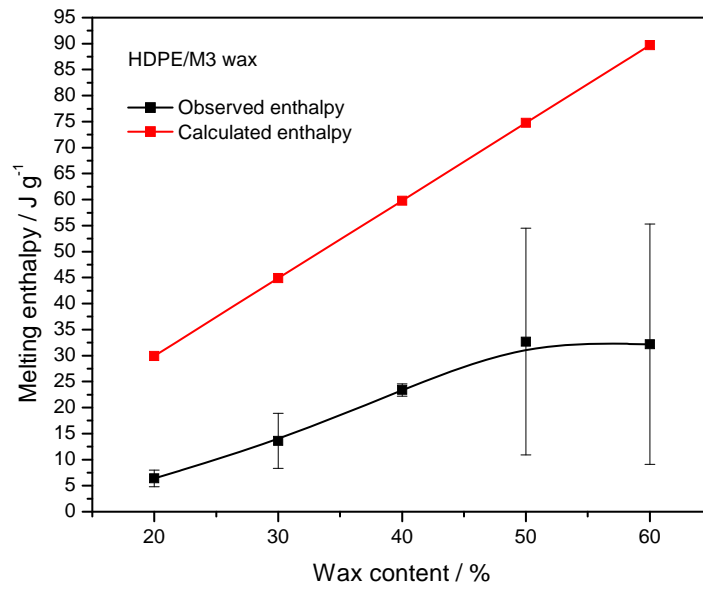


Figure 4.5 Comparison of experimental and calculated melting enthalpies of the M3 wax melting as a function of wax content in HDPE/M3 wax blends

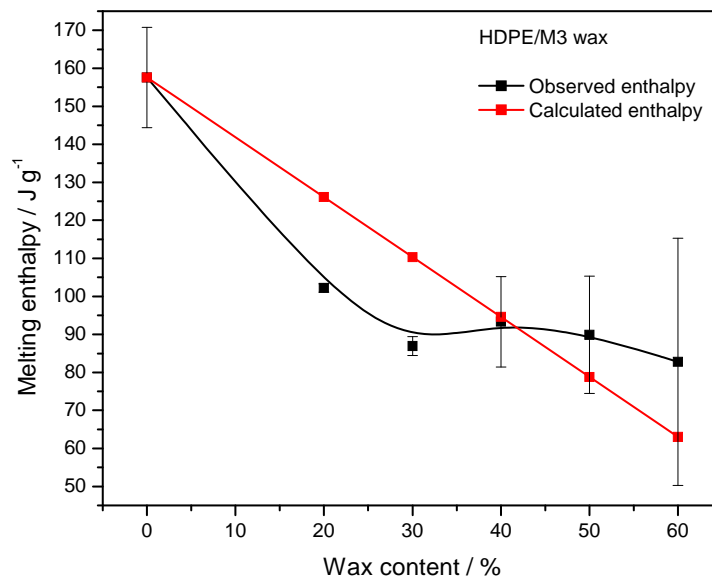


Figure 4.6 Comparison of experimental and calculated melting enthalpies of the HDPE melting as a function of wax content in HDPE/M3 wax blends

Figures 4.5 and 4.6 show the experimentally observed and calculated melting enthalpies, of respectively M3 wax melting and HDPE melting, as function of wax content. The experimentally observed melting enthalpies of the M3 wax are lower than the calculated enthalpies (Figure 4.5) for all the investigated wax contents. This may be the result of wax leakage from the blends during sample preparation. However, the difference between the two enthalpies increases with an increase in wax content. This probably indicates that some portion of the M3 wax partially co-crystallized with HDPE. The standard deviations are large at high wax contents. This shows the inhomogeneity of the PCM blends and uneven wax dispersion within the polymer matrix at higher wax contents. In case of HDPE melting (Figure 4.6), the experimentally observed melting enthalpies are lower than the calculated enthalpies at low wax contents. This may be due to the M3 wax plasticizing the HDPE matrix. However, the observed enthalpies are higher than the calculated enthalpies at higher wax contents, but the calculated enthalpies still fall within the error bars for the observed enthalpies. This supports the partial co-crystallization of the M3 wax with the HDPE at higher wax contents. Here the standard deviations for the observed melting enthalpies are also large at higher wax contents, which support the conclusion on the uneven distribution of the wax in the HDPE matrix.

The DSC heating curves of the HDPE/WF composites are shown in Figure 4.7. There is only one endothermic peak for all the composites. The melting peak temperatures of the composites remained fairly constant within experimental error with the incorporation of WF in HDPE matrix. As can be seen in Figure 4.8 and Table 4.1, the observed melting enthalpy of the composites is higher than the calculated enthalpy for 10% WF, but slightly lower (and still within experimental error) for 20% WF. It seems as if the WF particles acted as nucleating sites for the crystallization of HDPE at 10% WF, but when the WF content is higher, it seems as if the WF particles form aggregates/clusters (see SEM results) which immobilized the polymer chains and restricted the HDPE crystallization.

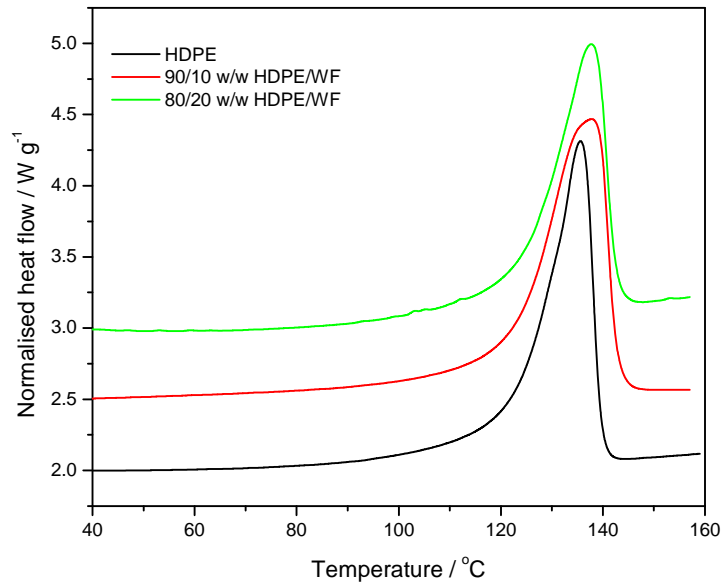


Figure 4.7 DSC heating curves of HDPE and the HDPE/WF composites

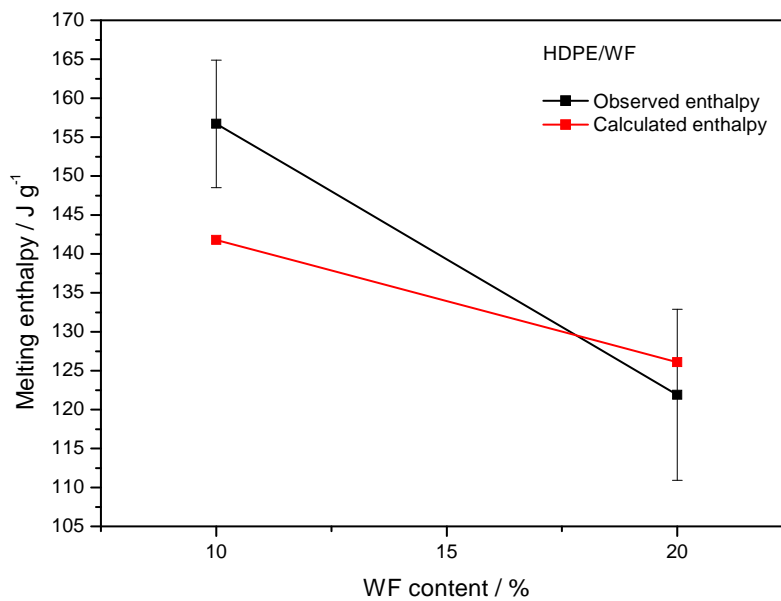


Figure 4.8 Comparison of experimental and calculated melting enthalpies of the HDPE melting as a function of WF content in HDPE/WF composites

Figures 4.9 and 4.10 depict the DSC heating curves of the HDPE/WF/M3 wax composites. The two figures show similar behaviour of two separate endothermic peaks (as in the case of the HDPE/M3 wax blends) for all the investigated M3 wax contents. This is a consequence of the high level of immiscibility of HDPE and M3 wax, even in the presence of WF. At low wax contents the melting temperatures of the wax are lower than that of pure wax, and the melting temperatures for the wax increased, whereas those of HDPE decreased with wax content (Table 4.1). The lower wax melting temperature at low wax contents are attributed to a lower wax crystallinity because most of the wax penetrated the WF pores which increased the amorphous fraction of the wax. At higher wax contents the WF pores were saturated with wax and the remaining wax crystallized around the WF particles. This increased the wax crystallinity and therefore the wax melting temperature. The decrease in HDPE melting temperature with increasing wax content is probably the result of the plasticizing effect of the molten wax in the polymer matrix.

The melting enthalpies of M3 wax at 10 and 20% WF contents are shown in Figures 4.11 and 4.12. In both cases, it can be seen that the experimentally observed enthalpies are lower than the calculated enthalpies and that the differences between them did not change significantly. This may be explained in terms of the following four situations: (i) since HDPE crystallizes first, there may be some inhibition of wax crystallization because of the isolation of single wax chains inside the amorphous phase of HDPE; (ii) part of the wax that was in contact with HDPE in the melt, may have co-crystallized with HDPE; (iii) part of the wax may have penetrated the pores of the WF particles, increasing the 'amorphous' part of the wax; (iv) part of the wax may have been adsorbed onto the surfaces of the WF particles, also increasing the 'amorphous' part of the wax. The standard deviations were fairly small, indicating that samples were more homogeneous.

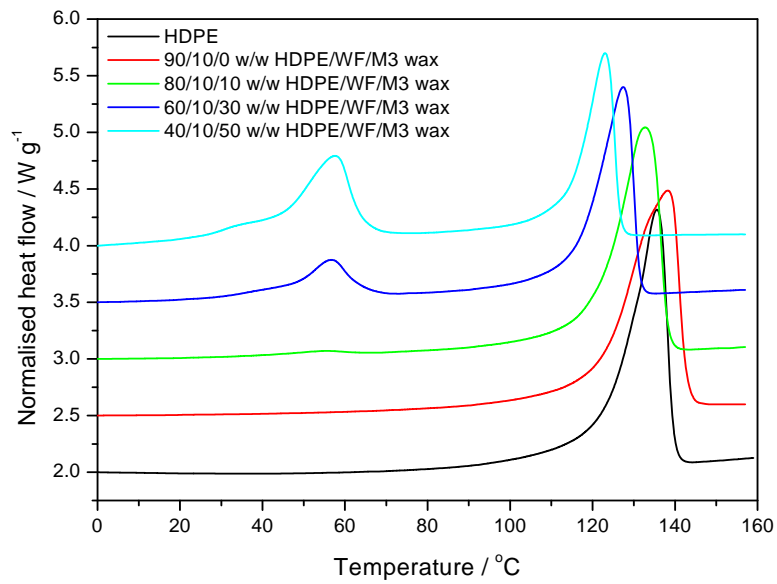


Figure 4.9 DSC heating curves of HDPE/WF/M3 wax PCM composites at 10% WF content

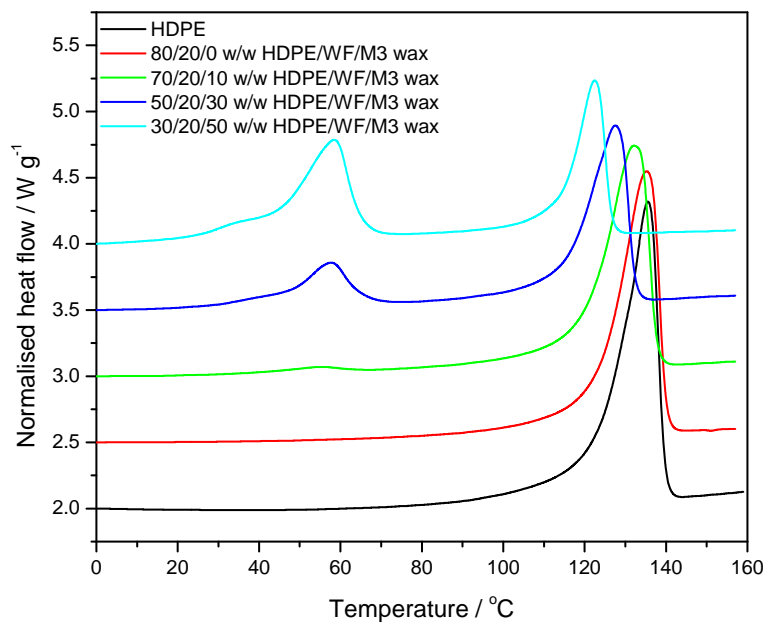


Figure 4.10 DSC heating curves of HDPE/WF/M3 wax PCM composites at 20% WF content

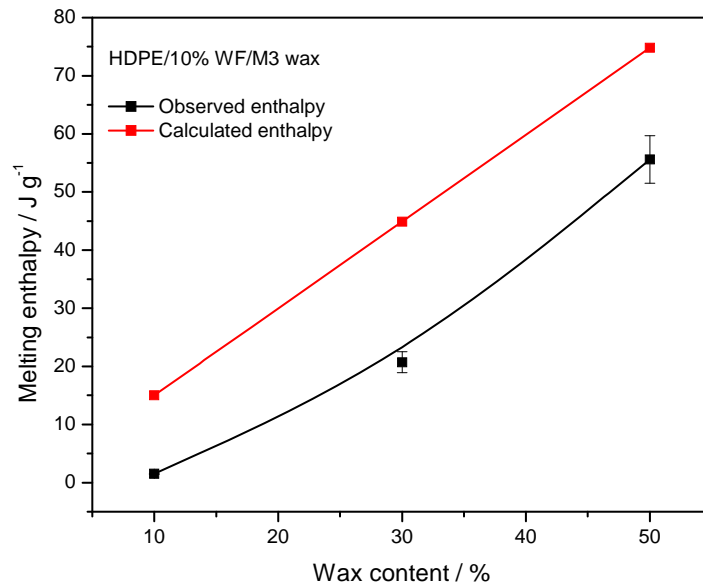


Figure 4.11 Comparison of experimental and calculated melting enthalpies of the M3 wax melting as a function of wax content in HDPE/10% WF/M3 wax composites

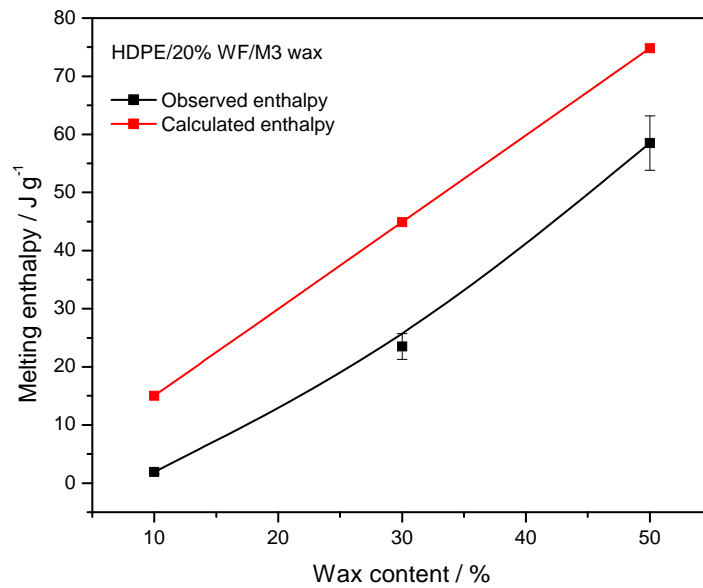


Figure 4.12 Comparison of experimental and calculated melting enthalpies of the M3 wax melting as a function of wax content in HDPE/20% WF/M3 wax composites

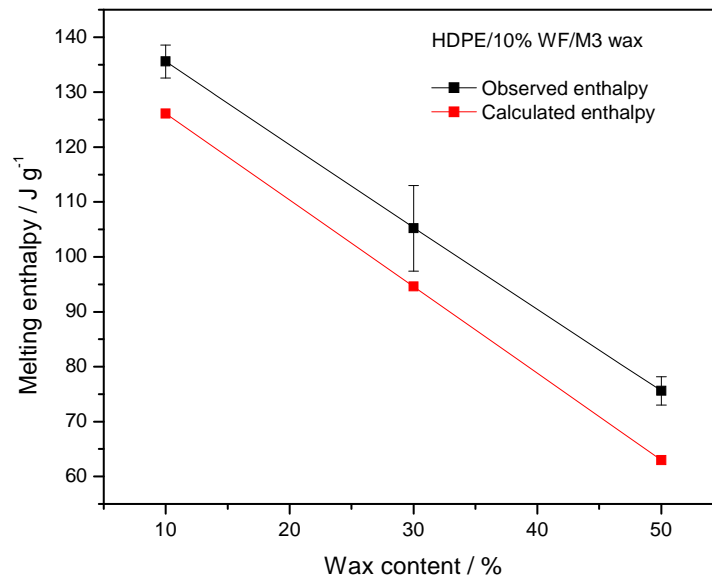


Figure 4.13 Comparison of experimental and calculated melting enthalpies of the HDPE melting as a function of wax content in HDPE/10% WF/M3 wax composites

The melting enthalpies of the HDPE in the HDPE/WF/M3 wax composites are shown in Figures 4.13 and 4.14 for the 10 and 20% WF content samples. In both cases, the experimentally observed enthalpies are higher than the calculated enthalpies with almost constant differences. This is probably the result of the partial co-crystallization of some of the M3 wax with the HDPE in the presence of WF. The standard deviations are small, indicating that the samples were fairly homogeneous.

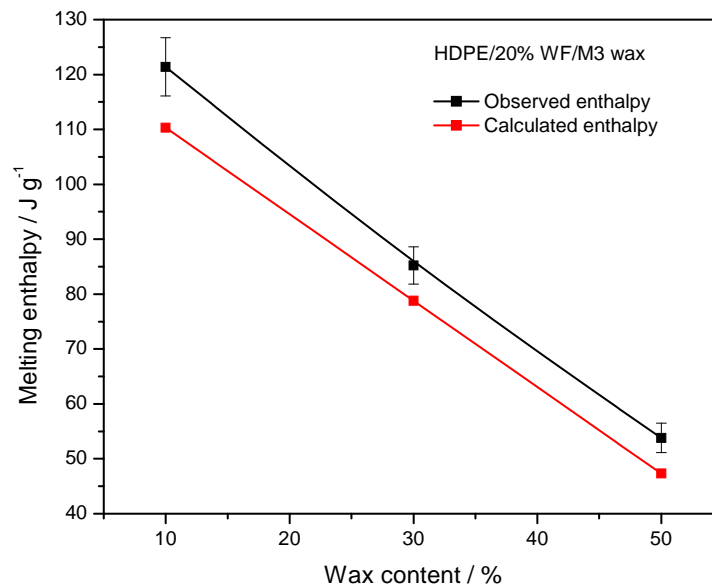


Figure 4.14 Comparison of experimental and calculated melting enthalpies of the HDPE melting as a function of wax content in HDPE/20% WF/M3 wax composites

4.2.2 HDPE/H1 wax blends and HDPE/WF/H1 wax composites

The DSC heating results of the HDPE/H1 wax blends and the HDPE/WF/H1 wax composites are shown in Figures 4.15 to 4.20, and the DSC data are summarized in Table 4.2. H1 wax has a broad melting temperature range and three endothermic peaks (Figure 4.15) at 83 (main peak), 93 and 105 °C. This wax has a melting enthalpy of 194 J g⁻¹, which is higher than that of HDPE. According to Luyt and Krupa [11] these multiple endothermic peaks for hard paraffin waxes are the result of the melting of crystalline fractions with different molecular weight distributions. The HDPE/H1 wax blends show two endothermic peaks, one in the melting temperature region of HDPE, and a second weak peak in the melting temperature region of H1 wax. This indicates that only part of the wax crystallized separately in the amorphous phase of HDPE, while some must have co-crystallized with HDPE. This indicates partial miscibility of the H1 wax with HDPE.

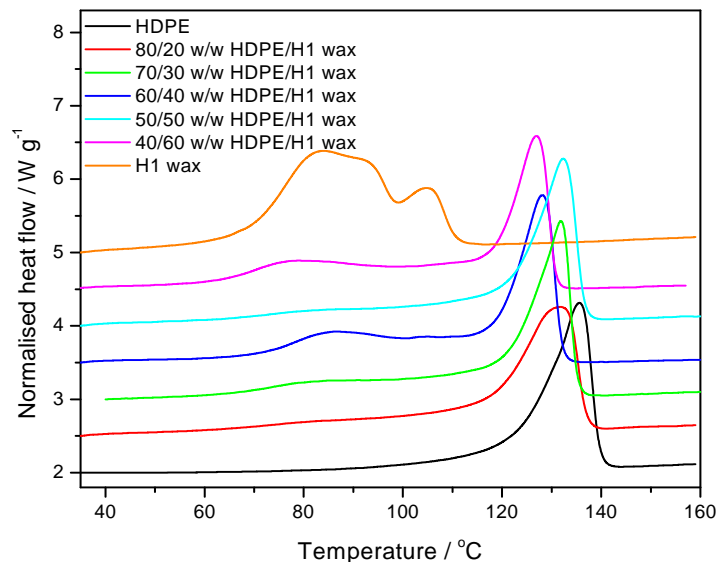


Figure 4.15 DSC heating curves of HDPE, H1 wax and the HDPE/H1 wax blends

The melting peak temperatures of the PCM blends are shown in Table 4.2. The presence of wax in HDPE seems to cause a slight decrease in melting temperature, but there is no definite trend. The graphs of experimentally observed enthalpies and calculated enthalpies as function of wax content are shown in Figure 4.16. The experimentally observed enthalpies are lower than the calculated enthalpies with an almost constant difference in values. However, the calculated enthalpies values fall within the experimental error of the observed enthalpies. If the differences are real, then it is most likely the consequence of small wax crystals in the amorphous phase of the polymer that must have influenced the polymer crystallization mechanism. There are large standard deviations on the experimentally observed enthalpies and this indicates that the wax was unevenly distributed in the blends.

Table 4.2 Summary of DSC results for HDPE/H1 wax blends and HDPE/WF/H1 wax composites

Samples	$T_{p,m} \pm s T_{p,m} / ^\circ\text{C}$	$\Delta H_m^{\text{obs}} \pm s \Delta H_m^{\text{obs}} / \text{J g}^{-1}$	$\Delta H_m^{\text{calc}} / \text{J g}^{-1}$
HDPE	135.9 ± 2.6	157.6 ± 13.2	-
H1 wax	$83.4^{\text{a}} \pm 2.6$ $92.7^{\text{b}} \pm 0.6$ $105.7^{\text{c}} \pm 0.6$	194.2 ± 10.9	-
HDPE/H1 wax (w/w)			
80/20	132.2 ± 0.7	154.4 ± 17.9	164.9
70/30	132.6 ± 2.0	156.6 ± 11.4	168.6
60/40	128.7 ± 1.1	164.2 ± 14.5	172.3
50/50	132.4 ± 0.5	166.2 ± 9.5	175.9
40/60	127.4 ± 1.7	172.9 ± 12.3	179.5
HDPE/WF (w/w)			
90/10	138.1 ± 0.5	156.7 ± 8.2	141.8
80/20	135.8 ± 1.9	121.9 ± 11.0	126.1
HDPE/WF/H1 wax (w/w)			
80/10/10	132.7 ± 0.3	143.1 ± 7.1	145.5
60/10/30	129.7 ± 0.5	152.8 ± 5.0	152.8
40/10/50	126.2 ± 0.4	154.0 ± 2.6	160.3
70/20/10	132.7 ± 0.4	120.2 ± 3.0	129.7
50/20/30	129.8 ± 1.0	130.7 ± 2.2	137.1
30/20/50	125.9 ± 0.4	146.0 ± 6.0	144.4

$T_{p,m}$, ΔH_m^{obs} , ΔH_m^{add} and s are respectively the peak temperature of melting, observed melting enthalpy, additive rule calculated melting enthalpy and standard deviation, while a, b and c respectively indicate the first (maxima), second (shoulder) and third (minor) peaks in the wax melting peak

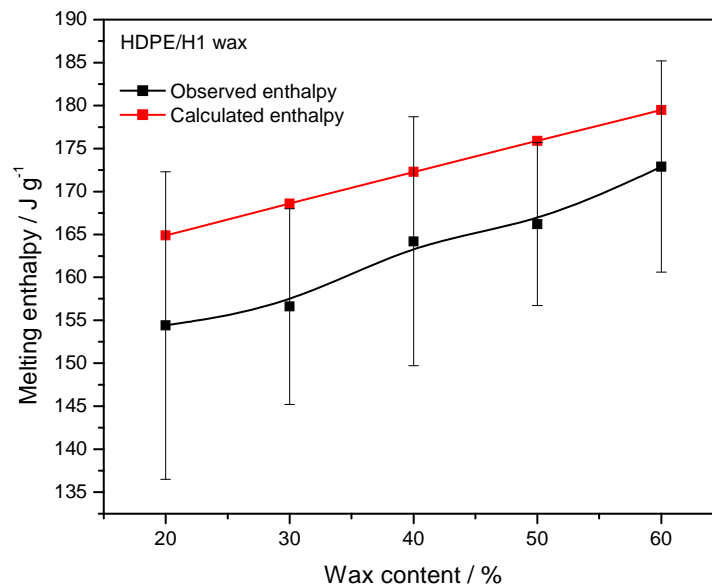


Figure 4.16 Comparison of experimental and calculated melting enthalpies as a function of wax content in HDPE/H1 wax blends

Figures 4.17 and 4.18 show the DSC curves of the HDPE/WF/H1 wax composites for 10 and 20% WF content. Only one endothermic peak is visible in the melting temperature region of the polymer (from both figures) for the lower wax content samples. This is indicative of the high level of miscibility of the wax and the polymer in the presence of WF. However, the emergence of a second peak is observed for higher wax contents, which is indicative of the partial immiscibility of the wax and polymer. It seems as if part of the H1 wax, at high wax contents, co-crystallizes with the polymer and part of it either crystallizes separately in the amorphous phase of the polymer, or crystallizes on the surfaces of the WF particles. Based on the SEM observations (section 4.1) the latter is more probable. A clear decrease in melting temperature of the HDPE in the composites with increasing wax content is observed (Table 4.2). This is attributed to the plasticizing effect of the wax.

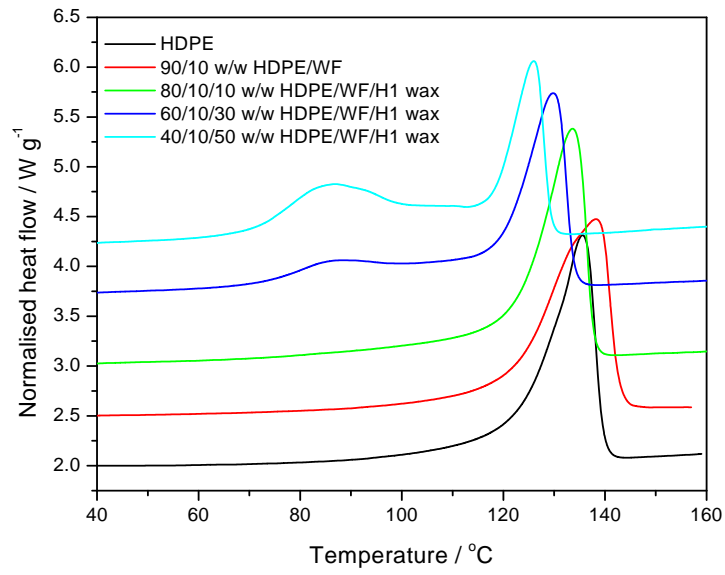


Figure 4.17 DSC heating curves of HDPE, the HDPE/WF composite and the HDPE/WF/H1 wax composites at 10% WF content

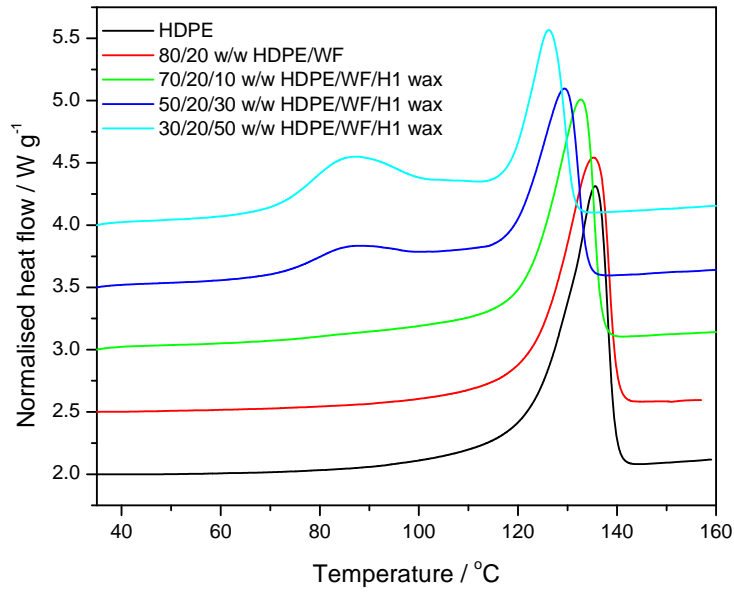


Figure 4.18 DSC heating curves of HDPE, the HDPE/WF composite and the HDPE/WF/H1 wax composites at 20% WF content

The curves of the experimentally observed and calculated enthalpies as function of wax content are shown in Figures 4.19 and 4.20. For the 10% WF containing samples, the experimentally observed enthalpies are lower than the calculated enthalpies with inconsistent differences as the wax content increases. The difference is large at the highest wax content. The standard deviations are significant at low wax contents and the calculated enthalpies fall within the experimental error. This is the result of the separate crystallization of H1 wax at the highest content, and the inhomogeneity of the composite samples. For the 20% WF containing composites (Figure 4.20), the experimental enthalpies are lower than the calculated ones, but the difference becomes smaller with increasing wax content until the values are almost the same at the highest wax content. The reason for this is not entirely clear, but the presence of WF particles covered by wax and/or the presence of wax crystals in the amorphous phase of the polymer obviously influenced the crystallization mechanism of the HDPE.

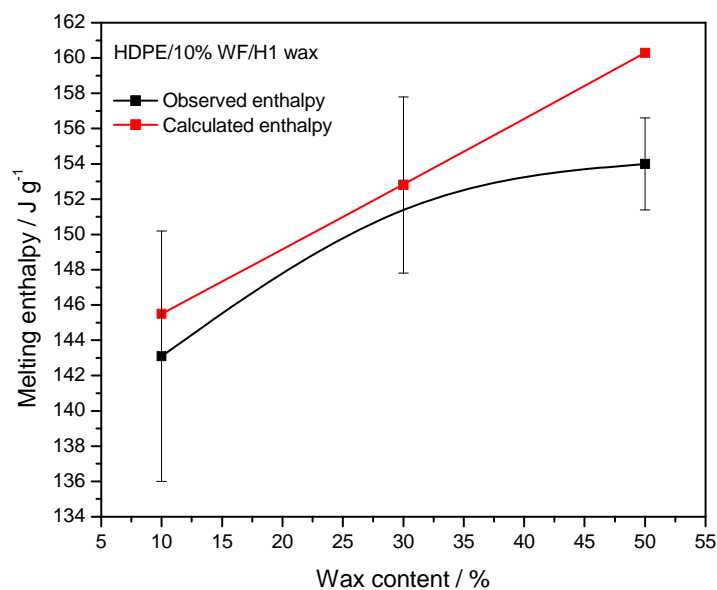


Figure 4.19 Comparison of experimental and calculated melting enthalpies as a function of wax content in HDPE/10% WF/H1 wax composites

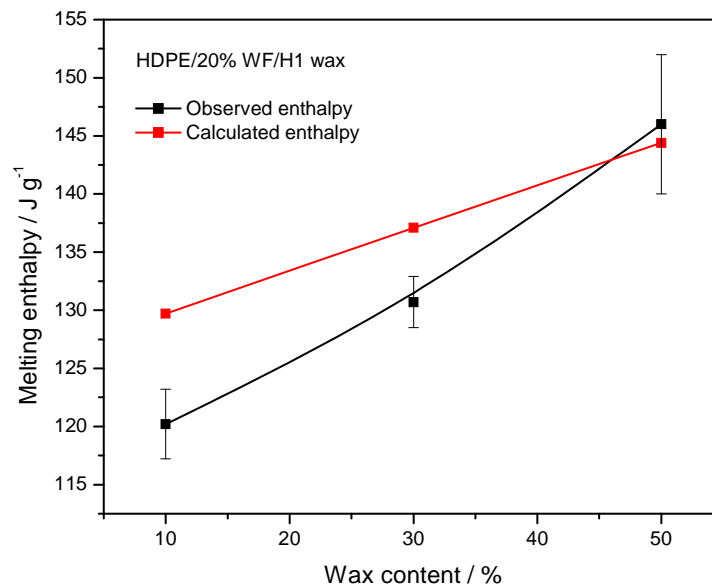


Figure 4.20 Comparison of experimental and calculated melting enthalpies as a function of wax content in HDPE/20% WF/H1 wax composites

4.3 Thermogravimetric analysis (TGA)

The TGA results of the HDPE/paraffin wax (M3 or H1) blends and the HDPE/WF/paraffin wax (M3 or H1) composites are shown in Figures 4.21 to 4.28. The thermal stabilities of all the samples were characterized in terms of the temperatures at 10 and 70% weight loss. A summary of the TGA results is presented in Tables 4.3 and 4.4 for the M3 and H1 wax containing blends and composites.

The TGA curves of the neat materials (HDPE, H1 wax, M3 wax and alkali-treated WF) are shown in Figure 4.21. The HDPE, H1 and M3 wax decomposed completely in a single step, whereas WF decomposed in multiple steps and yielded some residue. The HDPE matrix has the highest thermal stability, followed by the H1 wax, the WF, and then the M3 wax. In the TGA curve of the alkali-treated WF decomposition there is an initial weight loss step (5-6%) below 100 °C. This is the consequence of moisture evaporating from the sample. The second and major decomposition peak in the range of 250 to 360 °C is the result of the thermal depolymerization of hemicellulose and the glycosidic linkages of cellulose. The final

decomposition step of the alkali-treated WF starting above 360 °C may be the result of lignin decomposition, which finally contributes to the formation of char above 450 °C [21-23].

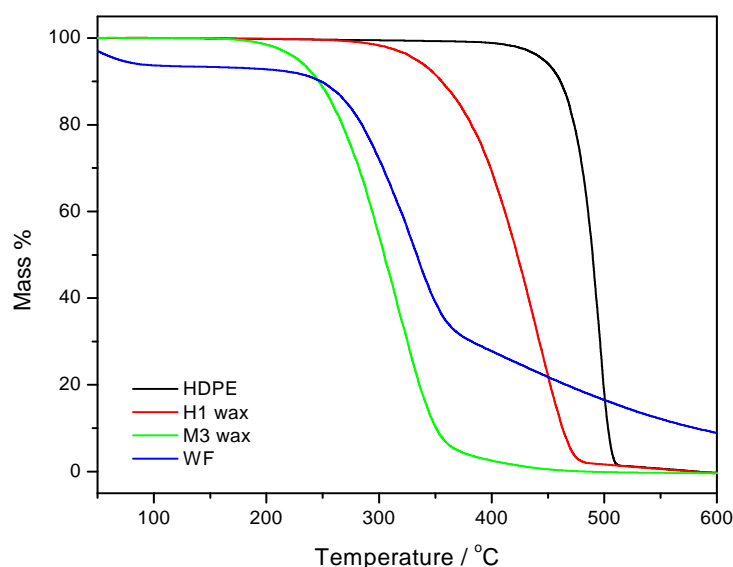


Figure 4.21 TGA curves of HDPE, H1 wax, M3 wax and alkali-treated WF

4.3.1 HDPE/M3 wax blends and HDPE/WF/M3 wax composites

The TGA results of the HDPE/M3 wax blends are shown in Figure. 4.22. The blends degraded in two-steps, with the M3 wax destabilizing the HDPE. Both degradation steps correspond with the relative amount of each component in blends according to the sample compositions. Therefore the first step is related to the degradation of M3 wax and the second to that of the HDPE matrix. This may be attributed to the immiscibility of the HDPE and the M3 paraffin wax, as already seen from both the DSC and SEM results (sections 4.1 and 4.2). Krupa *et al.* [9,10] reported similar behaviour for soft wax (Wax S) blended separately with PP and LDPE matrices. The values in Table 4.3 show that the thermal stabilities of the composites fall between those of the wax and the HDPE. This is probably because of both the low molecular weight and low thermal stability of the paraffin wax. The increased concentration of short wax chains, as well as fragments formed by chain scission, will have enough energy to escape from the matrix at lower temperatures [13,18,24]. The free radicals formed during wax degradation will also initiate HDPE degradation at lower temperatures.

Mpanza and Luyt [12] reported similar behaviour for LDPE/M3 wax blends at 10 wt% wax content.

Table 4.3 Summary of TGA results of HDPE/M3 wax blends and HDPE/WF/M3 wax composites samples

Sample w/w	T _{10%} / °C	T _{70%} / °C
HDPE	460.8	496.0
M3	245.7	323.7
WF	248.0	383.6
HDPE/M3 wax		
80/20	337.9	487.8
70/30	294.6	477.9
60/40	277.1	476.0
50/50	268.7	474.0
40/60	258.9	458.2
HDPE/WF		
90/10	380.1	499.0
80/20	332.2	498.0
HDPE/WF/M3 wax		
80/10/10	327.5	493.4
60/10/30	285.4	479.8
40/10/50	266.6	475.2
70/20/10	313.3	493.6
50/20/30	285.6	487.3
30/20/50	263.8	461.8

T_{10%} and T_{70%} means degradation temperatures at 10% and 70% weight loss respectively

The TGA results of the HDPE/WF composites in Figure 4.23 show two degradation steps. The relative amounts of the individual components also correlate with the weight loss in each of the degradation steps. The first step corresponds to the decomposition of WF and the second step to that of HDPE. The presence of WF does not have any influence on the thermal stability of HDPE, but HDPE seems to stabilise the WF. The T_{10%} is significantly higher for the 90/10 composite compared to that of the pure WF. The highly crystalline (and therefore highly stable) HDPE seems to protect the WF. However, at higher WF content the protection

seems to be less effective, probably because of incomplete covering of the WF by the HDPE matrix.

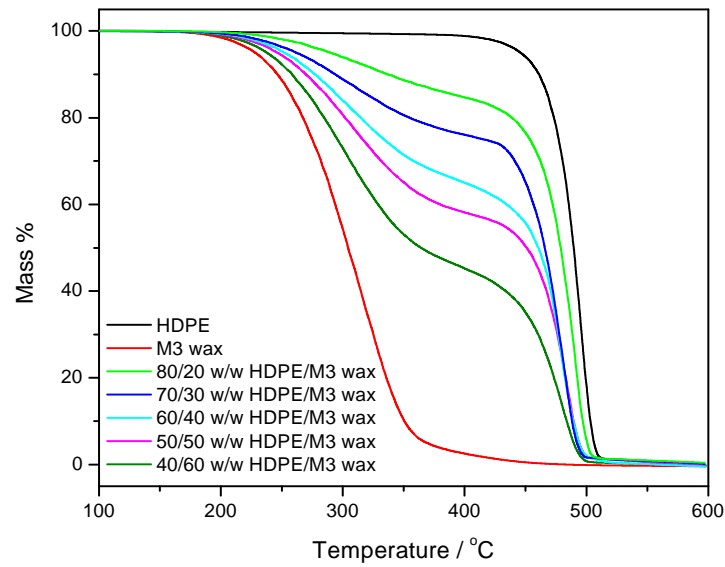


Figure 4.22 TGA curves of the HDPE/M3 wax blends

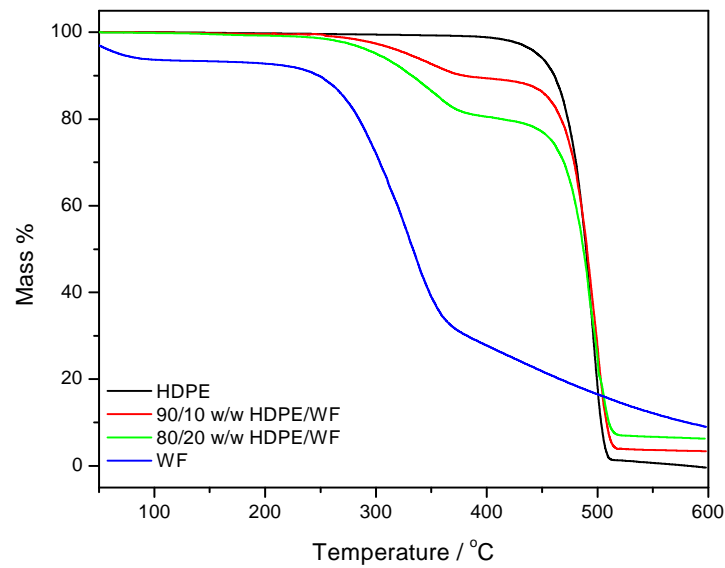


Figure 4.23 TGA curves of HDPE/WF composites

Figures 4.24 and 4.25 presents the TGA results of the HDPE/WF/M3 wax composites. All the PCM composites degraded in two steps. The percentage degradation during the first step corresponds to a combination of the amounts of WF and M3 wax initially mixed into the

sample, and the second to the initial content of HDPE. The first degradation step is an overlapping of the decompositions of WF and the M3 wax, with the M3 wax degrading first. For both WF contents, the presence of wax reduced the thermal stability of the composites (Table 4.3), but not more than that observed for the HDPE/M3 wax blends.

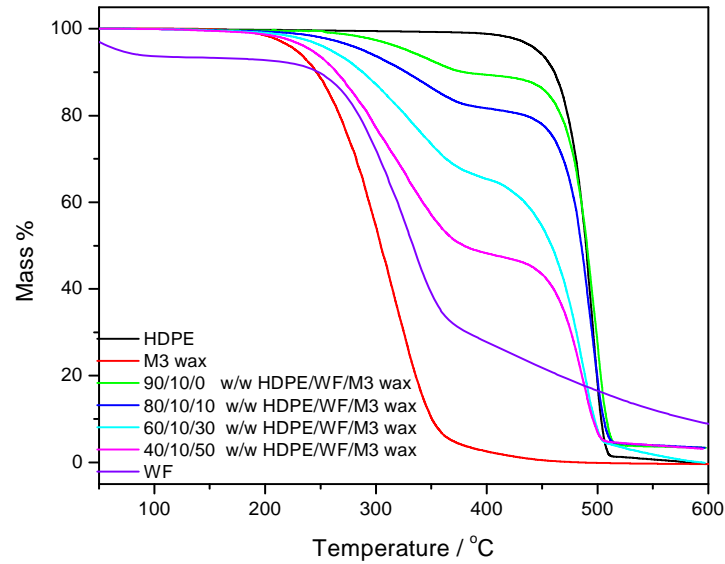


Figure 4.24 TGA curves of HDPE/10% WF/M3 wax composites

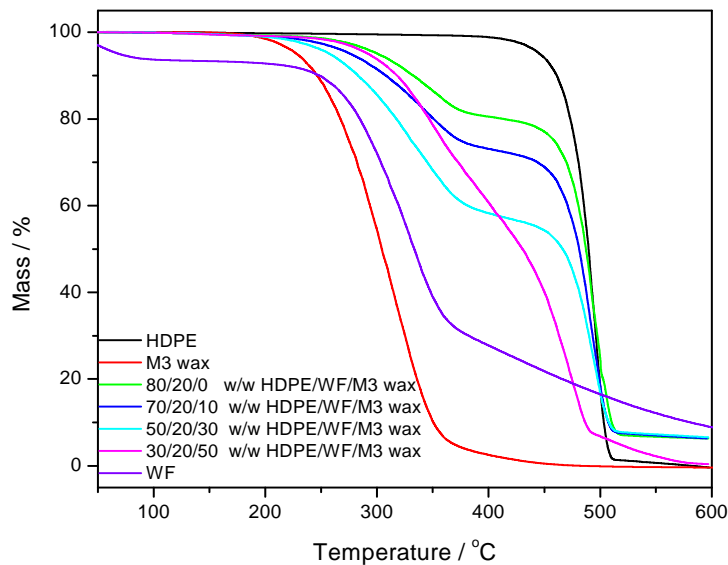


Figure 4.25 TGA curves of HDPE/20% WF/M3 wax composites

4.3.2 HDPE/H1 wax PCM blends and HDPE/WF/H1 wax composites

The TGA results of the HDPE/H1 wax blends and HDPE/WF/H1 wax composites are shown in Figures 4.26 to 4.28 and Table 4.4. The HDPE/H1 wax blends degrade in only one-step with no residue. The single step degradation shows some high level of miscibility (though not complete) of the HDPE and H1 wax as also seen from the SEM and DSC results (Sections 4.1 and 4.2). Similar behaviour was reported by Krupa *et al.* [9,10] in their investigation of PP/Wax FT and LDPE/Wax FT phase change materials. They explained this behaviour as indicating the higher level of compatibility and co-crystallization of the Fischer-Tropsch paraffin wax and the PP and LDPE matrices. The introduction of H1 wax into the HDPE matrix reduced the thermal stability of the blends (Table 4.4). However, the sample with 50% H1 wax seems to be slightly more stable (Figure 4.26 and Table 4.4), but so far we could not find an obvious explanation for this observation.

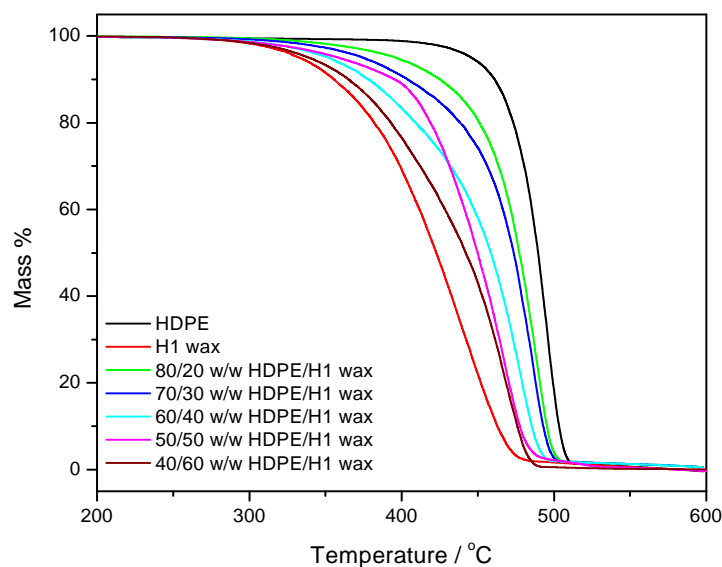


Figure 4.26 TGA curves of the HDPE/H1 wax blends

Figures 4.27 and 4.28 depict the thermal degradation results of the HDPE/WF/H1 wax composites at 10 and 20% WF respectively. Two degradation steps can be clearly seen for the lower wax contents, but they are less resolved for the higher contents. These peaks are related to the combined decomposition of H1 wax and WF (first step), and to that of the HDPE matrix (second step). The first step occurs at higher temperatures than that of neat WF, and it seems that the highly crystalline (and therefore more thermally stable) H1 wax stabilized the

WF. At both 10 and 70% weight loss (Table 4.4) all investigated composites samples showed reduced thermal stabilities as the wax content increased. This is the result of low thermal stability of the wax compared to the HDPE matrix.

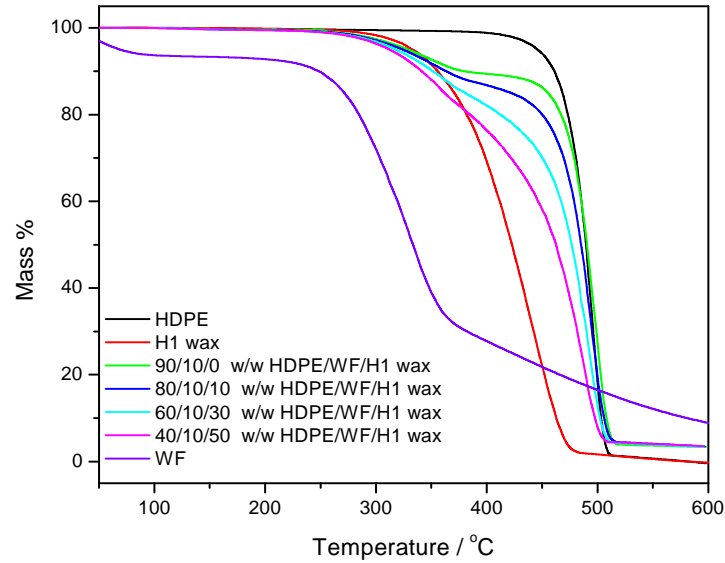


Figure 4.27 TGA curves of HDPE/10% WF/H1 wax PCM composites at various wax contents

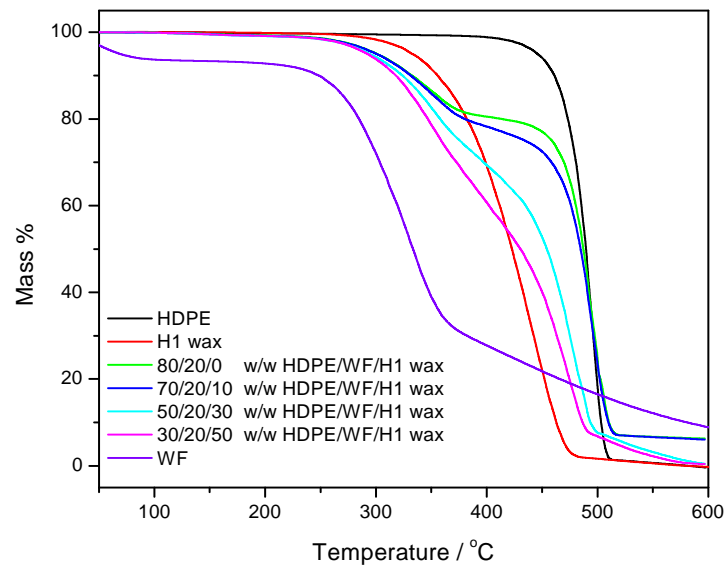


Figure 4.28 TGA curves of HDPE/20% WF/H1 wax PCM composites at various wax contents

Table 4.4 Summary of TGA results of HDPE/H1 wax blends and HDPE/WF/H1 wax composites samples

Sample w/w	T _{10%} / °C	T _{70%} / °C
HDPE	460.8	496.0
H1	356.1	441.2
WF	248.0	383.6
HDPE/H1 wax		
80/20	426.2	486.6
70/30	405.0	482.6
60/40	378.6	472.8
50/50	395.2	464.9
40/60	365.0	460.9
HDPE/WF		
90/10	380.1	499.0
80/20	332.2	498.0
HDPE/WF/H1 wax		
80/10/10	363.9	494.8
60/10/30	353.5	488.4
40/10/50	340.8	479.9
70/20/10	331.6	496.0
50/20/30	327.0	475.0
30/20/50	321.2	463.0

T_{10%} and T_{70%} means degradation temperature at 10% and 70% weight loss respectively

4.4 Dynamic mechanical analyses (DMA)

The DMA results of the investigated samples are depicted in Figures 4.29 to 4.36. The DMA storage modulus (E') and loss modulus (E'') properties are reported, while the damping factor curves (tan δ) were put in Appendix A. For the blends only the samples containing 20, 40 and 60 wt% wax were characterized, and for the composites only the samples with 20 wt% WF were analysed.

4.4.1 HDPE/M3 wax blends and HDPE/WF/M3 wax composites

The DMA storage and loss modulus of the HDPE/M3 paraffin wax blends are shown as a function of temperature in Figures 4.29 and 4.30. It can be seen in Figure 4.29 that HDPE has the highest storage modulus over the whole investigated temperature range. Depending on temperature interval, two opposite trends are noticed with increasing wax content. From -150 to -42 °C, samples with the highest wax content show a higher modulus, whereas from -42 to 60 °C the storage modulus decreases with increasing wax content. The blends show strain hardening, and an increase in modulus around 50 °C. This is probably the consequence of the wax solid-solid transition at 33 °C as observed by DSC (section 4.2, Figure 4.4 and Table 4.1).

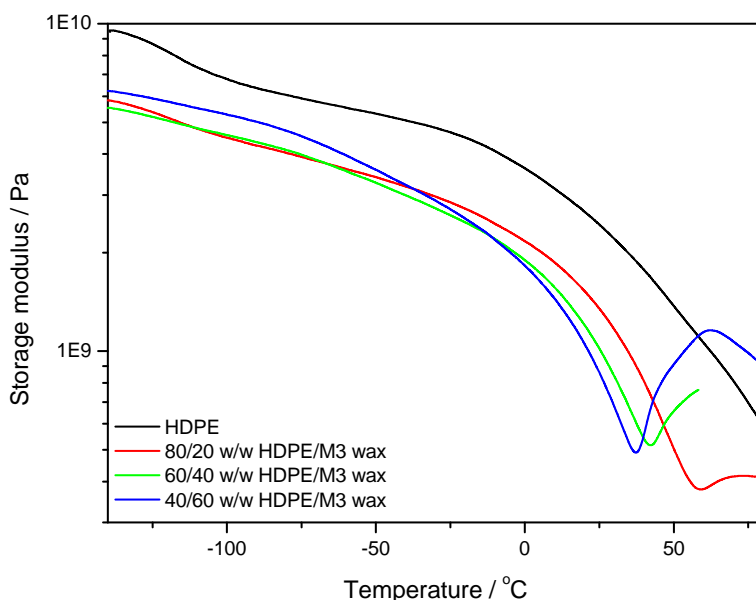


Figure 4.29 DMA storage modulus curves for the HDPE/M3 wax blends

The loss modulus curve of neat HDPE in Figure 4.30 shows two transition peaks. The first peak at -125 °C corresponds to the γ -transition and is the result of the crankshaft relaxation mechanism of the PE chains [28]. The second peak, at 46 °C, is the α -relaxation transition and it is related to the crystalline fraction in the semicrystalline material. In the case of the γ -transition there is virtually no change in the peak position with the addition of wax, but the position of the α -relaxation shifts to lower temperatures. This is the result of the reduced lamellar thickness of the blends as seen by DSC (section 4.2, Table 4.1 and Figure 4.4).

Sirotkin and Brooks [29] reported the association of the α -relaxation with c-shear within the crystalline lamellae, and concluded that this transition is dependent only on the lamellar thickness. The loss modulus curves of the samples with 40 and 60% M3 wax (Figure 4.30) show an additional peak at -75 °C, which is the β -relaxation. Linear polyethylenes (LPE) usually do not show a β -relaxation, which normally occurs in branched polyethylenes (BPE). This transition is the result of the motion in the interfacial regions (amorphous portion between crystallites) of the semicrystalline material, and depends on the degree of branching [29,30]. Djoković *et al.*[30] reported that the minimal interfacial content, which can produce a visible β -peak in the DMA curve of polyethylene, is about 10% of semicrystalline material. In LPE the interfacial content is about 3-4%, whereas in BPE (with only 0.6 mol % branches) it is about 11%. Long branches affect this relaxation more than shorter ones. The presence of a β -relaxation in the HDPE/M3 wax blends is therefore probably the result of an increase in the amount of the interfacial amorphous content as the wax content increases.

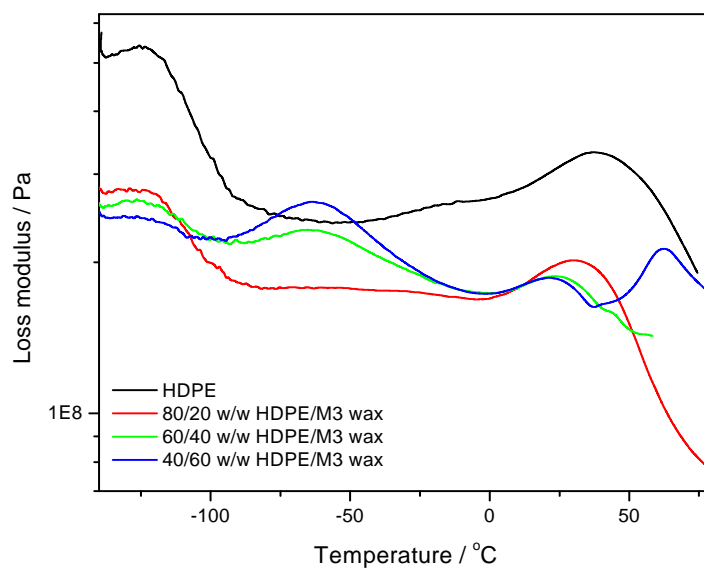


Figure 4.30 DMA loss modulus curves of HDPE/M3 wax blends

Figures 4.31 and 4.32 show the storage and loss modulus for the HDPE/WF/M3 wax composites. The storage modulus (Figure 4.31) of the 80/20 w/w HDPE/WF composite is higher than that of the neat HDPE throughout the investigated temperature range. All the storage moduli fall within the same order of magnitude, and no specific trends related to the presence of WF or wax content are observable. The addition of the WF to neat HDPE lowered the loss modulus (Figure 4.32), and it induced a shift of both the γ - and α - transitions towards high temperatures. This is attributed to a restriction of the motion of the main polymer chain, as well as increased lamellar thickness with WF loading. An additional peak at -14 °C is noticed after WF incorporation. We could not find an explanation for the origin of this transition, but this transition seems to be dependent on wax content. Also, as in the case of the HDPE/M3 wax blends (Figure 4.30), the position of α -relaxation transition shifts to lower temperatures as wax content increases, but it still appears at a higher temperature than that of the neat HDPE.

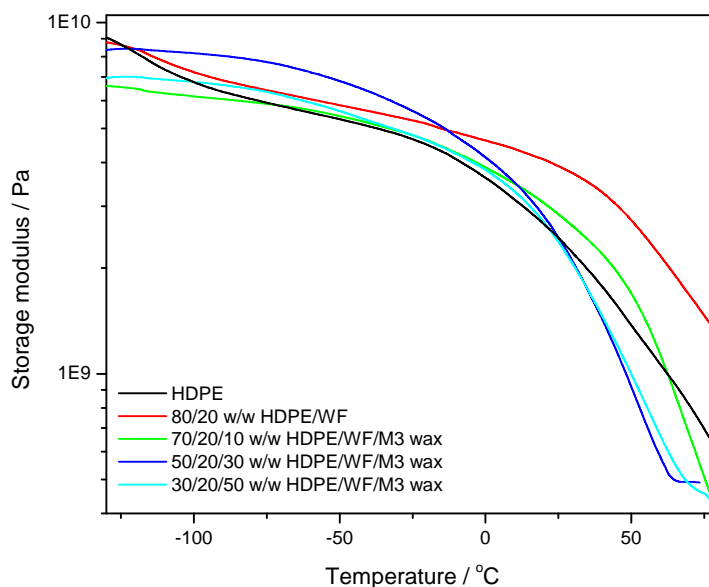


Figure 4.31 DMA storage modulus curves for HDPE/WF/M3 wax composites

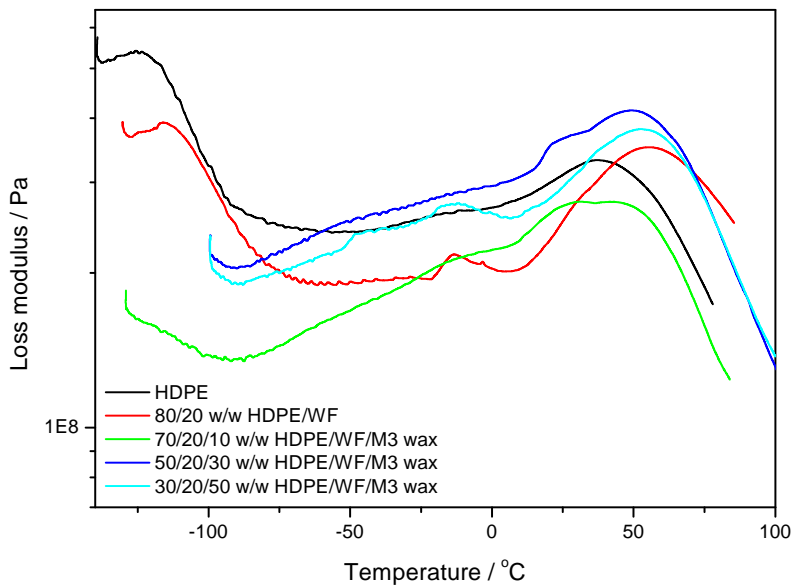


Figure 4.32 DMA loss modulus curves for HDPE/WF/M3 wax composites

4.4.2 HDPE/H1 wax blends and HDPE/WF/H1 wax composites

The storage and loss modulus curves of the HDPE/H1 wax blends are shown in Figures 4.33 and 4.34. It can be seen that the HDPE shows the highest storage modulus over the whole investigated temperature range (Figure 4.33). The introduction of H1 wax into the HDPE lowers the storage modulus, but there is no direct relation between the storage moduli and the wax content in the samples. The lower storage moduli are the consequence of the plasticizing effect of the wax on the HDPE matrix. The curves of the blends seem to converge at the temperature interval from 40 to 60 °C. In Figure 4.34 it can be noticed that the neat HDPE has the highest loss modulus throughout the experimental temperature range. The blends show two transitions (γ - and α -relaxation) that are characteristic of the neat HDPE. There are no changes in the peak position of the γ -relaxation, but the peak position of the α -relaxation shifts towards lower temperatures as the wax content increases. These changes in the peak position, in the case of α -relaxation transition, are the results of the reduced lamellar thickness in the presence of H1 paraffin wax. This behaviour is also seen by DSC (section 4.2, Table 4.2 and Figure 4.15).

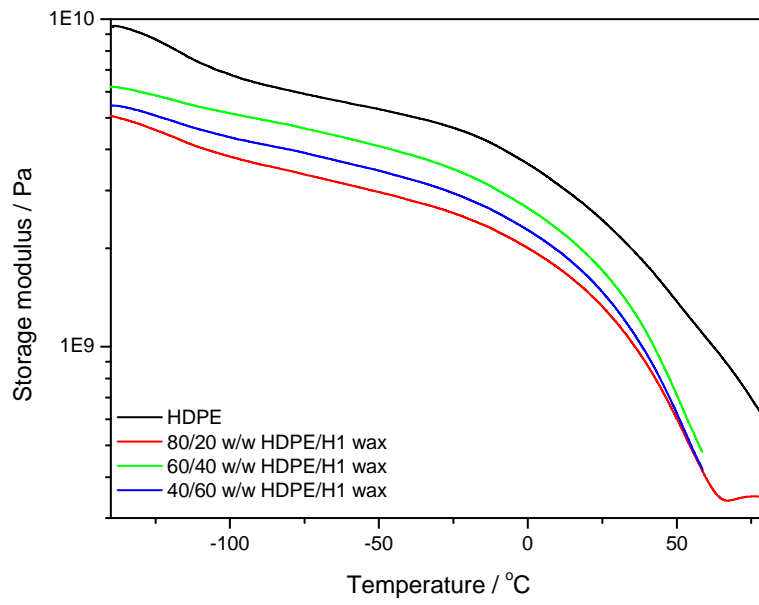


Figure 4.33 DMA storage modulus curves for the HDPE/H1 wax blends

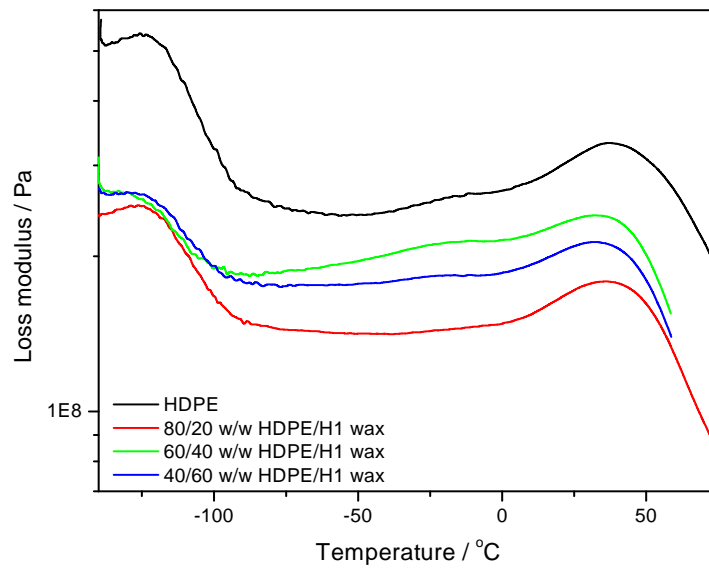


Figure 4.34 DMA loss modulus curves for the HDPE/H1 wax blends

Figures 4.35 and 4.36 show the storage and loss modulus graphs of the HDPE/WF/H1 wax composites. All the storage moduli fall within the same order of magnitude, and no specific trends related to the presence of WF or wax content are observable. The peak position of the α -transition for the HDPE/WF/H1 wax composites in Figure 4.36 shifts to higher temperatures with increasing H1 wax content. Although this peak position varies with wax content, it approaches that of the HDPE/WF composite. Contrary to the case of the HDPE/H1 wax blends (Figure 4.34), the position of the α -relaxation transition shifts to higher temperatures as the wax content increases, and its position is still at a higher temperature than that of the neat HDPE. The position of the observed additional peak seems to depend on the H1 wax content, and can be explained in a similar way than for the M3 wax based blend composites.

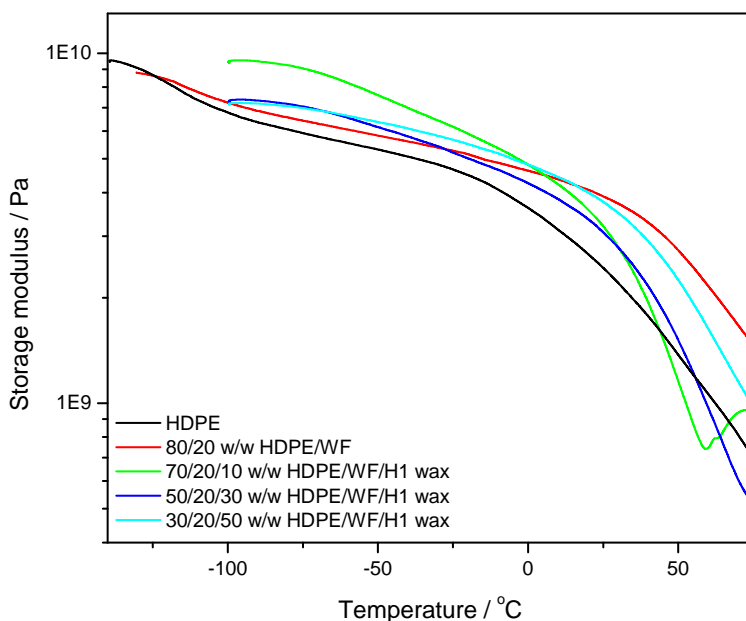


Figure 4.35 DMA storage modulus curves for HDPE/WF/H1 wax composites

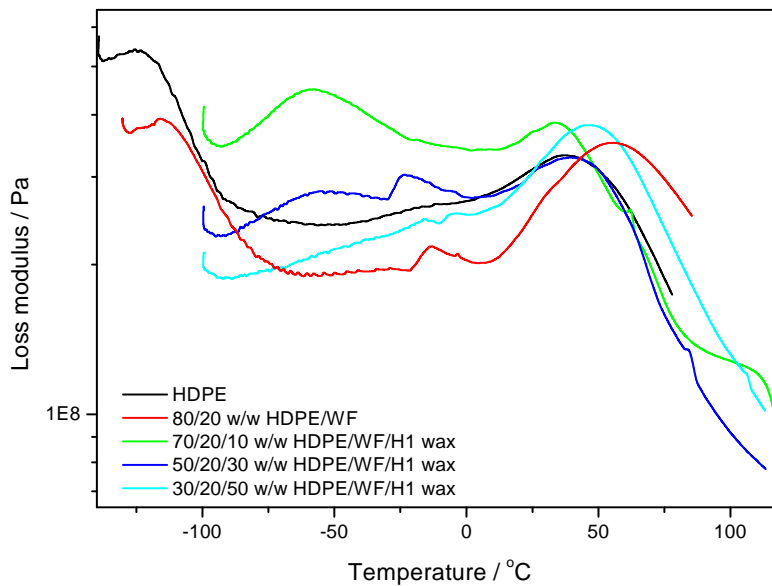


Figure 4.36 DMA loss modulus curves for HDPE/WF/H1 wax composites

4.5 Tensile testing (TT)

The tensile properties of the PCM blends and composites are depicted in Figures 4.37 to 4.45. The Young's modulus, elongation and stress at break, as well as elongation and stress at yield (where observed) are summarized in Tables 4.5 and 4.6. All the stress-strain results of the investigated samples were put in Appendix B.

4.5.1 HDPE/M3 wax blends and HDPE/WF/M3 wax composites

The stress-strain curves in Appendix B.1 show that the HDPE exhibited the typical characteristics of ductile polymers: stress whitening followed by necking and cold drawing after yielding. The HDPE has the highest values of elongation at break (588%) and modulus (653 MPa). When 20 wt% M3 wax is introduced, the blend shows strain softening after yielding. An increase in elongation at yield and a slight decrease in yield stress (Table 4.5, 80/20 w/w HDPE/M3 wax sample) can be noticed. This increase in elongation at yield may be the result of the plasticization effect of the M3 wax on the HDPE matrix, whereas the decrease in yield stress is because of the lower crystallinity of the blends as the wax content

increases (as seen by DSC, section 4.2). Samples with high wax contents did not show any yield point, and they were very brittle. Krupa and Luyt [15] showed that samples of LLDPE/wax, with 30 wt% and more wax contents do not have a yield point. They exhibit brittle rupture and did not undergo strain softening.

Figure 4.37 and Table 4.5 show the Young's modulus of the HDPE/M3 wax blends as function of wax content. A decrease in modulus with an increase in M3 wax content can be seen. This is the consequence of the decreased crystallinity of the blends with wax increase as seen by DSC (section 4.2). The tensile strength (Figure 4.38) varies with wax loading, and the elongation at break (Figure 4.39) of the blends decreases with increasing wax content. The lowered tensile strength may be the result of the decreased crystallinity of the blends with increasing wax content, and the shorter wax chains that may have partially co-crystallized with the HDPE, decreasing the average number of tie-chains between the HDPE lamellae. This led to a suppression of the cold drawing deformation of the polymer matrix [26]. The effect on the elongation at break is the consequence of the loss of drawability in the presence of high wax contents that leads to highly brittle blend samples [15].

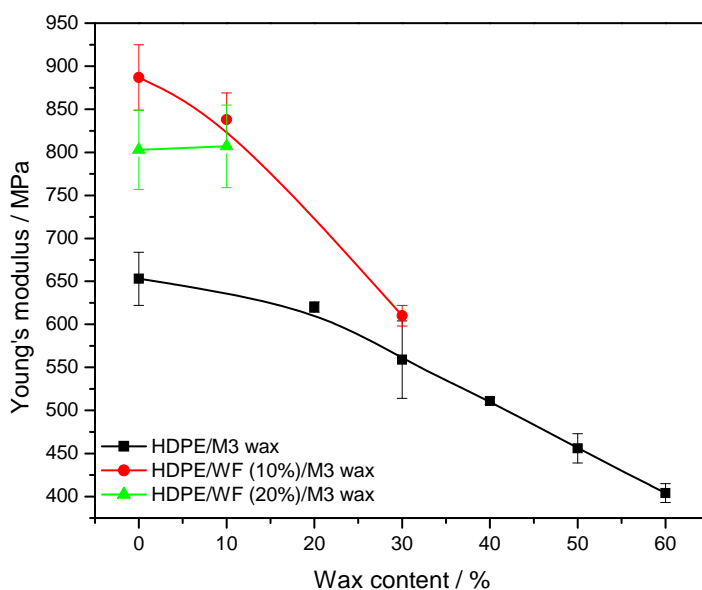


Figure 4.37 Young's modulus of HDPE/M3 wax blends and HDPE/WF/M3 wax composites as function of wax content

Table 4.5 Summary of tensile results for HDPE/M3 wax blends and HDPE/WF/M3 wax composites

Sample w/w	$\epsilon_y \pm s\epsilon_y$ / %	$\sigma_y \pm s\sigma_y$ / MPa	$\epsilon_b \pm s\epsilon_b$ / %	$\sigma_b \pm s\sigma_b$ / MPa	$E \pm sE$ / MPa
HDPE	11.3 ± 0.5	29.2 ± 1.1	587.5 ± 29	18.8 ± 0.8	653 ± 31.1
HDPE/M3 wax					
80/20	14.8 ± 0.2	28.6 ± 0.7	269.8 ± 8.9	15.3 ± 1.0	620 ± 6.1
70/30	-	-	14.1 ± 0.4	23.1 ± 0.3	559 ± 45.3
60/40	-	-	14.1 ± 1.3	21.0 ± 0.4	510.5 ± 3.5
50/50	-	-	10.7 ± 0.5	17.2 ± 0.3	455.9 ± 16.5
40/60	-	-	12.8 ± 0.3	16.7 ± 1.3	403.9 ± 10.9
HDPE/WF					
90/10	-	-	9.9 ± 1.2	25.0 ± 0.6	886.6 ± 37.8
80/20	-	-	4.4 ± 0.0	18.1 ± 0.2	802.5 ± 46.0
HDPE/WF/M3 wax					
80/10/10	-	-	10.9 ± 0.9	23.9 ± 0.8	838.2 ± 30.7
60/10/30	-	-	8.6 ± 0.7	22.3 ± 0.7	610 ± 11.8
70/20/10	-	-	5.4 ± 0.5	19.8 ± 1.2	807 ± 48.1

ϵ_y , σ_y , ϵ_b , σ_b and E are elongation at yield, yield stress, elongation at break, stress at break and Young's modulus of elasticity. The $s\epsilon_y$, $s\sigma_y$, $s\epsilon_b$, $s\sigma_b$ and sE are their respective standard deviations

The stress-strain curves in Appendix B.2 show that the incorporation of WF into HDPE gives stiff composites with no yield point. This subsequently leads to composites with higher Young's modulus values (Figure 4.40). This may be the result of the stiffer organic filler compared to neat HDPE, which results into a final product with higher stiffness [23]. The improved fibre-matrix adhesion as a result of fibre treatment with alkali may have contributed to the increased modulus (see SEM discussion, section 4.1) [31]. Although still higher than that of the neat HDPE, a slight drop in modulus of the composites with 20% WF can be noticed. This behaviour correlates with the observations by DSC (see section 4.2) where 20% WF gave composites with slightly lower crystallinity compared to the 10% WF composites.

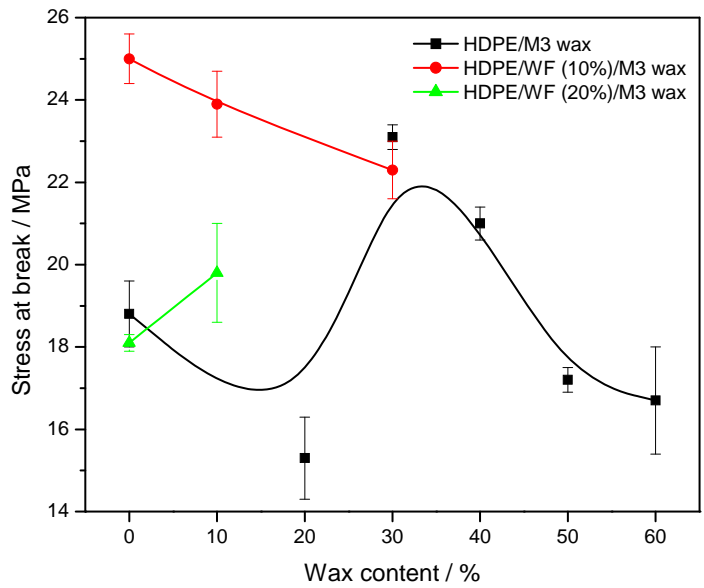


Figure 4.38 Stress at break of HDPE/M3 wax blends and HDPE/WF/M3 wax composites as function of wax content

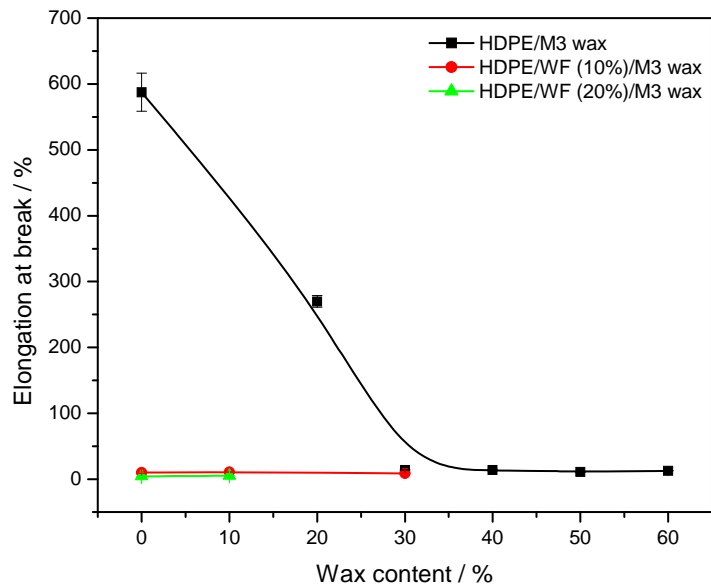


Figure 4.39 Elongation at break of HDPE/M3 wax blends and HDPE/WF/M3 wax composites as function of wax content

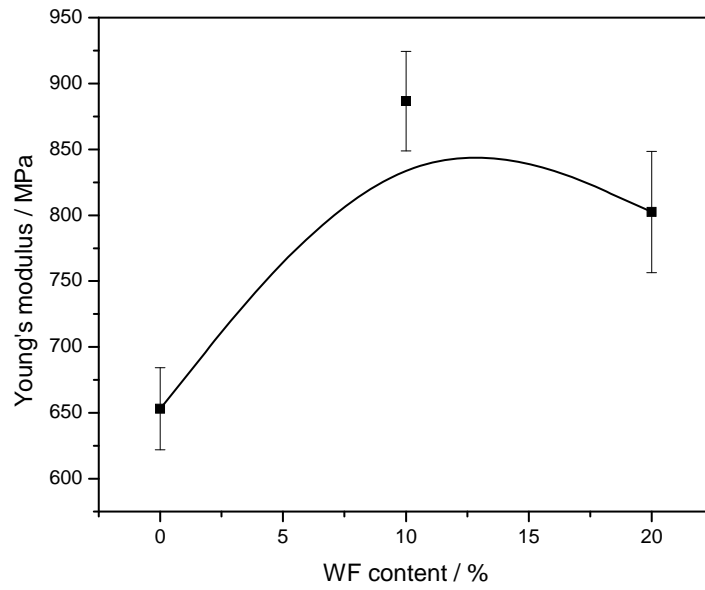


Figure 4.40 Young's modulus of HDPE/WF composites as function of WF content

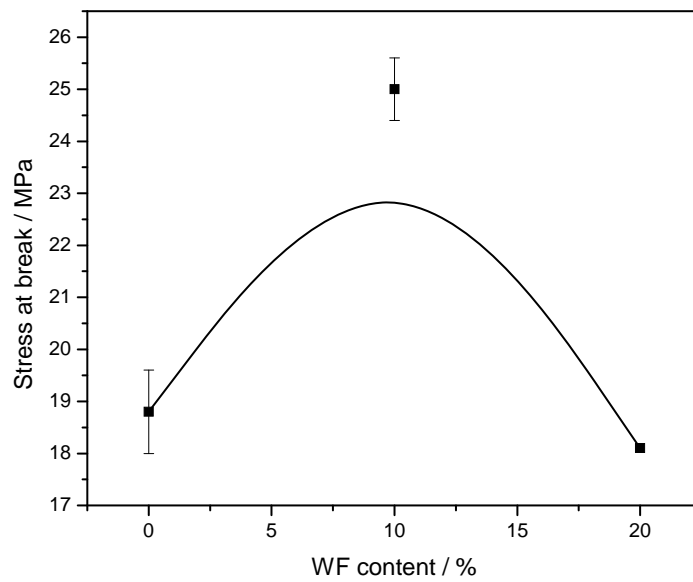


Figure 4.41 Stress at break of HDPE/WF composites as function of WF content

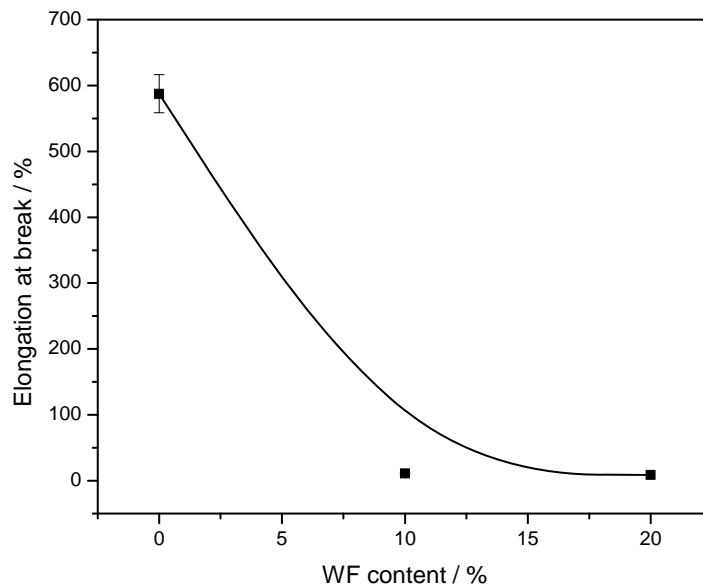


Figure 4.42 Elongation at break of HDPE/WF composites as function of WF content

The stress at break of the composites (Figure 4.41) shows an initial increase at 10% WF content, and a significant decrease at 20% WF. The initial increase in tensile strength is the consequence of increased crystallinity and more complete fibre coverage by the HDPE matrix. The decrease at higher WF content is probably the result of incomplete fibre coverage by the matrix and lowered crystallinity of the composites (see DSC, section 4.2 and Table 4.1). The elongation at break decreases with increasing WF content. This may be attributed to restricted mobility of the polymer chains giving rise to a rigid matrix in the presence of the solid WF particles, and to the WF particles that act as defect points [20,23,31,32].

The Young's modulus of the HDPE/WF/M3 wax composites (Figure 4.37) decreases with increasing wax content at 10 wt% WF content. This is because of reduced contact/interaction between the WF and the HDPE matrix in the presence of wax. As seen by SEM (section 4.1), the wax covered the WF particles and thus prohibited the mechanical interlocking interaction between WF and HDPE. As a result the wax has a considerable influence on the mechanical properties of the composites by reducing their stiffness. It may also be the consequence of the lower crystallinity of these composites as seen by DSC (section 4.2). Only samples with up to 30 wt% M3 wax content could be subjected to tensile tests because of the highly brittle samples at higher wax contents. However, there was an increase in Young's modulus with the

introduction of 10 wt% wax to composites containing 20% WF. This may probably be the result of too little wax available to cover all of the WF particles, and therefore some WF particles were directly in contact with the polymer matrix. Only the 10 wt% M3 wax composite could be characterized under tensile as the rest of the samples were also highly brittle.

The stress at break of the HDPE/WF (10%)/M3 wax composites decreased with increasing wax content (Figure 4.38). Since the tensile strength is a function of crystallinity, this is to be expected because of the decreased crystallinity as seen by DSC (section 4.2). It may also be the result of the poor interaction between WF and HDPE as seen for the HDPE/WF composites (discussed before and seen by SEM) even in the presence of wax [25]. In the case of the HDPE/WF (20%)/M3 wax composites (Figure 4.38), an increase in stress at break with increasing wax content is seen. Since there is more WF than wax in this system, it is probably the result of the existing interaction between the WF and the HDPE matrix.

The elongation at break of the HDPE/WF (10%)/M3 wax (Figure 4.39) decreases with an increase in wax content. This is the consequence of the restricted mobility of the polymer chains and reduced strain transfer in the presence of both WF and wax, which resulted into highly brittle composite samples. For the 20% WF composites, there is a slight increase in elongation at break (Table 4.5 and Figures 4.39). This may be the result of the plasticization effect of the M3 wax.

4.5.2 HDPE/H1 wax blends and HDPE/WF/H1 wax composites

The stress-strain curves in Appendix B.3 show that only the 80/20 w/w HDPE/H1 wax blends exhibited strain softening after yielding. The blend has a slightly lower elongation at yield and yield stress than neat HDPE. The reason for this is that the H1 wax, which crystallized in the amorphous phase of the polymer, acted as defect points. In the case of the yield stress it may be attributed to small wax crystals in the amorphous phase of the HDPE and their influence on the crystallinity of the blends as seen in the DSC results (Section 4.2, Figure 4.16 and Table 4.2).

The HDPE/H1 wax blends showed an increased Young's modulus with increasing wax content (Figure 4.43), and this is probably the result of the partial co-crystallization of H1 wax

with the HDPE matrix (see DSC results in section 4.2, Table 4.2), as well as more wax crystallized in the amorphous phase of the polymer [15]. At the highest wax contents (50 and 60%), however, there is a fairly constant modulus (with 60% wax sample showing large standard deviations), which is still high with respect to neat HDPE.

Table 4.6 Summary of tensile results for HDPE/H1 wax blends and HDPE/WF/H1 wax composites

Sample w/w	$\epsilon_y \pm s\epsilon_y$ / %	$\sigma_y \pm s\sigma_y$ / MPa	$\epsilon_b \pm s\epsilon_b$ / %	$\sigma_b \pm s\sigma_b$ / MPa	$E \pm sE$ / MPa
HDPE	11.3 ± 0.5	29.2 ± 1.1	587.5 ± 29.0	18.8 ± 0.8	653.0 ± 31.1
HDPE/H1 wax					
80/20	10.3 ± 0.3	28.9 ± 0.6	178.6 ± 5.5	15.6 ± 0.9	783.8 ± 40.9
70/30	-	-	7.1 ± 0.3	26.9 ± 0.9	799.0 ± 33.5
60/40	-	-	4.2 ± 0.2	21.4 ± 1.1	861.3 ± 6.0
50/50	-	-	5.2 ± 0.5	23.3 ± 1.7	854.3 ± 11.0
40/60	-	-	3.7 ± 0.2	22.5 ± 2.1	806.6 ± 51.8
HDPE/WF					
90/10	-	-	9.9 ± 1.2	25.0 ± 0.6	886.6 ± 37.8
80/20	-	-	4.4 ± 0.0	18.1 ± 0.2	802.5 ± 46.0
HDPE/WF/H1 wax					
80/10/10	-	-	8.1 ± 0.8	25.1 ± 0.6	934.5 ± 31.8
60/10/30	-	-	1.7 ± 0.1	12.6 ± 1.1	401.9 ± 22.0
70/20/10	-	-	3.9 ± 0.1	17.6 ± 1.5	837.0 ± 65.1

ϵ_y , σ_y , ϵ_b , σ_b and E are elongation at yield, yield stress, elongation at break, stress at break and Young's modulus of elasticity. The $s\epsilon_y$, $s\sigma_y$, $s\epsilon_b$, $s\sigma_b$ and sE are their respective standard deviations

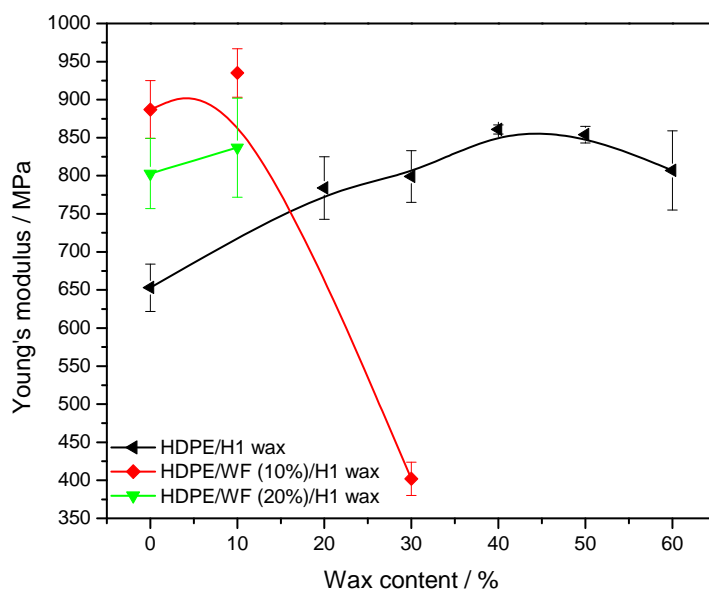


Figure 4.43 Young's modulus of HDPE/H1 blends and HDPE/WF/H1 wax composites as function of wax content

Figure 4.44 shows the stress at break of the HDPE/H1 wax blends. The stress at break increases with wax content, although it varies in such a way that it is not easy to correlate it with the available knowledge on the morphologies of the samples.

Figure 4.43 shows the Young's modulus values of the HDPE/WF/H1 wax composites as function of wax content. The presence of 10 wt% H1 wax resulted in a slightly increased modulus at both 10 and 20% WF contents. The 20% WF containing samples at higher wax contents could not be analysed because they were too brittle. An increase in wax content in the 10% WF composites gave a product with a significantly lower modulus. This is contrary to the increased crystallinity of the composites as observed by DSC (section 4.2), and there is no obvious explanation for this observation.

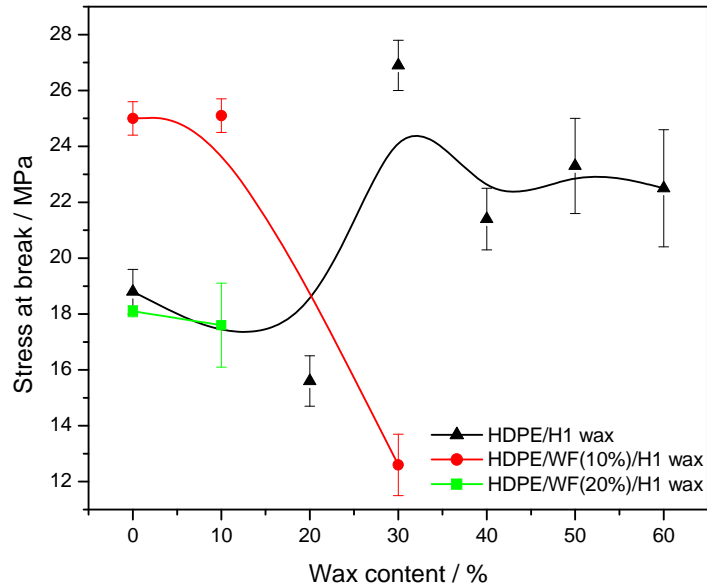


Figure 4.44 Stress at break of HDPE/H1 wax blends and HDPE/WF/H1 wax composites as function of wax content

The stress at break of these composites remained almost constant with the addition of 10% wax in both the 10 and 20% WF composites (Figure 4.44). However, the addition of 30 wt% H1 wax led to a significant decrease in tensile strength. There are three factors that may have contributed to this observation: (i) the incorporated shorter wax chains into the lamellae of the polymer during co-crystallization resulted to a decrease in the average number of tie-chains with increasing wax content; (ii) the low crystallinity of the composites; and (iii) the presence of WF particles which seems to act a defect points within the polymer matrix. Of these factors, the latter seems to be the more appropriate reason. The elongation at break (Figure 4.45) slightly decreases for the 10% WF composites (Table 4.6), and is fairly constant for 20% WF composites with wax loading. This is also because the WF particles act as defect points in the polymer matrix.

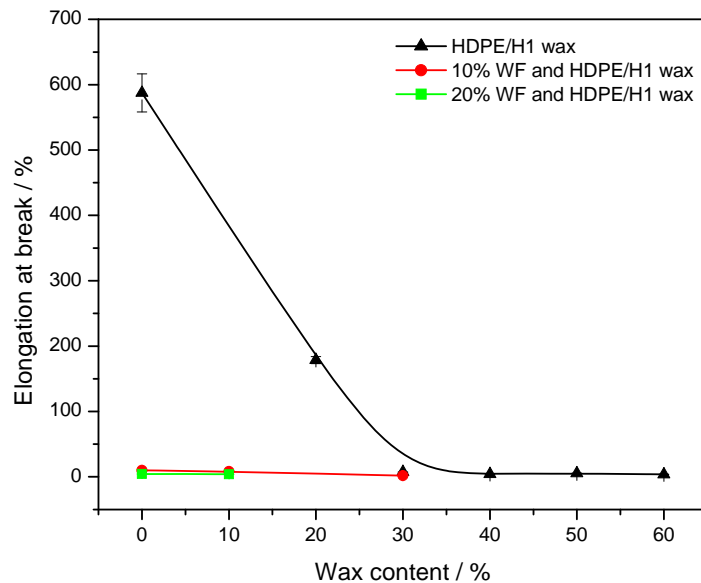


Figure 4.45 Elongation at break of HDPE/H1 wax blends and HDPE/WF/H1 wax composites as function of wax content

4.6 Water absorption

The water absorption results of the HDPE/WF composites, HDPE/WF/M3 wax and HDPE/WF/H1 wax composites are shown in Figures 4.46 to 4.50 and summarized in Table 4.7. Figure 4.46 depicts the water absorption curves of the HDPE/WF composites for both 10 and 20 wt% WF at different immersion times. The water uptake increases with immersion time and WF loading. Since a non-polar and hydrophobic thermoplastic (such as HDPE) has negligible or no water absorption, the water uptake of these composites is mainly because of the presence of the natural wood flour filler [20,33-35]. This is a consequence of the increased number of micro voids because of the large number of areas between the hydrophilic WF and the hydrophobic polymer matrix, which result from the weak interfacial bonding between these components (as seen by SEM in section 4.1) [36]. Because of the hydrophilic nature of the WF, these composites can absorb more water. The absorbed water tends to retain in the inter-fibrillar space of the cellulosic structure of the filler, as well as in the interface and micro voids present in the composites [33,36].

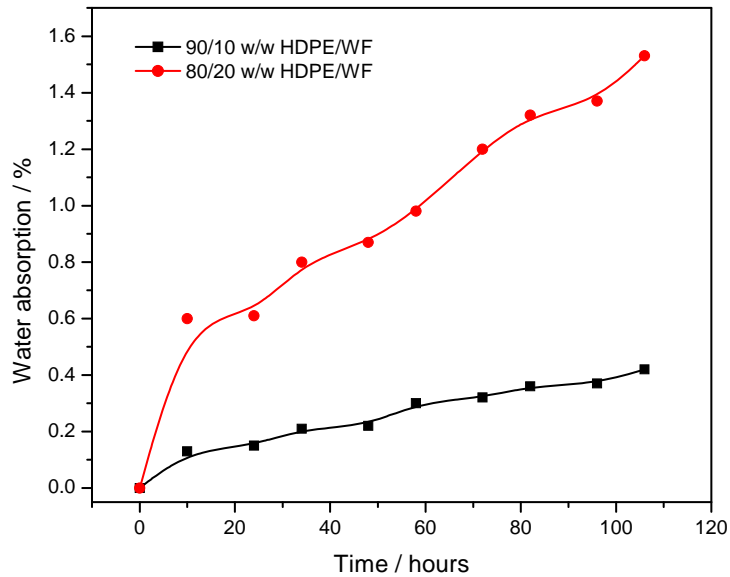


Figure 4.46 Water absorption curves of HDPE/WF composites

Figures 4.47 and 4.48 show the water absorption curves of the HDPE/WF/M3 wax composites, at 10 and 20 wt% WF. A decrease in water uptake is seen with increasing wax content. This is probably the result of the presence of wax that is water repellent in nature [15,18,24]. As seen by SEM and DSC (sections 4.1 and 4.2), the wax covers the WF surfaces in these composites and therefore limits the exposure of wood flour particles to water. At 10 wt% WF content, the differences between the water uptake of the composites at various wax contents is small, whereas at 20% it is significantly larger. This is because at low WF content (10%) almost all the WF particles are effectively covered by small amounts of wax. At high content of WF (20%), the low amounts of wax did not effectively cover all the WF particles, which remained exposed to water. However, as the wax content increased, most of the filler particles were effectively covered by wax, which has also filled the pores and limited water uptake by the composites.

Table 4.7 Summary of results for water absorption of HDPE/WF/M3 wax and HDPE/WF/H1 wax composites

HDPE/WF (w/w)	10 hrs	24 hrs	34 hrs	48 hrs	58 hrs	72 hrs	82 hrs	96 hrs	106 hrs
90/10	0.13	0.15	0.21	0.22	0.3	0.32	0.36	0.37	0.42
80/20	0.6	0.61	0.8	0.87	0.98	1.2	1.32	1.37	1.53
HDPE/WF/M3 wax (w/w)									
80/10/10	0.12	0.17	0.19	0.25	0.27	0.29	0.31	0.35	0.39
60/10/30	0.09	0.16	0.18	0.22	0.25	0.29	0.29	0.34	0.36
40/10/50	0.13	0.15	0.18	0.21	0.21	0.24	0.26	0.28	0.28
70/20/10	0.45	0.53	0.57	0.68	0.75	0.85	0.89	0.96	1.02
50/20/30	0.32	0.39	0.43	0.52	0.58	0.65	0.69	0.75	0.79
30/20/50	0.03 9	0.048	0.067	0.069	0.089	0.1	0.11	0.12	0.14
HDPE/WF/H1 wax (w/w)									
80/10/10	0.08 6	0.13	0.15	0.17	0.21	0.26	0.26	0.28	0.30
60/10/30	0.02 5	0.05	0.05	0.075	0.10	0.10	0.10	0.15	0.15
40/10/50	0.01 7	0.02	0.021	0.022	0.023	0.023	0.059	0.068	0.1
70/20/10	0.45	0.49	0.59	0.69	0.75	0.85	0.89	0.97	0.99
50/20/30	0.50	0.50	0.59	0.71	0.79	0.79	0.90	0.92	0.94
30/20/50	0.03 3	0.034	0.044	0.044	0.068	0.073	0.074	0.076	0.095

The water absorption is reported in percentages as given by Equation 3.1 in Chapter 3

The water absorption curves of the HDPE/WF/H1 wax composites are shown in Figures 4.49 and 4.50 for 10 and 20% WF contents, respectively. The water uptake of these composites also decreases with an increase in wax content. As in the case of M3 wax containing composites, this is the result of the affinity between the wax and the WF which shields the WF particles from the water, and which reduces the number of voids in and around the WF particles. The water uptake of the 10% WF containing composites is clearly lower than that of the 20% WF containing composites, and the explanation will be the same as that given above for the M3 wax containing composites.

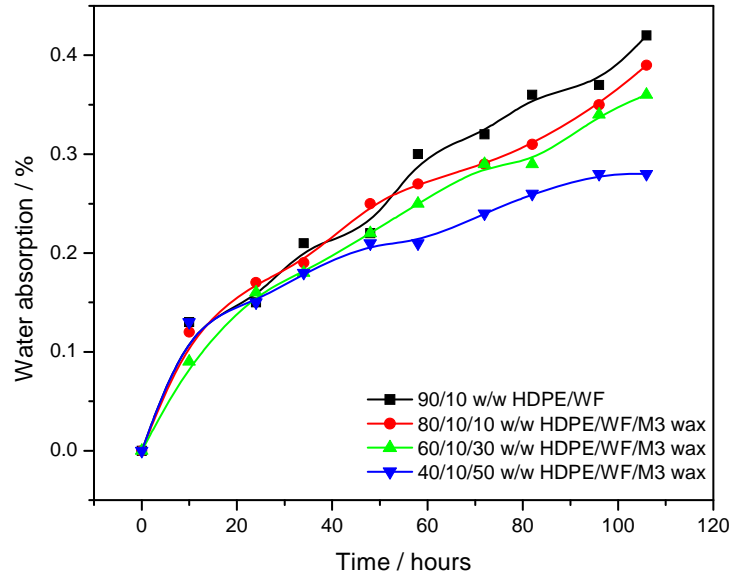


Figure 4.47 Water absorption curves of HDPE/WF/M3 wax composites at 10 wt% WF and various wax contents

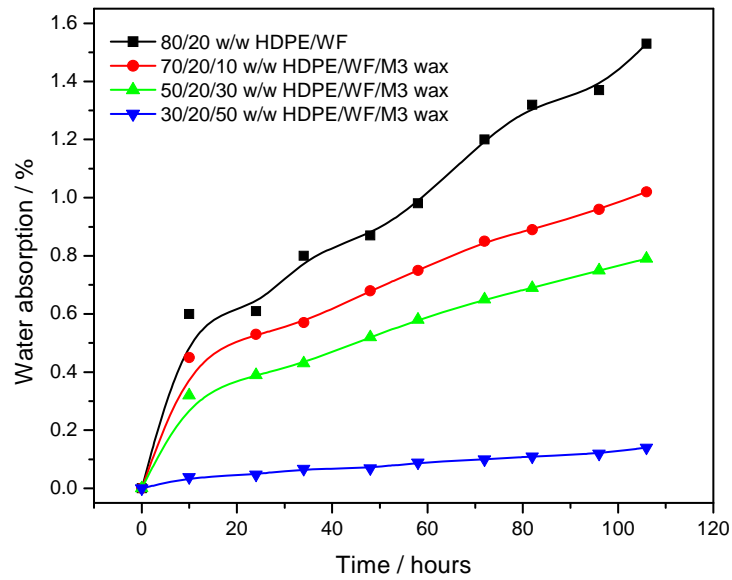


Figure 4.48 Water absorption curves of HDPE/WF/M3 wax composites at 20 wt% WF and various wax contents

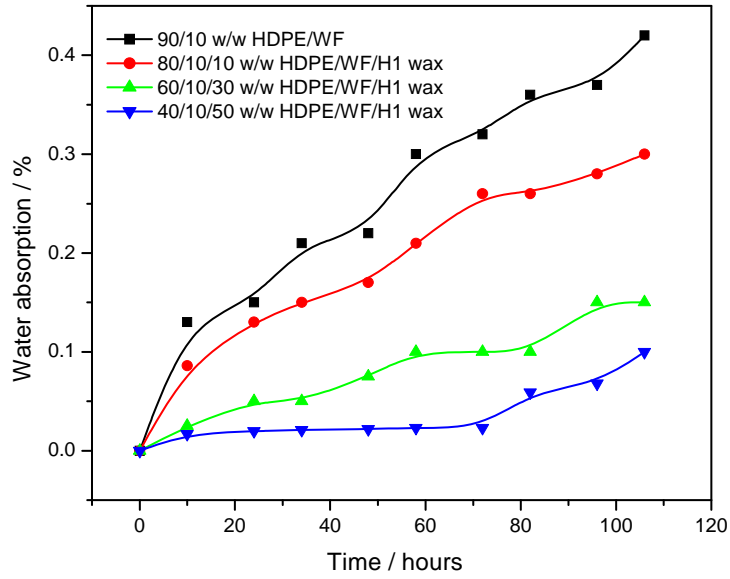


Figure 4.49 Water absorption curves of HDPE/WF/H1 wax composites at 10 wt% WF and various wax contents

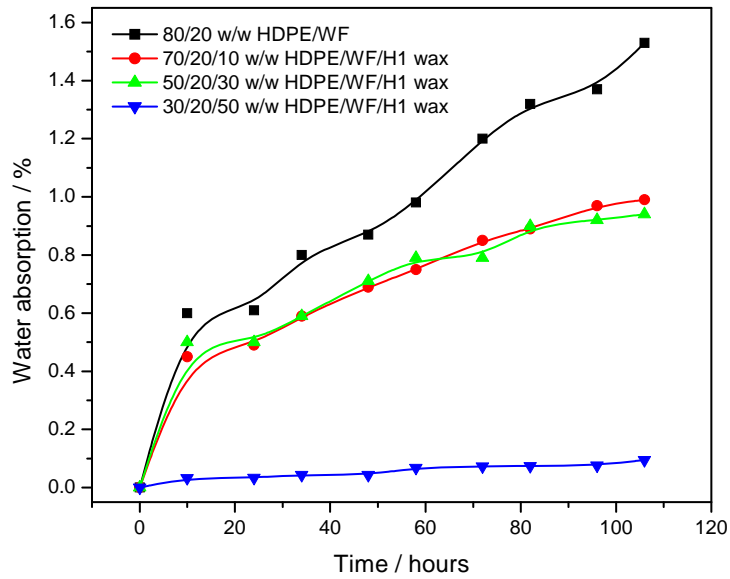


Figure 4.50 Water absorption curves of HDPE/WF/H1 wax composites at 20 wt% WF and various wax contents

4.7 References

1. M.J. John, R.D. Anandjiwala. Recent developments in chemical modification and characterization of natural fiber-reinforced composites. *Polymer Composites* 2008; 29(2):187-207 (DOI: 10.1002/pc.20461).
2. Y. Cao, S. Shibata, I. Fukumoto. Mechanical properties of biodegradable composites reinforced with bagasse fibre before and after alkali treatments. *Composites: Part A* 2006; 37:423-429.
3. M. Bengtsson, P. Gatenholm, K. Oksman. The effect of crosslinking on the properties of polyethylene/wood flour composites. *Composites Science and Technology* 2005; 65:1468-1479.
4. S.-M. Lai, F.-C. Yeh, Y. Wang, H.-C. Chan, H.-F. Shen. Comparative study of maleated polyolefins as compatibilizers for polyethylene/wood flour composites. *Journal of Applied Polymer Science* 2003; 87:487-496.
5. Y. Wang, F.-C. Yeh, S.-M. Lai, H.-C. Chan, H.-F. Shen. Effectiveness of functionalized polyolefins as compatibilizers for polyethylene/wood flour composites. *Polymer Engineering and Science* 2003; 43(4):933-945.
6. J. Z. Lu, Q. Wu, I.I. Negulescu. Wood-fibre/high-density-polyethylene composites: Coupling agent performance. *Journal of Applied Polymer Science* 2005; 96:93-102.
7. J. Z. Lu, I.I. Negulescu, Q. Wu. Maleated wood-fibre/high-density-polyethylene composites: Coupling mechanisms and interfacial characterization. *Composite Interfaces* 2005; 12(1-2):125-140.
8. S.H. Aziz, M.P. Ansell. The effect of alkalization and fibre alignment on the mechanical and thermal properties of kenaf and hemp bast fibre composites: Part I – Polyester resin matrix. *Composites Science and Technology* 2004; 64:1219-1230.
9. I. Krupa, G. Miková, A.S. Luyt. Polypropylene as a potential matrix for the creation of shape stabilized phase change materials. *European Polymer Journal* 2007; 43:895-907.
10. I. Krupa, G. Miková, A.S. Luyt. Phase change materials based on low-density polyethylene/paraffin wax blends. *European Polymer Journal* 2007; 43:4695-4705.
11. A.S. Luyt, I. Krupa. Thermal behaviour of low and high molecular weight paraffin waxes used for designing phase change materials. *Thermochimica Acta* 2008; 467:117-120.
12. H.S. Mpanza, A.S. Luyt. Comparison of different waxes as processing agents for low-density polyethylene. *Polymer Testing* 2006; 25:436-442.

13. S.P. Hlangothi, I. Krupa, V. Djoković, A.S. Luyt. Thermal and mechanical properties of cross-linked and uncross-linked linear low-density polyethylene-wax blends. *Polymer Degradation and Stability* 2003; 79:53-59.
14. D.G. Dikobe, A.S. Luyt. Morphology and properties of polypropylene/ethylene vinyl acetate copolymer/wood powder blend composites. *Express Polymer Letters* 2009; 3(3):190-199.
15. I. Krupa, A.S. Luyt. Thermal and mechanical properties of extruded LLDPE/wax blends. *Polymer Degradation and Stability* 2001; 73:157-161.
16. I. Krupa, A.S. Luyt. Physical properties of blends of LLDPE and an oxidized paraffin wax. *Polymer* 2001; 42:7285-7289.
17. M.J. Hato, A.S. Luyt. Thermal fractionation and properties of different polyethylene/wax blends. *Journal of Applied Polymer Science* 2007; 104:2225-2236.
18. I. Krupa, A.S. Luyt. Thermal properties of uncross-linked and cross-linked LLDPE/wax blends. *Polymer Degradation and Stability* 2000; 70:111-117.
19. A.S. Luyt, V.G. Geethamma. Effect of oxidized paraffin wax on the thermal and mechanical properties of linear low-density polyethylene-layered silicate nanocomposites. *Polymer Testing* 2007; 26:461-470.
20. D.G. Dikobe, A.S. Luyt. Effect of filler content and size on the properties of ethylene vinyl acetate copolymer-wood fiber composites. *Journal of Applied Polymer Science* 2007; 103:3645-3654.
21. N.E. Marcovich, M.A. Villar. Thermal and mechanical characterization of linear low-density polyethylene/wood flour composites. *Journal of Applied Polymer Science* 2003; 90:2775-2784.
22. C. Albano, J. González, M. Ichazo, D. Kaiser. Thermal stability of blends of polyolefins and sisal fiber. *Polymer Degradation and Stability* 1999; 66:179-190.
23. M.G. Salemane, A.S. Luyt. Thermal and mechanical properties of polypropylene-wood powder composites. *Journal of Applied Polymer Science* 2006; 100:4173-4180.
24. T.N. Mtshali, I. Krupa, A.S. Luyt. The effect of cross-linking on the thermal properties of LDPE/wax blends. *Thermochimica Acta* 2001; 380:47-54.
25. A.S. Luyt, M.E. Malunka. Composites of low-density polyethylene and short sisal fibres: the effect of wax addition and peroxide treatment on thermal properties. *Thermochimica Acta* 2005; 426:101-107.

26. A.S. Luyt, M.J. Hato. Thermal and mechanical properties of linear low-density polyethylene/low-density polyethylene/wax ternary blends. *Journal of Applied Polymer Science* 2005; 96:1748-1755.
27. V. Djoković, T.N. Mtshali, A.S. Luyt. The influence of wax content on the physical properties of low-density polyethylene-wax blends. *Polymer International* 2003; 52:999-1004 (DOI:10.1002/pi.1180).
28. N.J. Heaton, R. Benavente, E. Pérez, A. Bello, M. Pereña. The γ relaxation in polymers containing ether linkages: conformational dynamics in the amorphous phase for a series of polybibenzoates containing oxyethylene spacers. *Polymer* 1996; 37(17):3791-3798.
29. R.O. Sirotkin, N.W. Brooks. The dynamic mechanical relaxation behaviour of polyethylene copolymers cast from solution. *Polymer* 2001; 42:9801-9808.
30. V. Djoković, D. Kostoski, M.D. Dramićanin. Viscoelastic behavior of semicrystalline polymers at elevated temperatures on the basis of a two-process model for stress relaxation. *Journal of Polymer Science: Part B: Polymer Physics* 2000; 38:3239-3246.
31. K. Joseph, S. Thomas, C. Pavithran. Effect of aging on the physical and mechanical properties of sisal-fibre-reinforced polyethylene composites. *Composites Science and Technology* 1995; 53:99-110.
32. P.W. Balasuriya, L. Ye, Y.-W. Mai. Mechanical properties of wood flake-polyethylene composites. Part I: Effects of processing methods and matrix melt flow behaviour. *Composites: Part A* 2001; 32:619-629.
33. A. Arbelaiz, B. Fernández, J.A. Ramos, A. Retegi, R. Llano-Ponte, I. Mondragon. Mechanical properties of short flax fibre bundle/polypropylene composites: Influence of matrix/fibre modification, fibre content, water uptake and recycling. *Composites Science and Technology* 2005; 65:1582-1592.
34. S. Panthapulakkal, M. Sain. Agro-residue reinforced high-density polyethylene composites: Fiber characterization and analysis of composite properties. *Composites: Part A* 2007; 38:1445-1454.
35. W. Wang, M. Sain, P.A. Cooper. Study of moisture absorption in natural fibre plastic composites. *Composites Science and Technology* 2006; 66:379-386.
36. H.-S. Yang, H.-J. Kim, H.-J. Park, B.-J. Lee, T.-S. Hwang. Water absorption behavior and mechanical properties of lignocellulosic filler-polyolefin bio-composites. *Composite Structures* 2006; 72:429-437.

Chapter 5: Conclusions

The purpose of this study was to investigate whether the incorporation of natural filler (wood flour) in PCM blends could improve their mechanical properties and thermal stability, as well as to compare the performance of two types of paraffin wax as PCMs in an HDPE matrix.

5.1 HDPE/WF composites

From the SEM results, there was poor filler dispersion within the HDPE matrix with no visible WF fractures. Although there may have been improved interaction (through mechanical interlocking) between the WF and HDPE as a result of the pre-treatment of the WF with an alkali, there was clearly still a poor interfacial adhesion between these components. From the DSC results, the melting peak temperatures of the composites remained fairly constant within experimental error. The observed melting enthalpy of the composites was higher than the calculated enthalpy for 10% WF, but slightly lower for 20% WF. It seemed as if the WF particles acted as nucleation sites for the crystallization of HDPE at low WF content, but when the WF content is higher, it seemed as if the WF particles formed aggregates/clusters which immobilized the polymer chains and restricted the HDPE crystallization. The TGA results of the HDPE/WF composites showed two degradation steps. The presence of WF did not have any influence on the thermal stability of HDPE, but HDPE seemed to stabilise the WF. However, at higher WF content the protection seems to be less effective, probably because of incomplete covering of the WF by the HDPE matrix. The storage modulus of the 80/20 w/w HDPE/WF composite is higher than that of the neat HDPE. The addition of the WF to HDPE lowered the loss modulus, and caused a shift of both the γ - and α - transitions towards high temperatures. This is attributed to a restriction of the motion of the main polymer chain, as well as increased lamellar thickness with WF loading. An additional peak at -14 °C is noticed after WF incorporation. We could not find an explanation for the origin of this transition. The incorporation of WF into HDPE gave stiff composites with no yield point. These composites had a higher Young's modulus as a result of the stiffer organic filler compared to neat HDPE. The improved fibre-matrix adhesion as a result of fibre treatment with alkali, as seen by SEM, may have contributed to the increased modulus. Although still higher than that of the neat HDPE, a slight drop in modulus of the composites

with 20% WF was noticed, probably because of the reduced crystallinity as seen by DSC. The stress at break of the composites initially increased at 10% WF content, and decreased significantly at 20% WF. The initial increase in tensile strength is the consequence of the increased crystallinity and more complete fibre coverage by the HDPE matrix. The decrease at higher WF content is probably the result of incomplete fibre coverage by the matrix and lowered crystallinity of the composites as seen by DSC. The elongation at break decreased with increasing WF content. This may be attributed to restricted mobility of the polymer chains, giving rise to a rigid matrix in the presence of the solid WF particles, and to the WF particles that acted as defect points. The water absorption (WA) increased with immersion time and WF loading. The water uptake of these composites was mainly because of the presence of the natural wood flour filler. This is a consequence of the large number of micro voids because of the areas between the hydrophilic WF and the hydrophobic polymer matrix, which resulted from the weak interfacial bonding between these components as seen by SEM.

5.2 HDPE/M3 wax blends and HDPE/WF/M3 wax composites

From the SEM results, the blends and composites with M3 wax showed immiscibility of the polymer matrix with wax at all the investigated compositions. It was difficult to observe individual WF particles, and to distinguish between the HDPE and wax phases at high wax contents. This was probably the result of the higher affinity between WF and the wax, as well as the separately crystallized wax in the amorphous phase of the HDPE. Both the M3 and H1 waxes had a higher affinity for the WF.

The DSC results of the HDPE/M3 wax blends also showed the immiscibility character of these blends. The melting temperatures of HDPE decreased as wax content increased as a result of the plasticization effect of the M3 wax on the HDPE matrix. From the observed lower than expected experimental enthalpies of the wax, there might have been wax leakage from the blends during sample preparation, as well as partial co-crystallization of some portion of the M3 wax with HDPE. In the case of HDPE melting, the experimentally observed melting enthalpies were lower than the calculated enthalpies at low wax contents, but higher than the calculated enthalpies at higher wax contents. This further supported the observed partial co-crystallization. The blends were inhomogeneous and there was uneven wax dispersion within the polymer matrix at higher wax contents. The TGA showed that the blends degraded in two distinguishable steps confirming partial immiscibility as seen by SEM

and DSC. The presence of wax lowered the thermal stability of the blends. This is probably because of both the low molecular weight and low thermal stability of the paraffin wax. The DMA results showed reduced storage modulus of the blends with wax incorporation, although this was dependant on temperature interval. Of the two relaxation transitions (i.e. γ - and α -relaxation) observed for the neat HDPE matrix by DMA, the presence of M3 wax only induced a shift in the α -relaxation peak position towards lower temperatures. This was the result of the reduced lamellar thickness of the blends as seen by DSC. The loss modulus curves of the samples with 40 and 60% M3 wax showed an additional peak at -75 °C, which is the β -relaxation. The presence of a β -relaxation in the HDPE/M3 wax blends is therefore probably the result of an increased amount of the interfacial amorphous content as the wax content increased.

From the tensile results, the blend showed strain softening after yielding when 20 wt% M3 wax was introduced. An increase in elongation at yield and a slight decrease in yield stress were noticed. The increased elongation at yield may be the result of the plasticization effect of the M3 wax on the HDPE matrix, whereas the decreased yield stress was because of the lower crystallinity of the blends as the wax content increased as seen by DSC. Samples with high wax contents were very brittle. A decrease in modulus with an increase in M3 wax content was seen. This was the consequence of the decreased crystallinity of the blends with wax increase as seen by DSC. The tensile strength varied with wax loading, and the elongation at break of the blends decreased with increasing wax content. The lowered tensile strength may be the result of the decreased crystallinity of the blends with increasing wax content, and suppression of the cold drawing deformation of the polymer matrix. The effect on the elongation at break was a consequence of the loss of drawability in the presence of high wax contents that led to highly brittle blend samples.

The HDPE/WF/M3 wax composites at both 10 and 20% WF contents showed similar miscibility behaviour of HDPE and M3 wax, as in the case of the HDPE/M3 wax blends, even in the presence of WF. There was lower wax crystallinity (at low wax content) in the composites because most of the wax penetrated the WF pores increasing the amorphous fraction of the wax. At higher wax contents the WF pores were saturated with wax and the remaining wax crystallized around the WF particles, increasing the wax crystallinity and therefore the wax melting temperature. A plasticizing effect of the molten wax in the polymer matrix was also observed, even in the presence of WF. The experimentally observed

enthalpies of M3 wax at 10 and 20% WF contents were lower than the calculated enthalpies, but with insignificant differences between them. This was explained in terms of the following four situations: (i) inhibited wax crystallization inside the amorphous phase of HDPE; (ii) co-crystallization of some part of the wax with HDPE; (iii) penetration of the pores of the WF particles by wax, increasing the ‘amorphous’ part of the wax; (iv) adsorption of part of the wax onto the surfaces of the WF particles, also increasing the ‘amorphous’ part of the wax. The experimentally observed melting enthalpies of the HDPE in the HDPE/WF/M3 wax composites at both 10 and 20% WF were higher than the calculated enthalpies. This was probably the result of the partial co-crystallization of some of the M3 wax with the HDPE in the presence of WF. The samples were fairly homogeneous. All the PCM composites degraded in two steps. The first degradation step was an overlapping of the decompositions of WF and the M3 wax, with the M3 wax degrading first. For both WF contents, the presence of wax reduced the thermal stability of the composites, but not more than that observed for the HDPE/M3 wax blends. From the DMA results, all the storage moduli fell within the same order of magnitude, and no specific trends related to the presence of WF or wax content were observable. An observed additional peak at -14 °C was noticed after WF incorporation, and seemed to be dependent on the wax content. Also, as in the case of the HDPE/M3 wax blends, the position of α -relaxation transition shifted to lower temperatures as M3 wax content increased, but it still appeared at a higher temperature than that of the neat HDPE.

The Young’s modulus of the HDPE/WF/M3 wax composites decreased with increasing wax content at 10 wt% WF content. This was because of reduced contact/interaction between the WF and the HDPE matrix in the presence of wax. It may also have been a consequence of the lower crystallinity of these composites as seen by DSC. However, there was an increase in Young’s modulus with the introduction of 10 wt% wax to composites containing 20% WF. This may have been the result of too little wax available to cover all of the WF particles, and therefore some WF particles were directly in contact with the polymer matrix. The stress at break of the HDPE/WF (10%)/M3 wax composites decreased with increasing wax content. Since the tensile strength is a function of crystallinity, this was to be expected because of the decreased crystallinity as seen by DSC. It may also have been the result of the poor interaction between WF and HDPE as seen for the HDPE/WF composites in SEM, even in the presence of wax. In the case of the HDPE/WF (20%)/M3 wax composites, an increase in stress at break with increasing wax content was seen. Since there was more WF than wax in this system, it is probably the result of the existing interaction between the WF and the HDPE

matrix. The elongation at break of the HDPE/WF (10%)/M3 wax decreased with an increase in wax content. This was a consequence of the restricted mobility of the polymer chains and reduced strain transfer in the presence of both WF and wax. For the 20% WF composites, there was a slight increase in elongation at break. This may have been the result of the plasticization effect of the M3 wax.

5.3 HDPE/H1 wax blends and HDPE/WF/H1 wax composites

Although it varied with the H1 wax content, the crystalline structure of HDPE was clearly visible in the composites. This may have been a consequence of the higher level of miscibility of the H1 wax with the HDPE matrix as observed in the DSC results. For the highest wax content composite samples, there was a phase separation and hence partial immiscibility of the wax and the polymer matrix as observed from both the SEM and the DSC results.

The HDPE/H1 wax blends had two endothermic peaks, indicating that only part of the wax phase separated from the HDPE matrix, while some must have been partially co-crystallized with HDPE. The presence of wax in HDPE caused a slight decrease in melting temperature, but with no definite trend. The experimentally observed enthalpies were lower than the calculated enthalpies with an almost constant difference in values. However, the calculated enthalpies values fell within the experimental error of the observed enthalpies. If the differences are real, then it is most likely the consequence of small wax crystals in the amorphous phase of the polymer that must have influenced the polymer crystallization mechanism. There was an uneven distribution of wax in the blends. The TGA results of HDPE/H1 wax blends showed only a one-step degradation with no residue. This indicated a high level of miscibility of the HDPE and H1 wax as was also seen from the SEM and DSC results. The introduction of H1 wax into the HDPE matrix reduced the thermal stability of the blends. However, the sample with 50% H1 wax seems to be slightly more stable, but so far we could not find an obvious explanation for this observation.

HDPE showed the highest storage and loss modulus, and the introduction of H1 wax into the HDPE lowered the storage modulus with no direct relation between the storage moduli and the wax content in the samples. The lower storage moduli were a consequence of the plasticizing effect of the wax on the HDPE matrix. The curves of the blends seemed to converge at the temperature interval from 40 to 60 °C. There were no changes in the peak

position of the γ -relaxation, but the peak position of the α -relaxation shifted towards lower temperatures as the wax content increased. These changes in the case of the α -relaxation transition were the result of reduced lamellar thickness in the presence of H1 paraffin wax. This behaviour was also seen by DSC.

The 80/20 w/w HDPE/H1 wax blends exhibited strain softening after yielding. The blend had a slightly lower elongation at yield and yield stress than neat HDPE. The reason for this was that the H1 wax crystals, which formed in the amorphous phase of the polymer, acted as defect points. In the case of the yield stress it may be attributed to small wax crystals in the amorphous phase of the HDPE and their influence on the crystallinity of the blends as seen in the DSC results. Young's modulus increased with increasing wax content, and this was probably the result of the partial co-crystallization of H1 wax with the HDPE matrix as seen by the DSC results, as well as to more wax crystallized in the amorphous phase of the polymer. At the highest wax contents (50 and 60%), however, there was a fairly constant modulus (with 60% wax sample showing large standard deviations), which was still high with respect to neat HDPE. The stress at break increased with wax content, although it varied in such a way that it was not easy to correlate it with the available knowledge on the morphologies of the samples.

The HDPE/WF/H1 wax composites for 10 and 20% WF content showed one endothermic peak in the melting temperature region of the polymer for the lower wax content samples. This is indicative of the high level of miscibility of the wax and the polymer in the presence of WF. However, the emergence of a second peak was observed for higher wax contents, which was indicative of the partial immiscibility of the wax and the polymer. Seemingly part of the H1 wax, at high wax contents, co-crystallized with the polymer and part of it either crystallized separately in the amorphous phase of the polymer, or crystallized on the surfaces of the WF particles. Based on the SEM observations the latter is more probable. The plasticization effect of the wax was more visible in the presence of WF. For the 10% WF containing samples, the experimentally observed enthalpies were lower than the calculated enthalpies with inconsistent differences as the wax content increased. This was the result of the separate crystallization of H1 wax at the highest content, and the inhomogeneity of the composite samples. For the 20% WF containing composites, the experimental enthalpies were lower than the calculated ones, but the difference became smaller with increased wax content. The reason for this was not entirely clear, but the presence of WF particles covered by wax

and/or the presence of wax crystals in the amorphous phase of the polymer obviously influenced the crystallization mechanism of the HDPE. The TGA results of these composites displayed two degradation steps that were clearly seen for the lower wax contents, but were less resolved for the higher contents. The first step occurred at higher temperatures than that of neat WF, and it seemed that the highly crystalline (and therefore more thermally stable) H1 wax stabilized the WF. All the investigated composite samples showed reduced thermal stabilities as the wax content increased. This was the result of low thermal stability of the wax compared to that of the HDPE matrix.

From the DMA results the peak position of the α -transition for the HDPE/WF/H1 wax composites shifted to higher temperatures with increased H1 wax content. Although this peak position varied with wax content, it approached that of the HDPE/WF composite. Contrary to the case of the HDPE/H1 wax blends, the position of the α -relaxation transition shifted to higher temperatures as the wax content increased, and its position was still at a higher temperature than that of the neat HDPE. The position of the observed additional peak seemed dependent on the H1 wax content. The presence of 10 wt% H1 wax resulted in a slightly increased modulus at both 10 and 20% WF contents. The 20% WF containing samples at higher wax contents could not be analysed because they were too brittle. An increase in wax content in the 10% WF composites gave a product with a significantly lower modulus. This was contrary to the increased crystallinity of the composites as observed by DSC, and there was no obvious explanation for this observation. The stress at break of these composites remained almost constant with the addition of 10% wax in both the 10 and 20% WF composites. However, the addition of 30 wt% H1 wax led to a significant decrease in tensile strength. There are three factors that may have contributed to this observation: (i) the incorporated shorter wax chains into the lamellae of the polymer during co-crystallization resulted to a decreased average number of tie-chains with increasing wax content; (ii) the low crystallinity of the composites; and (iii) the presence of WF particles which seemed to act as defect points within the polymer matrix. Of these factors, the latter seemed to be the more appropriate reason. The elongation at break slightly decreased for the 10% WF composites, and was fairly constant for 20% WF composites with wax loading. This was also because the WF particles acted as defect points in the polymer matrix. The water absorption properties of the HDPE/WF/H1 wax composites also decreased with increased wax content. As in the case of M3 wax containing composites, this was the result of the affinity between the wax and the WF which shielded the WF particles from the water, and which reduces the number of voids

in and around the WF particles. The water uptake of the 10% WF containing composites was clearly lower than that of the 20% WF containing composites.

Both the thermal stability and mechanical properties of these blend and composite systems seemed better in the presence of WF. However, the M3 wax containing systems had inferior properties in comparison with the H1 wax containing system.

Effective energy storage requires the phase change material (in this case the waxes) to be immiscible with the matrix material (in this case HDPE), so that energy can be stored and released through the solid-liquid phase transition of the wax. However, if the wax co-crystallizes with the polymer, it does not melt at a lower temperature. Based on the discussed results there are advantages and disadvantages for the studied blend and composite systems. The H1 wax has a high melting enthalpy than the M3 wax, which would make it a better energy storage material. However, the H1 wax had a high level of co-crystallization with the polymer matrix, thus making it unfavourable. Although the M3 wax has a lower melting enthalpy, its high level of immiscibility makes it the material of choice as an energy storage material when blended with HDPE. It seems that the presence of wood flour reduced co-crystallization of the waxes with HDPE, because it seemed to interact more strongly with the wax so that the wax primarily crystallized around the WF particles. This resulted in a somewhat greater portion of the wax being available for energy storage.

ACKNOWLEDGEMENTS

The preparation of this thesis would not have been possible without the will of the Almighty God and the support, hard work and endless efforts of a large number of individuals and institutions.

I would like to thank my supervisor, **Prof. Adriaan Stephanus Luyt**, for his great efforts to explain things clearly and simply, and his guidance during my research. I express my deep sense of gratitude for his guidance, cloudless source of inspiration and constant support all through the course of the study. Throughout my thesis-writing period, he provided encouragement, sound advice, good teaching, good company, and lots of good ideas. His overly enthusiasm and integral view on research and his mission for providing 'only high-quality work and not less', has made a deep impression on me. I owe him lots of gratitude for having shown me this way of research. He could not even realize how much I have learned from him.

I would like to gratefully acknowledge the enthusiastic co-supervisor, **Dr. Igor Krupa**, during this work, who shared with me a lot of his expertise and research insight.

I acknowledge the University of the Free State at large by proving me with an opportunity to study.

Many thanks to Dr. Vladimir Djoković and my fellow polymer science research group (Dr. B. Hlangothi, Dr. S. Mishra, Dr. A. Mishra, Dr. S. Ochigbo, Mr. Mohammad Essa Ahmad, Mr. Mfiso. Mngomezulu, Mr. Tshwafo. Motaung, Mr. Samson Lulu Mohomane, Mr. Lefu. Nhlapo, Ms. Julia Puseletso Mofokeng, Mr. Jeremia Sefadi, Mr. Thabang Mokhothu, Mr. Bongile Tshabalala, Mr. Thabo Phelephe, Mr. Tsietse Tsotetsi, Mrs Seadimo Mojaki, Mrs Nomampondomise Molefe and Neo Moji), for all their help, support, interest and valuable hints. Especially I am obliged, to Mrs. M. Mokoena, Mrs. D.G. Mosiangaoko.

Appendix A

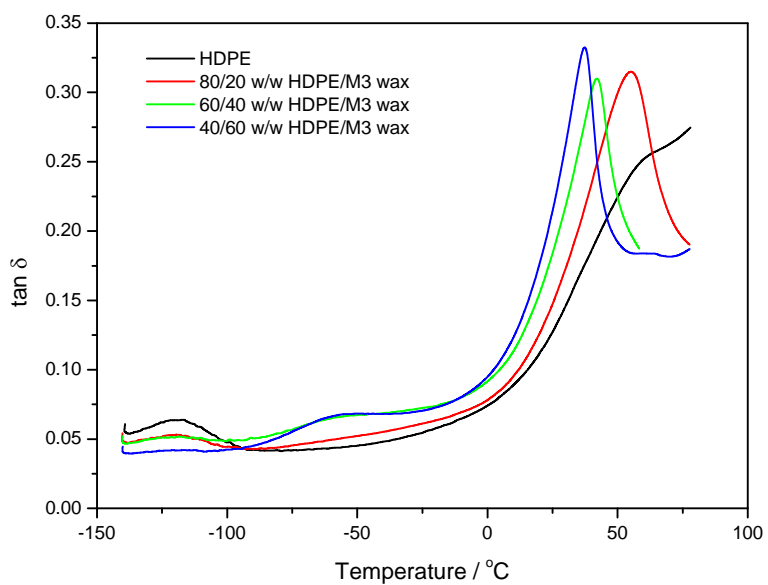


Figure A.1 DMA damping factor ($\tan \delta$) curves for the HDPE/M3 wax blends

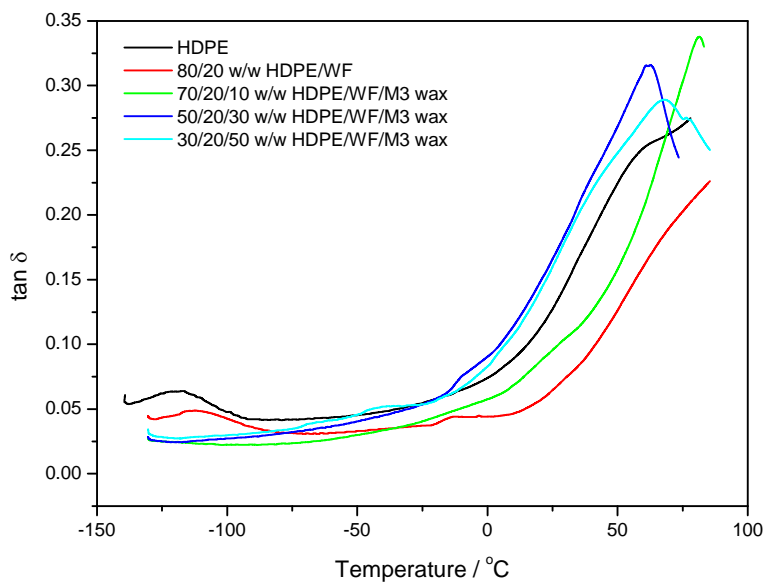


Figure A.2 DMA damping factor ($\tan \delta$) curves for the HDPE/WF/M3 wax composites

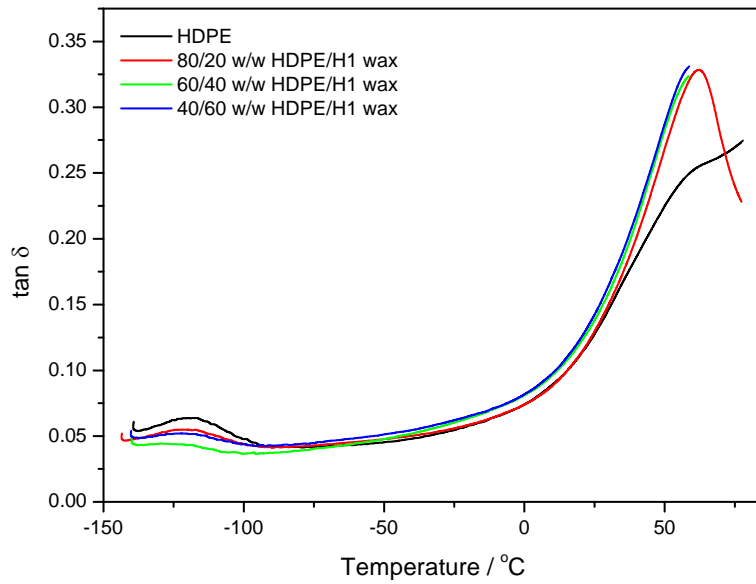


Figure A.3 DMA damping factor ($\tan \delta$) curves for the HDPE/H1 wax blends

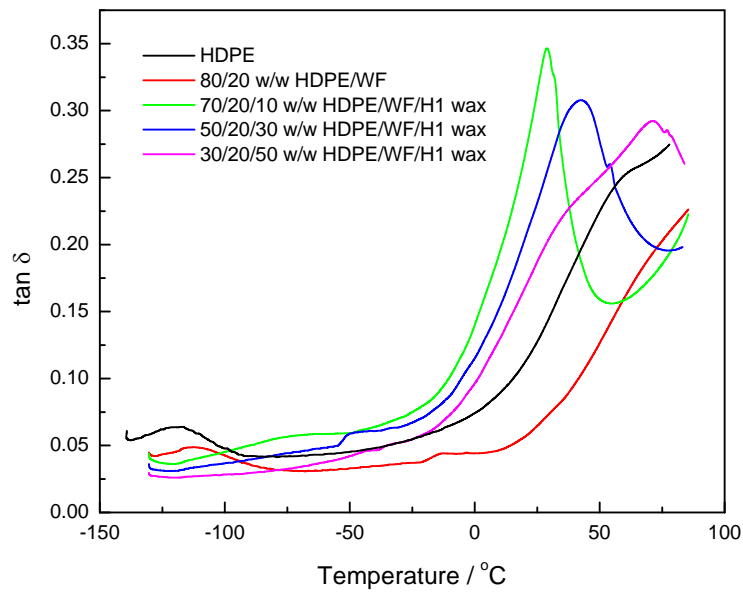


Figure A.4 DMA damping factor ($\tan \delta$) curves for the HDPE/WF/H1 wax composites

Appendix B

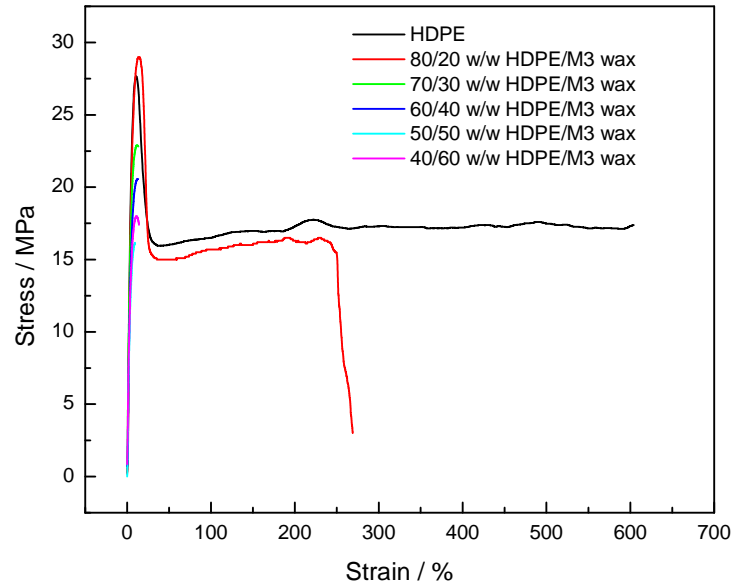


Figure B.1 Stress-strain curves of HDPE/M3 wax PCM blends at various wax contents

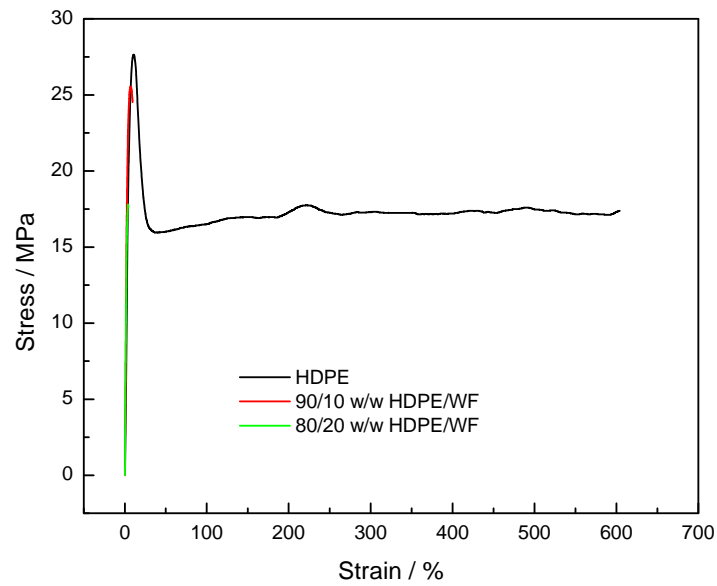


Figure B.2 Stress-strain curves of HDPE/WF composites

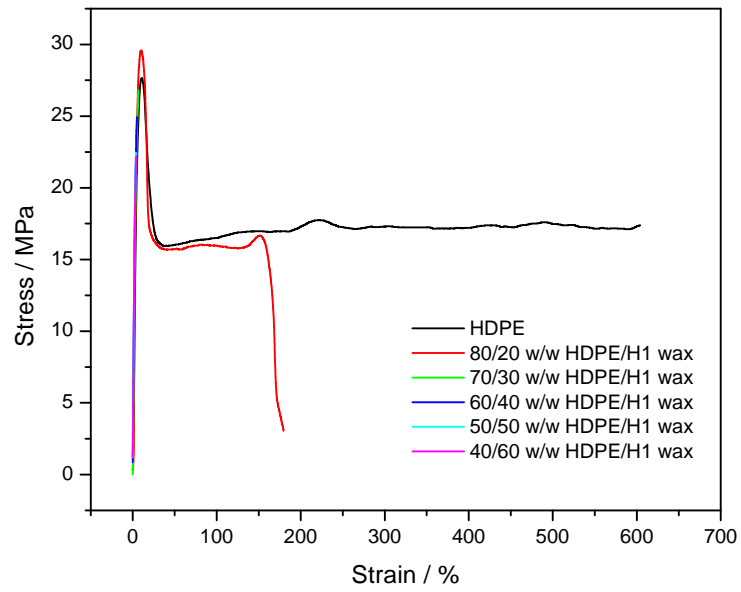


Figure B.3 Stress-strain curves of HDPE/H1 wax PCM blends at various wax contents